Dissertation

submitted to the

Combined Faculties for the Natural Sciences and for Mathematics

of the Ruperto-Carola University of Heidelberg, Germany

for the degree of

Doctor of Natural Sciences

presented by

Jovana Bojcevski, dipl. Phys.

born in Belgrade, Serbia

Oral Examination:

23.05.2017.

Calcium-mediated mechanisms of retinal ganglion cell degeneration during autoimmune optic neuritis

Referees: **Prof. Dr. Hilmar Bading**

Prof. Dr. Ricarda Diem

Acknowledgments

First of all I would like to thank Prof. Dr. Ricarda Diem for allowing me to start the amazing journey in the field of neuroscience; for her incredible support and care.

I would like to thank the following people for their contribution to this thesis:

Prof. Dr. Himar Bading for knowledgeable and constructive comments regarding my thesis, as my official supervisor and as a member of my thesis advisory committee. I would also like to thank Prof. Ana Martin-Villalba for being a part of my advisory committee and for her useful comments regarding my thesis.

Dr. Richard Fairless for scientific guidance, discussions and advices regarding experimental designs.

Dr. Sarah Williams for her valuable comments during my thesis.

Dr. Dorit Hoffmann for giving me a great introduction into my thesis.

Marika Dienes for her excellent technical assistance; for many time she was professional-level translator and lawyer; for her kindness, patience and friendship.

To all the people with whom I have interacted during my thesis work, in DKFZ and University of Heidelberg, specially Dr. Carlos Bas-Orth, Constanze Depp and people from G370 and G160 - who were kind enough to share their knowledge and skills; all members of AG Diem, great Master and MD students and fellow PhD student Kira Pichi.

To my friends who have always supported me throughout my studies; and made my life “pretty pretty good”.

To my amazing family, who have been coping with my unpredictable choices since ever, but have always been open-minded, understanding and most importantly loving.

To Dr. Aleksandar Stojic without whom this all would have never been possible; for being my life and science partner “come rain or come shine”.

Abstract

Optic neuritis (ON) is a common early symptom in multiple sclerosis (MS). It is characterized by disruption of the blood-brain barrier (BBB), inflammatory demyelination, and reactive gliosis in addition to axonal and somatic degeneration of retinal ganglion cells (RGCs) within the optic nerve and retina, respectively. ON can be modelled in animals, in particular by immunization of Brown Norway (BN) rats with myelin oligodendrocyte glycoprotein (MOG). In addition to the hallmarks of ON, RGC degeneration in BN autoimmune optic neuritis (AON) has been reported to begin during the induction phase of the disease (iAON) prior to lymphocyte infiltration and inflammatory demyelination in the optic nerve (Fairless at al., 2012). This may have parallels with observations of retinal degeneration in some MS patients even in the absence of clinically defined ON associated with demyelination (Green at al., 2010; Saidha et al., 2011).

Previous studies from our group have shown that this early RGC loss is timed with blood-retinal barrier (BRB) disruption, increase in retinal Ca^{2+} and activation of the Ca^{2+}-activated protease, calpain (Hoffmann et al., 2013), with subsequent elevation of optic nerve Ca^{2+}. We hypothesise that an initial retinal pathology may lead to Ca^{2+}-mediated cytoskeleton reorganization and axonal transport deficits in the optic nerve that could affect axonal integrity, as observed during iAON by electron microscopy (Fairless et al., 2012).

In this study, we examined the potential accumulation of axonal transport proteins along optic nerves, with particular focus on the optic nerve head (ONH) where RGC axons are naturally unmyelinated and therefore potentially more exposed to stress. No such anomalies were observed prior to the appearance of inflammatory demyelinating lesions. However, the axonal actin network dynamics within the optic nerve was changed starting iAON. This correlated with a decrease in protein expression of the Ca^{2+}-dependent actin binding protein gelsolin, and an increase in fractin, a cleaved product of the actin monomer; both proteins being implicated in apoptotic processes. Intravitreal injection (IVI) of MK801, an NMDA receptor blocker, during iAON significantly rescued RGCs and reverted axonal actin changes to the values observed in healthy animals.

In order to investigate downstream mechanisms of NMDA activity, a primary RGC culture was established. Based on qPCR data that Na+/Ca2+ exchanger 1 (NCX1), involved in regulating Ca^{2+} homeostasis, is elevated during iAON, its role in Ca^{2+} dynamics of isolated RGCs was investigated. Although this primary culture did not fully reflect RGC in vivo pathology (for example, cultured RGCs were seen not to retain sensitivity to glutamate excitotoxicity), blockade with an inhibitor targeting reverse NCX1 function (SEA0400) significantly reduced Ca^{2+} responses to glutamate stimulation.

However, SEA0400 treatment during iAON in vivo did not affect either RGC survival or optic nerve actin dynamics.

Collectively, data presented in this thesis provide further evidence that early neurodegenerative processes involved in AON pathology precede inflammatory driven demyelination of the optic nerves. Initial RGC loss observed in iAON is tightly connected to NMDA receptor activity in the retina, whereby prolonged intracellular Ca^{2+} increase may be one of the possible initiators of RGC death. These findings could be relevant for the development of potential neuroprotective treatment strategies in MS patients, particularly for a sub-set of MS patients characterized by retinal pathology in the absence of clinically-defined ON.

Zusammenfassung

Die autoimmune Optikusneuritis (AON) ist eine der häufigsten Erstmanifestationen einer Multiplen Sklerose (MS). Pathophysiologische Merkmale der AON sind Störungen der Bluthirnschranke, entzündliche Demyelinisierung und reaktive Gliose sowie axonale und somatische Degeneration von retinalen Ganglienzellen. Dabei handelt es sich um die Neurone, deren Axone den Sehnerven bilden. Für das Tiermodell der AON werden Brown Norway Ratten mit Myelin-Oligodendrozyten-Glykoprotein immunisiert. Es konnte gezeigt werden, dass die Degeneration von retinalen Ganglienzellen bei der AON schon während der Induktionsphase der Erkrankung (iAON) beginnt und zwar bevor Lymphozyten den Sehnerven infiltrieren und es zu einer Demyelinisierung kommt (Fairless et al. 2012). Dazu passen Beobachtungen an Patienten mit MS, bei denen eine Degeneration der retinalen Nervenfaserschicht nachweisbar ist auch wenn sich klinisch keine AON gezeigt hatte (Green et al., 2010; Saidha et al., 2011).

Vorangegangene Studien unserer Arbeitsgruppe konnten zeigen, dass der frühe Verlust der retinalen Ganglienzellen zeitlich parallel mit einer Störung der Blut-Retina-Schranke, einem erhöhten retinalen Ca^{2+}-Gehalt und einer Aktivierung der Ca^{2+}-aktivierten Protease Calpain (Hoffmann et al., 2013) auftritt. Wir nehmen an, dass die frühe Degeneration retinaler Ganglienzellen zu einer Ca^{2+}-abhängigen Zytoskelettreorganisation und Axontransportstörung im Sehnerven führt und somit die axonale Integrität beeinflusst, was bereits im Stadium der iAON elektronmikroskopisch sichtbar ist (Fairless et al., 2012).

In der vorliegenden Studie untersuchten wir die mögliche Akkumulation von axonalen Transportproteinen im Sehnerven, wobei der Fokus der Untersuchungen auf dem Sehnervenkopf lag. Dort sind die Axone der retinalen Ganglienzellen natürlicherweise nicht myelinisiert und somit

möglicherweise einem erhöhten Stress ausgesetzt. Vor dem Auftreten von inflammatorisch demyelinisierenden Läsionen im Sehnerven konnten wir keine Einschränkungen des axonalen Transports feststellen. Jedoch fanden sich zu Beginn der iAON Veränderungen in der Dynamik des axonalen Aktinnetzwerks. Dies korrelierte mit einer verringerten Proteinexpression des Ca^{2+}-abhängigen Aktinbindeprotein Gelsolin und der Erhöhung von Fractin, einem Spaltungsprodukt von Aktinmonomeren. Beide Proteine spielen eine Rolle bei der Apoptose. Intravitreale Injektionen von MK801, einem NMDA Blocker, während der iAON führte zu einem verbesserten Überleben der retinalen Ganglienzellen und verhinderte die axonalen Aktin-Veränderungen.

Um die nachgeschalteten Mechanismen einer NMDA-Rezeptor-Aktivierung in retinalen Ganglienzellen zu untersuchen, wurde eine primäre Kultur retinaler Ganglienzellen etabliert. Im Rahmen von qPCR-Untersuchungen konnte eine erhöhte Expression des Na^{+}/Ca^{2+}- Austauschers 1 (NCX1), der beteiligt ist an der Regulation der Ca^{2+}-Homöostase, nachgewiesen werden. Deswegen wurden die Ca^{2+}-Dynamiken von isolierten retinalen Ganglienzellen untersucht. Es zeigte sich, dass die Primärkulturen nicht die komplette in vivo Pathologie, wie z.B. die Sensitivität gegenüber Glutamatexzitoxizität, aufwiesen. Dennoch war es möglich mit Hilfe eines Inhibitors (SE0400), der die NCX1 Funktion umkehrt, die Ca^{2+} Antwort in retinalen Ganglienzellen nach Glutamat-Stimulation signifikant zu reduzieren. Allerdings zeigte die Behandlung mit SEA0400 bei iAON im Rahmen einer in vivo Studie weder ein verbessertes Überleben retinaler Ganglienzellen noch beeinflusste es die Aktindynamiken im Sehnerven positiv.

Zusammenfassend lässt sich sagen, dass diese Arbeit Mechanismen der frühen Neurodegeneration im Rahmen der AON aufzeigt. So ist der frühe Verlust retinaler Ganglienzellen die Folge einer Aktivierung von NMDA-Rezeptoren mit konsekutivem Anstieg der intrazellulären Ca2+ Konzentration. Auch scheinen Veränderungen im Aktin-Netzwerk das frühe Sterben von retinalen Ganglienzellen zu begünstigen. Diese Ergebnisse könnten relevant sein für die Entwicklung von potenziell neuen neuroprotektiven Behandlungen der MS.

List of publications

Hoffmann D.B., Williams S.K., Bojcevski J., Müller A., Stadelmann C., Naidoo V., Bahr B.A., Diem R., Fairless R. (2013) Calcium influx and calpain activation mediate preclinical retinal neurodegeneration in autoimmune optic neuritis. J Neuropathol Exp Neurol. 72(8):745-57.

Table of contents

1 Introduction …*1*

1.1 Multiple sclerosis ...***1***

1.1.1 Genetic and environmental risk factors in MS ...***1***

1.1.2 MS disease course …***2***

1.1.3 Pathology of MS …***4***

1.1.3.1 White matter pathology …***4***

1.1.3.2 Grey matter pathology …***5***

1.1.3.3 Pathology of ON …***5***

1.1.4 Neurodegeneration in MS …***6***

1.2 Experimental autoimmune encephalomyelitis …***9***

1.2.1 MOG-induced EAE in Brown Norway rats …***10***

1.3 Axonal cytoskeleton and transport …***12***

1.3.1 Axonal cytoskeleton …***12***

1.3.2 Axonal transport …***13***

1.3.3 Cytoskeleton and transport deficits in EAE …***14***

1.4 RGC death in experimental models …***15***

1.4.1 Optic nerve injury …***15***

1.4.2 Glutamate excitotoxicity in the retina …***15***

1.4.3 RGC loss in AON …***16***

1.5 The role of Ca^{2+} in neurodegeneration …***17***

1.5.1 The role of Ca^{2+} in apoptosis …***19***

1.5.2 Apoptotic and Ca^{2+} dependent modulation of actin cytoskeleton …***20***

1.6 Summary …***21***

2 The aim of the study …*23*

3 Methods …*24*

3.1 Animals …***24***

3.2 MOG-EAE induction and animal scoring …***24***

3.3 Retinal excitotoxicity model – IVI of glutamate …***25***

3.4 IVI of cholera toxin subunit B-Alexa Fluor 488 conjugate …***26***

3.5 Isolation and culture of primary RGC …***26***

3.6 Tissue collection and processing …***28***

3.6.1 Retinal whole-mounts ...***28***

3.6.2 Preparation of frozen tissue sections …***29***

3.7 Histopathology …***29***

3.7.1 Luxol Fast Blue …***29***

3.7.2 Bielschowsky´s Silver Impregnation …***30***

3.8 Immunofluorescent staining – general protocol …***30***

3.8.1 Immunocytochemistry …***32***

3.8.2 Immunofluorescent staining retinal whole–mounts …***33***

3.9 Terminal deoxynucleotidyl transferase dUTP nick end labelling (TUNEL) assay …***34***

3.10 Preparation of tissue lysates …***34***

3.10.1 Western blotting …***35***

3.10.2 Globular versus filamentous actin ratio assay …***36***

3.11 Live dead assay …***37***

3.12 Ca^{2+} imaging …***37***

3.13 Quantitative Real Time - Polymerase Chain Reaction (qRT-PCR) …***39***

3.14 MK801 and SEA0400 treatment studies during iAON …***41***

3.15 Statistical analyses …***41***

4 Results …*42*

4.1 Disease course …***42***

4.2 Early RGC loss detection with the anti-Rbpms immunostaining of retinal whole-mounts …***43***

4.3 Axonal transport deficits during AON …***43***

4.3.1 Axonal transport profile in the ONH …***44***

4.3.2 Axonal transport profile in the distal optic nerve …***46***

4.3.3 Cholera Toxin B subunit A488-conjugate for detection of axonal transport deficits during AON …***50***

4.4 Actin network profile in optic nerves during AON …***51***

4.4.1 G/F-actin ratio is increased along the course of AON …***51***

4.4.2 Expression of proteins associated with actin cytoskeleton changes during AON …***52***

4.5 Intravitreal injection of glutamate as a model of primary RGC loss …***52***

4.5.1 RGC loss following IVI of glutamate …***53***

4.5.2 Axonal transport profile following IVI of glutamate …***54***

4.5.3 G/F-actin ratio is increased in optic nerves following IVI of glutamate …***55***

4.6 Blockade of the NMDA receptor protects RGCs and reverses actin network changes in the optic nerve during iAON …***55***

4.7 mRNA expression of Ca^{2+}-permeable channels in RGC is regulated during the course of AON …***58***

4.8 Utilization of primary RGC cultures for studying Ca^{2+} responses following glutamate stimulation …***59***

4.8.1 Primary RGC culture is not prone to glutamate excitotoxicity …***60***

4.8.2 Ca^{2+} dynamics in primary RGCs following glutamate receptor stimulation …***60***

4.8.3 Role of NCX in Ca^{2+} dynamics following glutamate stimulation of RGCs …***63***

4.9 Treatment study with NCX1 receptor blocker SEA0400 in AON …***66***

5 Discussion …*67*

5.1 Anti-Rbpms staining can be used for detection of RGC loss in iAON …***67***

5.2 Axonal transport deficits do not precede RGC loss during iAON …***69***

5.3 Actin cytoskeleton as a marker of axonal stress in AON …***70***

5.4 NMDA glutamate receptor is involved in RGC neurodegeneration during iAON …***72***

5.5 Invulnerability of RGCs to glutamate excitotoxicity in vitro …***74***

5.6 Role of NCX1 in Ca2+ dynamics following glutamate receptor stimulation in cultured RGCs …***75***

5.7 SEA0400 blocker application during iAON did not protect RGCs …***76***

5.8 Summary …***77***

References …*79*

Abbreviations …*112*

1. Introduction

1.1 Multiple Sclerosis

Multiple sclerosis (MS) is the most common cause of chronic neurological disability in young adults with an average onset between the ages of 20 and 40 (Hauser and Oksenberg, 2006). MS is seen as an immune-mediated demyelinating disease of the central nervous system (CNS) accompanied by neurodegeneration that eventually leads to permanent neurological disability. It has become an increasingly interesting topic amongst the neurological community considering that it represents a great burden on the quality of individual life and society.

The first disease diagnostic criteria, as well as the correlation of neurological symptoms with post mortem CNS pathology, came from the work of "the Father of Neurology" Dr. Jean Martin–Charcot. In the late 1860s, he published studies from the autopsy brains of his patients and described and illustrated the so–called *"la sclerose en plaques"* (Charcot, 1868). By the middle of the 20th century, MS was defined as a distinct entity with more known about its diverse neurological outcomes, and the first studies on disease origin and risk factors were conducted (Compston & Coles, 2008). Unfortunately, even today there are still many unanswered questions regarding the origin, nature and pathophysiological mechanisms behind this devastating disease.

1.1.1 Genetics and environmental risk factors in MS

The origin of MS remains unknown, but the disease seems to be more common amongst certain ethnic populations and under specific environmental conditions. MS is recognized as complex genetic disorder with modest disease risk heritability and multifaceted gene–environment interactions. Genetic heritage as a risk factor emerged after studies on ethnicity (Rosati G., 2001; Langer et al., 2013) and familial re-occurrence (Sadovnick et al., 1996; Ebers et al., 1995; Ebers et al., 2000). The strongest MS susceptibility genes recognized so far are the major histocompatibility complex (MHC) class II, DR beta 1 gene (HLA – DRB1), interleukin‑2 receptor complex (IL2R) and interleukin-7 receptor (IL7R) (Oksenberg et al., 2004; Gregory et al., 2007). In the following years, additional new candidates were observed, mostly in immune-related genes, with some exceptions such as ribosomal protein L5, kinesin family member 21B (Kif21B) and GRIN2A gene which encodes the NR2A subunit of the *N*-methyl-D-aspartate receptor (NMDAR; Hafler et al., 2007; Sawcer et al., 2014; Baranzini et al., 2009).

The role of different environmental factors in MS emerged following studies conducted on migration (Alter et al., 1978; Rosati, 2001). One prominent environmental risk factor is the Epstein Barr virus

(Haahr et al., 2004; Lucas et al., 2011; Ascherio & Munger, 2007a). Other factors include vitamin D (Munger et al., 2006; Soilu-Hänninen et al., 2005; Ascherio & Munger, 2007b) and smoking (Hedström et al., 2009), etc. All of these, and many other environmental factors, are believed to contribute to MS incidence and disease progression, although strong and persuasive evidences are still missing.

1.1.2 MS disease course

Neurological symptoms commonly associated with MS include various physical (weakness, tiredness, pain, visual disturbances, etc.), emotional (stress, depression, mood swings, etc.) and cognitive (remembering, problem solving, learning, etc.) disturbances. These symptoms represent underlying pathological changes in different parts of the CNS whose hallmark is the appearance of inflammatory demyelinating lesions (Compston and Coles, 2008). The first attacks are generally unpredictable and need to persist for at least 24 hours to be considered as a relapse. Following initial symptoms, MS is diagnosed only after the specific McDonald's criteria are met based on magnetic resonance imaging (MRI) examination (Polman et al., 2011).

The currently used classification of different MS subtypes was established in 2013 by the International Advisory Committee on Clinical Trials of MS (Lublin et al., 2014). The following subtypes are recognized:

- Clinically Isolated Syndrome (CIS)
- Radiologically Isolated Syndrome (RIS)
- Relapsing remitting MS (RRMS)
- Primary Progressive MS (PPMS)
- Secondary Progressive MS (SPMS).

CIS is an initial presentation of neurologic symptoms characteristic for MS which does not yet meet the aforementioned criteria for a diagnosis of MS (dissemination in time and space). In 80% of MS patients, CIS is the first manifestation of disease. Most prominent markers in predicting the conversion from CIS to clinically diagnosed MS (CDMS) are MRI lesion load and the presence of oligoclonal bands in cerebrospinal fluid (CSF; Kuhle et al., 2015).

RIS represents the case in which incidental MRI shows the presence of a CNS lesion in the absence of clinical symptoms characteristic of MS. RIS might raise the suspicion of MS based on morphology and location of the lesions. It was recently evaluated that 33% of people with RIS develop MS within the next 5 years (Lebrun et al., 2009).

RRMS is the most common MS subtype. Approximately 80% of MS patients are initially diagnosed with RRMS (Trapp and Nave, 2008). It has clearly defined attacks (relapses) of new or increasing neurologic symptoms that are followed by a remission phase during which symptoms may partially or totally disappear (Figure 1.A).

SPMS commonly follows from a period of RRMS and together they represent the most common biphasic MS type. Within 25 years, 90% of RRMS patients progress to SPMS. Relapses can still continue with the continuous presence of increasing neurological deficits (Noseworthy et al., 2000; Trapp and Nave, 2008; Figure 1.B).

PPMS is initially diagnosed in around 15% of MS patients. It is characterized by a worsening of clinical symptoms without episodes of remission from the beginning of the disease course. Compared to RRMS, PPMS patients have more spinal cord than brain lesions (Miller & Leary, 2007; Figure 1.C).

Based on the heterogeneity of different clinical subtypes and neurological symptoms, it is still debatable if what we call MS today is a single disease with many faces or separate phenomena classified under the same name (Stys et al., 2012; Lassmann, 2013).

Optic neuritis (ON) is a syndrome associated with primary inflammation of the optic nerve. It is a presenting feature of MS in about 20% of patients, with about 50% incidence at some point during the disease course (Balcer, 2006). Reoccurrences of ON in patients that develop MS is around 30% during the 10 year follow up (Beck et al., 2004). Clinical symptoms of acute ON associated with MS are monocular visual impairments. These include problems in colour distinction (in particular, the red colour appears “washed out”), blurry vision or acute vision loss. Pain while moving the eye is common in around 90% of patients (Balcer, 2006). ON is diagnosed cinicallz and by measurement of visually evoked potentials (Balcer et al., 2015).

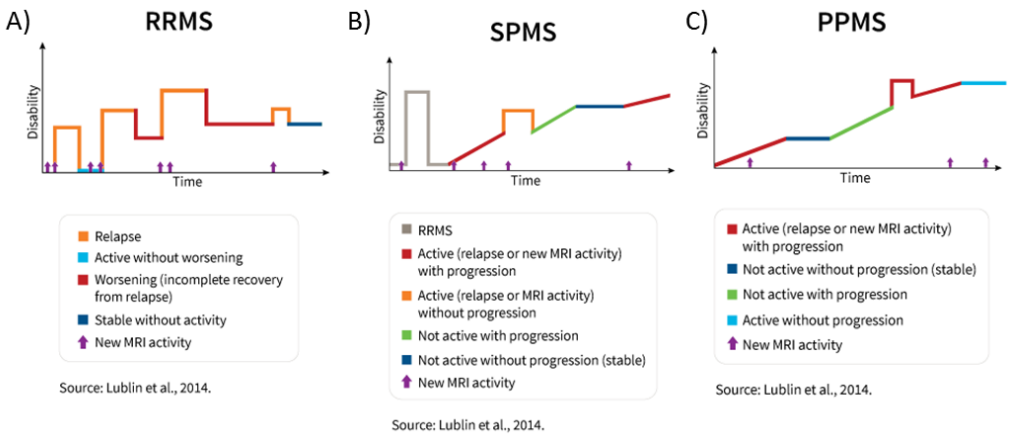

Figure 1.1.2 MS disease course (adapted from National Multiple Sclerosis Society web page).

1.1.3 Pathology of MS

MS assumes three distinct patterns of CNS pathology: inflammatory demyelination in white matter, diffuse pathology in normal-appearing white matter and grey matter demyelination. It is currently unclear whether these patterns appear interdependently or independently.

1.1.3.1 White matter pathology

White matter (WM) lesions have long been considered as a hallmark of MS pathology. These lesions are areas of focal demyelination accompanied by blood-brain barrier (BBB) disruption, infiltration of lymphocytes and monocytes from the periphery as well as a variable degree of CNS tissue destruction. They are highly dynamic structures that change their morphology and inflammatory profile with time. In their active state, the centre of the lesion is enriched with inflammatory infiltrates which leads to demyelination and, to various extents, the loss of both oligodendrocytes and axons. Four different types of WM lesions have been recognized (Lucchinetti et al., 2000).

Pattern I has the "basic" character shared with all the other lesion types, the presence of macrophages and T cells and, to a lesser extent, B cells. Specific for Pattern II is the presence of antibody and complement deposition. Patterns III and IV have a common feature of vast oligodendrocyte death. The loss of oligodendrocytes in type III lesions is mainly through the process of apoptosis while in type IV it is more of a necrotic nature. Another difference between these two types is an uneven loss of different myelin proteins. In Pattern III lesions there is a preferential loss of myelin-associated glycoprotein (MAG). The feature of pattern III lesions is having an ill-defined shape; in contrast, the other patterns have a well-defined lesion edge which is usually centred around the blood vessels. With time, different patterns mature into a more homogeneous, chronic state (Breij et al., 2008). These chronic lesions are characterized by a lack of myelin in their centre and a redistribution of inflammatory cells (mainly macrophages) at their rims/periphery. In their inactive state, the lesion centre is hypo-cellular with a sparse presence of macrophages and lymphocytes, but a strong astrocytic gliosis (Kipp et al. 2012).

Besides these well-established WM lesions recognizable by standard Gd-enhanced MRI examination due to the presence of BBB leakage, there are also the so-called "normal-appearing white matter" (NAWM) lesions. NAWM pathology is predominantly present in PPMS (Suhy et al., 2000). Hallmarks of NAWM lesions include mild BBB disturbances and monocyte infiltration, some activation of astrocytes and microglia, and minor demyelination and axonal loss. Interestingly, in NAWM, together with the presence of pro-inflammatory and cell damaging markers, many cellular stress markers involved in anti-inflammatory and protective mechanisms were also detected (Fu et al., 1998; Zeis et al., 2009; Cunnea et al., 2011; Pedre at al., 2011; Graumann et al., 2003).

1.1.3.2. Grey matter pathology

Grey matter (GM) pathology in MS has been largely neglected until recent advances in the sensitivity of histopathological markers and MRI provided substantial evidence of its presence and correlation with neurological symptoms (Honce, 2013). Lesions have now been observed both in the cortex and in the deep GM of the CNS including the caudate nucleus, hippocampus, thalamus, putamen and the spinal cord (Haider et al., 2014; Koenig at al., 2014; Gilmore at al., 2008; Vercellino et al., 2009). Nonetheless, cortical lesions are now recognised to be a very prominent feature, and are classified based on their location (Peterson et al., 2001):

- type1 "leukocortical" lesions – spanning deep layers of GM together with underlying WM
- type 2 "intracortical" lesions – located entirely within the cortical GM
- type 3 lesions – located within sub-pial cortical layers, usually not spreading below cortical layers 3 and 4
- type 4 lesions - extend over the entire width of the cortex, do not spread into the subcortical WM, and might extend over several gyri or entire lobes.

The inflammatory profile of these lesions is different from their WM counterparts. GM lesions have a relative lack of parenchymal lymphocyte infiltration, antibody and complement deposition and BBB disruption compared to WM lesions (Peterson et al., 2001; Bö et al., 2003). However, they have increased activation of residential microglia and astrocytes (Peterson et al., 2001; Brink et al., 2005; van Horssen et al., 2007; Vercellino et al., 2009; Haider et al., 2014; Calabrese et al., 2015).
Cortical lesions are present during all stages and in all types of MS (Kutzelnigg et al., 2005; Vercellino et al., 2005; Lucchinetti et al., 2011). GM pathology has been observed early on following disease onset (Dalton et al., 2004; De Stefano et al., 2003; Lucchinetti et al., 2011). Its load accumulates with disease progression, sometimes overcoming WM pathology (Kutzelnigg and Lassmann, 2005; Gilmore et al., 2008). Interestingly, MS patient disability was shown to correlate better with GM than WM pathology (Vercellino et al., 2005; Calabrese et al., 2012; Honce, 2013).

1.1.3.3 Pathology of ON

Optic nerves are the second pair of cranial nerves that belong to the CNS. They are composed of retinal ganglion cell (RGC) axons. These neurons have a distinct compartmentalization of their cell bodies, which reside in the innermost layer of the retina and myelinated axons in the optic nerves. The initial segment of these axons are unmyelinated and located within the retina forming the retinal

nerve fibre layer (RNFL) and the most proximal part of the optic nerve, the optic nerve head (ONH). Most of these axons terminate in the lateral geniculate nucleus (LGN) from where further projections lead to the visual cortex.

Similar to WM lesions, the main feature of ON is the presence of inflammatory demyelinating lesions in the optic nerve accompanied by visual disturbances (Roed et al., 2005; Söderström et al., 1993; Chalmoukou et al., 2015). Due to a lack of published autopsy reports, the pathological mechanisms in ON are suggested based on functional testing and MRI. Gd-enhanced MRI confirms BBB breakdown (indicative of the presence of inflammatory lesions), while altered visual evoked responses, such as prolonged latency and decreased amplitude of the signal imply demyelination and axonal injury, respectively. In addition to the pathology in the optic nerve, loss of RGCs and also neurons in the inner nuclear layer (INL) together with thinning of the RNFL can be detected in the retina (Green et al., 2010; Syc et al., 2012; Kupersmith et al., 2016). Changes in outer retinal parts, such as the outer plexiform layer as well as outer nuclear and photoreceptor segments, have also been observed (Kaushik et al., 2013; Al-Louzi et al., 2015). Surprisingly, thinning of RGC neuronal and axonal layers has even been observed in non-ON eyes of MS patients (Saidha et al., 2011; Walter et al., 2013).

There are several mechanisms implicated in this observed retinal pathology. On one side, due to axonal loss following inflammatory demyelination, it is thought that retrograde trans-synaptic and Wallerian-like degeneration, dying of the distal axon following injury, contribute to retinal atrophy through depletion of trophic factors coming from the brain (Klistorner et al, 2007; Rocca et al., 2013). However, there are findings showing that retinal pathology might originate within the retina itself through microcystic macular oedema, and breakdown of the blood-retinal barrier (BRB) with or without microglial inflammation, that is associated with INL atrophy (Gelfland et al., 2012; Cennamo et al., 2015; Kaufhold et al., 2013).

Based on the aforementioned pathological observations, it is clear that MS has been dominantly characterized through its temporal and spatial inflammatory and demyelinating profile. However, additional mechanisms implicated in MS also include autoimmunity, gliosis, and neurodegeneration (Stys, 2013). In the last decades, interest in the neurodegenerative aspect of MS has gained momentum since many different immunomodulatory therapies have failed to prevent the progressive neurological deterioration visible in most MS patients.

1.1.4 Neurodegeneration in MS

Current disease-modifying therapies have been able to supress inflammatory-mediated relapses, although they have proved not to be effective in decreasing or postponing neurological disabilities during progressive stages of MS. Neurodegeneration, though observed since the times of Charcot, has been neglected in MS research for a long time (Charcot, 1868; Kornek & Lassmann, 1999).

However, increasing neurological disability in SPMS and PPMS is found to correlate with the accumulation of widespread neurodegeneration and the inability of the CNS to compensate for it (Trapp & Nave, 2008). Axonal swellings and transections together with oligodendrocyte stress and loss have been detected in post-mortem tissue (Ferguson et al., 1997; Trapp et al., 1998; Ganter et al. 1999; Lovas et al. 2000). In addition, using MRI and magnetic resonance spectroscopy (MRS), neurodegeneration was observed to correlate with decreased levels of N-acetyl-aspartate (NAA), mostly present within axons (Matthews et al., 1996; Bjartmar et al. 2000; Fu et al. 1998). Besides overall cortical atrophy, more subtle changes such as synaptic loss were also detected (Wegner et al., 2006; Dutta et al., 2011; Tur et al., 2016; Jürgens et al., 2016).
Some of the neurodegenerative mechanisms suggested to be involved in MS pathology are (Kwachi & Lassmann, 2017; Macrez et al., 2016):

- virtual hypoxia as a consequence of both demyelination and direct action of reactive oxygen and nitrogen species (ROS/RNS)
- glutamate excitotoxicity
- Wallerian-like degeneration.

In demyelinated axons, “virtual hypoxia” might happen due to an increased pressure on mitochondria for adenosine triphosphate (ATP) production. Demyelination leads to a disruption in the nodes of Ranvier which in turn causes a redistribution of voltage-gated Na^+ channels (NaV). In order to maintain efficient conduction velocity in the absence of salutatory action potential propagation there is an increase of Na^+ influx into the axon. This imposes a higher demand for ATP by the ATP-dependent Na^+/K^+ pump responsible for Na^+ extrusion, in turn leading to mitochondrial injury through respiratory chain dysfunction (Mahad et al., 2015). In addition, nitric oxide (NO) can induce a respiratory burden on the axon. Inducible nitric oxide synthases (iNOS), one of the key enzymes involved in NO synthesis is expressed on activated microglia/microphages and is found to be upregulated in inflammatory MS lesions (Bö et al. 1994, Liu et al. 2001, Smith & Lassmann, 2002; Trapp & Nave, 2008). Elevated NO levels can damage axons by modifying the action of key channels, like NaV and Na^+/K^+ pump (Renganathan et al., 2002; Muriel et al., 2003) and glycolytic enzymes (McDonald & Moss, 1993). Activated microglia/microphages are also seen as mediators of oxidative damage via production of reactive oxygen species (ROS) contributing further to demyelination and free radical-mediated tissue injury (Fischer et al., 2012; Hohlfeld et al, 1997; Stys et al., 2012). Astrocytes, the most abundant cells of the CNS, are also associated with neurodegeneration due to their impaired function in the suppression of iNOS and in clearance of glutamate (Cambron et al., 2012).

The role for glutamate, the main excitatory CNS neurotransmitter, has been suggested in MS pathology since increased levels of glutamate have been detected in all patterns of MS pathology (Srinivasan et al., 2005; Baranzini et al., 2010; Tisell et al., 2013; Muhlert et al., 2014). Over stimulation of glutamate receptors, expressed on both neurons and oligodendrocytes, is believed to cause excitotoxicity predominantly through resultant increases in intracellular Ca^{2+} to toxic levels. Among many other downstream pathways, increased intracellular Ca^{2+} leads to activation of proteases, many of which are involved in the regulation of apoptosis (see chapter 1.11). In active and chronic WM lesions, increased levels of Ca^{2+}-activated proteases (calpains) have been detected (Diaz-Sanchez et al., 2006). The source of elevated extracellular glutamate within inflammatory lesions might come from neutrophils, macrophages, microglia and dendritic cells. All of them are capable of releasing glutamate through the cysteine/glutamate anti-porter Xc^- (Collard et al., 2002; Pampliega et al., 2011; Evonuk et al., 2015; Pacheco et al., 2006; Domercq et al., 2005; Micu et al. 2016). Increases in extra-synaptic glutamate from degenerating neurons could cause further injury to other neighbouring neurons. Simultaneously, its inappropriate buffering by compromised astrocytes which no longer express sufficient levels of membrane glutamate transporters or intracellular enzymes involved in maintaining the glutamate-glycine cycle could additionally affect neighbouring neurons (Vercellino et al., 2009; Castegna et al., 2011). In NAWM, the axons could also be the source of glutamate via inappropriate synaptic vesicle docking and glutamate vesicle release due to axonal transport failure. Such axonal glutamate release has been shown to affect oligodendrocytes and to disturb normal physiological communication between these two cell types (Micu et al., 2016; Saab et al, 2016).

Wallerian degeneration is a simple experimental model of axonal degeneration following axonal transection or crush used to describe the dying back of the distal axonal part in both peripheral nervous system and CNS neurons (Waller, 1850). This axonal loss is predominantly thought to occur because of the lack of materials delivered via axonal transport from the cell body to the detached axon (De Vos et al., 2008; Coleman, 2005). In the CNS, the hallmark of this process is the appearance of axonal swellings and spheroids prior to final axonal disruption and the appearance of axonal fragments (Beirowski et al. 2010). T cell-mediated axonal transection, hence true Wallerian degeneration, has been described in MS, though these events are considered to be relatively rare (Trapp et al. 1998).

Wallerian-like degeneration occurs in many neurodegenerative diseases, especially those where axonal transport is impaired (Coleman & Freeman, 2010). Focal axonal swellings are observed to occur without overt axonal disintegration and it is debatable if these swellings precede future transection or whether they are part of a reversible process that would make them candidate targets for neuroprotective strategies. Whatever the precise mechanism of axonal degeneration, axonal

spheroids likely contribute to significant functional impairment. There are numerous causes for the appearance of axonal spheroids and swellings: focal axolemmal failure with subsequent ionic dysregulation causing cytoskeletal damage (Stone et al., 2004; Kornek et al., 2000), local impairment of axonal transport (Stokin et al., 2005; Ferreirinha et al., 2004), neuronal autophagy (Komatsu et al., 2007; Wang et al., 2012), etc. Wallerian-like degeneration is observed to be the most prominent feature of early MS axonal loss in WM lesions and NAWM (Rocca et al., 2013; Dziedzic et al., 2010). This MS Wallerian-like degeneration was at first connected with demyelinated axons due to the lack of glial support (Trapp & Nave, 2008). However, axonal damage was observed in NAWM, and it became clear that inflammatory-mediated injury is more wide-spread than previously thought. Axonal transport failure could be one of the reasons since certain kinesin superfamily proteins involved in axonal transport were found to be decreased in WM lesions and NAWM (Hares et al., 2016) as well as in non-lesioned GM (Hares et al., 2014).

It is hoped that through the discovery and understanding of neurodegenerative mechanisms, new MS treatment strategies will be developed. This approach is necessary in order to stop or at least delay the progression of neurological deficits in MS patients and to improve their life quality. In order to achieve this, different animal models of MS have been developed, which have already provided tremendous advances in our understanding and anticipation of disease mechanisms.

1.2 Experimental autoimmune encephalomyelitis

Experimental autoimmune encephalomyelitis (EAE) is the principal animal model used in MS research. It can be induced in different animal species (primates and rodents) which results in heterogeneous pathological mechanisms similar to those observed in MS - from non-demyelinating monophasic clinical disease to secondary progressive neurodegenerative disease (Baker & Amor, 2012). In most EAE variants, the main pathological feature is the presence of inflammatory, demyelinating lesions in the WM (Storch et al., 1998; Kornek et al., 2000). The induction of EAE can be achieved by three different mechanisms:

- spontaneous EAE
- adoptive transfer EAE
- actively induced EAE

Spontaneous EAE is not a naturally occurring phenomenon but it has been observed in some transgenic mice strains, such as transgenic mice expressing a T cell-specific myelin basic protein receptor (Goverman et al., 1993; Madsen et al., 1999; Krishnamoorthy et al., 2006).

Adoptive transfer EAE is induced by transferring auto-reactive T cells (Ben-Nun et al., 1981). These antigen-specific T cells are isolated from the lymph nodes of an animal that previously developed EAE and are subsequently injected into a naïve donor.

Actively induced EAE is initiated after immunization using purified myelin, CNS tissue homogenates, or, more commonly, different myelin proteins/peptides, like myelin basic protein (MBP) proteolipid protein (PLP) and myelin oligodendrocyte glycoprotein (MOG). Such active immunizations usually require the use of adjuvants to boost the immune response and in some cases additional injection of *Bordetella pertussis*-derived toxin is required in order to facilitate break-down of the BBB (Linthicum et al., 1982) and expansion of autoreactive T cells (Hofstetter et al., 2002).

1.2.1 MOG-induced EAE in Brown Norway rats

In most animal strains, EAE pathology is driven by T cells while the activation of the humoral immune system, commonly observed in MS, is missing (Krishnamoorthy and Wekerle, 2009). The Brown Norway (BN) rat strain was previously declared as resistant to the development of EAE following immunizations with guinea pig CNS homogenate and some myelin proteins (Gasser et al., 1973). However, it was later shown to be highly susceptible to EAE induction by immunisation with MOG. This resulted in an extensive antibody-mediated demyelinating pathology, occurring in both the spinal cord and optic nerve due to the high expression of MOG within these structures. This strong humoral immune component is attributed to the genetic background of BN rats which have different RT1 haplotypes to other rat strains, but are analogous to the MHC in humans (Stefferl *et al.*; 1999). The pathological profile in spinal cords of BN rats resemble that observed in MS (Kornek *et al.*, 2000). The incidence of autoimmune optic neuritis (AON) in this model is about 90% of all animals that develop neurological symptoms indicative of spinal cord pathology (Meyer et al., 2001; Fairless et al., 2012). It shares common features with those observed in human ON, including inflammatory demyelinating lesions (Meyer *et al.* 2001) accompanied by retinal atrophy (Hein et al., 2012), RGC loss and visual deterioration (Meyer et al., 2001). In this model, the loss of RGCs precedes classical optic nerve pathology (Hobom et al., 2004; Fairless et al., 2012) and BBB leakage (Boretius et al., 2008). This finding makes the BN-EAE model important in addressing the retinal neurodegenerative mechanisms that might mimic pathology detected in MS patients. This is especially true due to potential correlation with RGC degeneration observed in the non-ON eyes of MS patients – see chapter 1.3.4.

Recent work on this model included the investigation of the origins and downstream molecular pathways involved in AON pathology, therefore with focus on the mechanisms involved in mediating the earliest neurodegenerative events prior to onset of classical optic nerve lesion formation. AON can be separated into two phase: the induction AON (iAON) during which RGC loss, microglial

activation and disruption of BRB was observed; followed by the clinical AON (cAON) with inflammatory optic nerve lesions formation and demyelination. Some of the mechanisms that could be involved in early RGC loss might originate from the observed BRB disruption and activation of microglia and astrocytes within the retina as well as in the ONH (Fairless et al., 2012). Though at this time point optic nerves seem unchanged, ultrastructural modifications were detected in their still myelinated axons such as vacuolization of the peri-axonal space (Fairless et al., 2012) and disruption of axonal domains (Stojic, PhD thesis 2016). Dynamic intracellular connection between the two compartments, retina and optic nerve, is established through axonal transport that rely on cytoskeleton integrity. Axonal cytoskeleton and transport changes in BN AON require investigation in order to see whether neurodegenerative mechanisms similar to those observed in MS are occurring (see chapter 1.1.4 – Wallerian-like degeneration) and also whether this might serve as a link between observed retina/ONH disturbances and further upstream disruptions in the axonal cytoskeleton. Indeed in iAON, breakdown of the cytoskeletal component spectrin and de-phosphorylation of neurofilaments in the optic nerves have been previously reported (Hoffman et al., 2013; Stojic, PhD thesis 2016).

Further on, early RGC loss in iAON was shown to be apoptotic in nature (Fairless et al., 2012) and this loss was observed to correlate with increased Ca^{2+} tissue levels in both retina and optic nerves. Systemic application of calpeptin, a blocker of calpain – a Ca^{2+}-dependent protease, was shown to ameliorate disease severity and axonal loss during clinical inflammatory demyelination of optic nerves and also to protect RGCs during both induction and clinical phases of AON (Hoffmann et al., 2013). These findings opened the question of the role of Ca^{2+} increases in both RGC loss and axonal integrity. What initiates these observed Ca^{2+} increases; is this phenomenon happening simultaneously in both retina and optic nerves; or alternatively does the initial insult originate within one compartment with subsequent disturbances progressing in an anterograde or retrograde direction? In the case of retinal Ca^{2+} increase, glutamate excitotoxicity, one of the neurodegenerative mechanisms implicated in MS (see chapter 1.1.4 – glutamate excitotoxicity), may be involved. RGC loss might be initiated and accompanied via intracellular Ca^{2+} increase following overstimulation of RGC glutamate receptors. Further on, this Ca^{2+} increase could diffuse and initiate axonal degeneration. However, extracellular glutamate increase could also originate within RGC axons, following synaptic vesicles docking and glutamate vesicular release along the axons due to upstream axonal transport deficits in the ONH.

The relevance of EAE models and mechanisms involved in EAE pathology to the ones suggested for MS is confirmed by the current success of immunomodulatory MS therapies, like Natalizumab (Yednock et al., 1992; del Pilar Martin et al., 2008; Stüve et al., 2006) or FTY720 (Fujino et al., 2003; Kappos et al., 2010). However, immunomodulation has not been able to address the persistent

problem of ongoing neurodegeneration, and currently no neuroprotective therapies are available to MS patients. And thus, the quest to better understand neurodegenerative processes under an autoinflammatory environment continues to be as relevant as ever.

1.3 Axonal cytoskeleton and transport

1.3.1 Axonal cytoskeleton

Neuronal maintenance and physiological functioning depends on and is influenced by the state of its axonal cytoskeleton and transport infrastructure. Proteins which form the cytoskeleton exist as either free cytosolic monomers or are assembled into highly dynamical structures that form and support the axon. The three main constituents of the (axonal) cytoskeleton are (Figure 2):

- ***Neurofilaments (NFs)*** belong to the family of intermediate filaments and contribute to radial axonal growth (axonal diameter) and consequently axonal conductance (Yuan et al., 2012). NFs are composed of three polypeptides: light (NFL, 60 – 70 kDa; Fliegner & Liem, 1991), medium (NFM, 130 – 170 kDa) and heavy (NFH; 180 – 200 kDa) chains, defined by molecular weight, which form complexes with α-internexin (Yuan et al., 2006). Under normal physiological conditions in myelinated axons, NFs are phosphorylated on their side arms (Pant, 1995). They have been implicated in different neurodegenerative diseases, such as amyloid lateral sclerosis (ALS), where NF accumulation is the hallmark of disease pathology (Rudrabhatla, 2014). In MS, the presence of non-phosphorylated NFs in axons is considered to be a stress marker and is readily observed in demyelinated, swollen and transacted axons (Trapp et al., 1998).
- ***Microtubules*** are seen as long-term railways for the transport of organelles and vesicles. Microtubule filaments are dynamic, ATP-dependent heterodimers composed of α and β-monomer tubulin subunits (both ~ 50 kDa; Fletcher & Mullins, 2010). There are different proteins involved in microtubule stabilization. Tau is one of them, and has been implicated in neurodegenerative diseases, where its hyper-phosphorylation and accumulation is considered the cause of neurodegenerative processes in Parkinson's (PD) and Alzheimer's (AD) disease (Rudrabhatla, 2014). In MS, though not considered to be the primary cause of neurodegeneration, tau accumulation has also been observed (Anderson et al., 2008).
- ***The Actin network*** consists of filamentous actin (F-actin) built from ATP-dependent binding of globular monomeric, 42 kDa protein (G-actin; Fletcher & Mullins, 2010). A third structure has been recently described – ring-like structures of actin and spectrin spaced at intervals of ~180 nm, known as actin rings. They have been detected in the axonal initial segment, dendrites and at the Nodes of Ranvier (Xu et al., 2013; Lukinavičius et al., 2014; D'Este et al.,

2015). Actin has been implicated in diseases like PD and Down's syndrome (Bernstein et al., 2011). In MS patients, levels of blood gelsolin, one of a family of actin-severing proteins, was found to be decreased (Kułakowska et al., 2010), and the presence of actin in CSF is found to correlate with disease neurological severity (Semra et al., 2002).

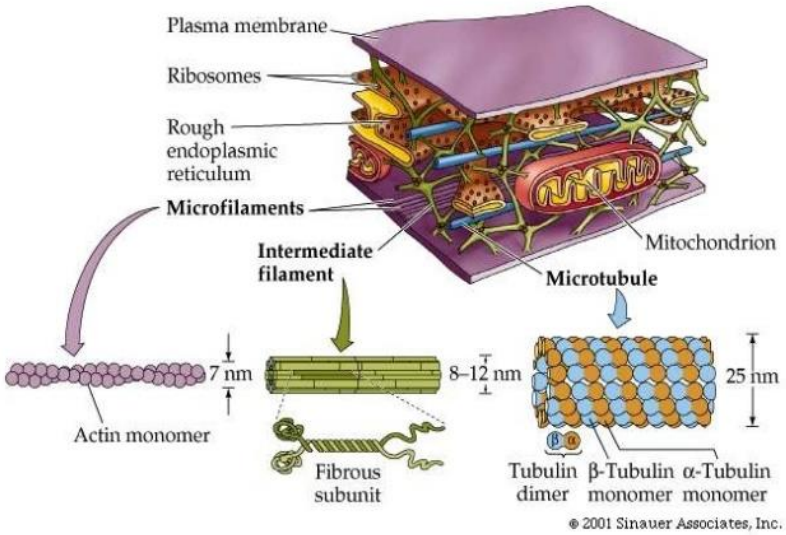

Figure1.3.1. Cell cytoskeleton. (copyright ©Sinauer Associates Inc. 2001)

1.3.2 Axonal transport

Axonal transport is one of the ways a neuronal cell body communicates with its dendrites, axons and their synapses. The axonal transport machinery involves "transport rails" consisting mainly of microtubule filaments, the ATP-dependent motor proteins kinesin and dynein as "transport engines", and transported proteins and organelles as "transport cargo". Briefly, axonal transport is divided based on the average rate of movement into a fast component (FC, 50 - 400 mm/day) and two subtypes of slow component (SCa 0.2 - 3 mm/day; SCb 2 - 10 mm/day) (Black, 2016). FC is associated with microtubule ATP-dependent kinesin/dynein transport of membranous organelles, like mitochondria and synaptic vesicles. SC involves the transport of proteins that make up the cytoskeleton and cytosol of the axons (Dahlström et al., 1992; Brown, 2009). Axonal transport depends simultaneously on cell body viability to synthesise proteins that are then transported further on, their attachment to kinesin/dynein, mitochondrial respiration for ATP needs and finally cytoskeletal stability.

Some neurodegenerative diseases as a main pathological hallmark have lesions with misfolding, fibrillization and aggregation of disease-specific proteins that affect axonal transport. In the ALS animal model, it has been shown that an anomaly in the SOD1 gene leads to axonal transport deficits

through damage to both the mitochondria (De Vos et al., 2007) and the cargo through the promotion of cargo disassembly from transport motors (Jung et al. 2005,Wagner et al. 2004). In AD, β-Amyloid (Aβ) peptides that result from amyloid precursor protein (APP) cleavage, accumulate along the axons where they damage transport through affecting different cargoes and mitochondria (Hiruma et al. 2003, Rui et al. 2006). The microtubule-binding protein tau has been also found to interfere with kinesin-microtubule binding (Seitz et al. 2002). In MS, axonal swelling, blebbing and transection are detected, with accumulation of β-Amyloid precursor protein (βAPP) and SMI32 markers (Ferguson et al., 1997; Trapp et al., 1998). In addition, a decrease in the transport motor protein kinesin was detected within, and in the vicinity of, demyelinating lesions (Hares et al., 2016).

1.3.3 Cytoskeleton and transport deficits in EAE

Axonal damage in EAE has been shown to be of heterogeneous origins. In general, axonal transection following inflammatory demyelination is considered to be the main cause of axonal degeneration (Trapp & Nave, 2008). Demyelinated axons are perceived as more vulnerable since they are exposed to potentially disruptive agents coming from the inflammatory cells and damaged oligodendrocytes. This can lead to mitochondrial damage and axonal transport deficits, and induction of spheroid formation leading to axonal transection. Some of these pathological events have been observed in the EAE model. In the adoptive transfer EAE model with autoreactive MBP-primed T cells, it was shown that T cells are the main mediators of axonal damage (Shriver et al., 2006). In another study, it was shown that microglial activity following breakdown of the BBB and fibrinogen leakage was the main driver of axonal damage (Davalos et al., 2012). The increased presence of ROS/ reactive nitrogen species (RNS) has been found to interfere with mitochondrial transport along axons within inflammatory lesions. However, axonal transport deficits have also been found to precede demyelination and axonal degeneration (spheroid formation and transection). This implies that inflammatory damage might be more widespread than previously though and could affect the transport machinery prior to demyelination. More importantly, axonal transports deficits were reversible in morphologically normal-appearing axons which are of great importance in developing potential therapeutic strategies (Nikic et al., 2010; Sorbara et al., 2014). In the AON model, following inflammatory demyelination, accumulation of voltage-gated Ca^{2+} channels was observed along axonal tracts. Additionally, application of a channel blocker increased the survival of healthy axons, having higher efficiency if applied during the iAON, prior to clinical optic nerve pathology. It was subsequently suggested that premature docking of channel-bearing vesicles along the axon might be an early sign of axonal transport deficits (Gadjanski et al., 2009).

1.4 RGC death in experimental models

Understanding neurodegenerative pathways in complex animal models like EAE-AON where various inflammatory and neurodegenerative mechanisms happen in parallel, influencing each other in both suppression and promotion, might not be possible without comparison with more controlled neurodegenerative models, like optic nerve transection and intravitreal injection (IVI) of glutamate-receptor agonists.

1.4.1 Optic nerve injury

The most widely-used model to investigate molecular pathways involved in axonal degeneration and transport deficits and their influence on neuronal viability is optic nerve transection. Activation of apoptotic cell death pathways are observed in RGCs following nerve transection. The main reason for retrograde RGC cell death is connected with the loss of retrograde-trophic support coming from the brain. Indeed, phosphorylation of Akt via phosphoinositide 3-kinase (PI3K), an anti-apoptotic pathway dependent on trophic receptor stimulation, was shown to be reduced in RGCs after *in vivo* axotomy (Kermer et al., 1999). Also, caspase activity and DNA fragmentation were observed (Kermer et al., 1999). Bax family proteins (Bcl-2 and Bax), which play an important role in regulation of apoptosis, were found to be upregulated in retina following optic nerve crush (Isenmann & Bähr, 1997).

In models of nerve injury, the axonal compartment also goes through dynamic changes. In an *in vitro* model of axonal transection, the distal part of the axon goes through a process known as Wallerian degeneration (see chapter 1.1.4). Following transection, the initial phase is characterized by the formation of axonal spheroids - this morphological change is accompanied by high Na^+ and Ca^{2+} influx through different ion channels (George et al., 1995), massive cytoskeleton reorganization through calpain-mediated mechanisms and lysosomal activity (Billger et al. 1988; Johnson et al. 1991; Kerschensteiner et al., 2005; Knöferle et al., 2010). The whole process is referred to as axonal apoptosis, since it is highly organized and controlled in nature (Wang et al., 2012).

1.4.2 Glutamate excitotoxicity in the retina

Following pre-synaptic glutamate release, activation of ionotropic (N-methyl-D-aspartate, NMDA; α-amino-3-hydroxyl-5-methyl-isoxazol-4-propionic acid, AMPA and kainate) and metabotropic (mGlu) glutamate receptors leads to intracellular increases in Na^+ and Ca^{2+} ions which leads to the depolarization of the post-synaptic neuron (Hare et al., 2011). However, upon overstimulation of glutamate receptors, toxicity can also be induced, termed glutamate excitotoxicity, due to the

elevation of Na^+ and Ca^{2+} to toxic levels capable of activating downstream pathways leading to cell death (Olney, 1969; Obrenovitch et al., 2000). Glutamate excitotoxicity first emerged as a as concept following studies on neonatal mice where subcutaneous injection of glutamate led to neuronal loss, preferentially in the inner retina and hippocampus (Lucas & Newhouse, 1975; Olney et al., 1969). In general, almost all glutamate receptor subtypes are confirmed to be involved in mediating excitotoxicity, but ionotropic receptors are recognized as the key players in this process (Choi, 1988; Tymianski, 1996).

In the retina, glutamate excitotoxicity can be induced following IVI of toxic levels of glutamate receptor agonists (NMDA, AMPA and glutamate; Siliprandi et al., 1992; Pellegrini & Lipton, 1993; Pang et al., 1999; Luo et al., 2001; Chidlow et al., 2008). RGCs are especially vulnerable since it is known that these cells have a high density of glutamate channels on their dendrites (Aizenman et al., 1988; Massey & Miller, 1990; Diamond & Copenhagen, 1993). Besides RGC apoptosis, changes in their axonal compartments were also observed following IVI of NMDA (Saggu et al., 2010; Kuribayashi et al., 2010).

1.4.3 RGC loss in AON

In the model of AON, the initial insults and downstream pathways of RGC degeneration are currently not clear. In AON, evidence for both primary and secondary RGC death has been observed. Secondary RGC death refers to retrograde cell body loss following axonal injury – such as that which occurs following axotomy – and is observed during cAON, where it is connected with inflammatory demyelination in the optic nerve. During this disease stage, both axonal loss and accompanying Ca^{2+} increases of the optic nerve, and more specifically the axons, could be detected (Gadjanski et al., 2009; Hoffmann et al., 2013). In addition to the reduction in surviving RGCs at this stage of the disease, evidence of neurodegenerative pathways being activated in RGCs include positivity for Bax and capase-3 (Hobom et al., 2004), and also DNA degradation as detected by TUNEL (terminal deoxynucleotidyl transferase dUTP nick end labelling) (Fairless et al., 2012).

In AON, a case for primary RGC death has been made for that occurring during iAON, since during this period inflammatory demyelination and axonal injury in the optic nerve are not observed to occur, and thus no clear mechanism of secondary degeneration is apparent. Additionally, despite no pathological changes being seen in the optic nerve, retinal disturbances such as increased permeability of the BRB and activation of resident microglia could be seen which may directly affect the integrity of the RGC soma. Although RGC degeneration is much less in iAON than that seen during the later cAON, similar apoptotic signalling could be seen (Hobom et al., 2004; Fairless et al., 2012). Glutamate excitotoxicity might be implicated in primary RGC loss during iAON. Treatment with minocycline, an anti-inflammatory and neuroprotective antibiotic, was shown to reduce glutamate

levels in the retina already in iAON correlating with protection of RGCs against degeneration (Maier et al., 2007). In addition, systemic application of memantine and MK801 (NMDA-receptor blockers) were shown to be neuroprotective when applied during both iAON and cAON (Sühs et al., 2014). In addition, elevated Ca^{2+} levels in both retina and optic nerves were observed during AON implying the role of Ca^{2+} in early RGC loss (Hoffmann et al., 2013).

1.5 The role of Ca^{2+} in neurodegeneration

Ca^{2+} is the main intracellular secondary messenger of all eukaryotic cells including neurons. It regulates some of the most important cellular physiological functions: membrane excitability (Krnjevic et al., 1989; Schwartzkroin & Stafstrom, 1980), cytoskeletal integrity (Schlaepfer & Zimmerman, 1985; Trifaro & Vitale, 1993), exocytosis and synaptic activity (Robitaille et al, 1993; Llinas et al., 1992; Smith & Augustine, 1988) and gene expression through nuclear signalling (Bading, 2013). To maintain intracellular Ca^{2+} homeostasis, neurons must be able to control the influx of extracellular Ca^{2+} which is about 100,000 times higher than intracellular cytosolic Ca^{2+}. Because of this high Ca^{2+} gradient and the need for homeostasis, neurons have very sophisticated machinery to regulate Ca^{2+}, including control of its: influx (ion channels), buffering (Ca^{2+}-binding proteins, endoplasmic reticulum and mitochondria), intracellular diffusion, internal storage (endoplasmic reticulum and mitochondria) and its efflux (ionic pumps) (Tymianski & Tator, 1996).
In addition to the role of glutamate receptors as described above, Ca^{2+}influx is also connected with voltage-gated Ca^{2+} channels (VGCC), while its efflux is mostly regulated by plasma membrane Ca^{2+} ATPases (PMCA) and the Na^{+}-Ca^{2+} exchangers (NCX).

- **VGCC** classification is based on their physiological properties and sensitivity to known toxins: high voltage-activated, Cav1.1-4 channels, Cav2.2 (N-type) and Cav2.1 (P/Q-type); intermediate voltage-activated, Cav3.1-2 and Cav3.3 (T-type) and low voltage-activated, Cav2.3 channel (R-type; Catterall et al., 2005). In RGCs, all types of VGCCs were detected (Karschin & Lipton, 1989; Taschenberger & Grantyn, 1995). Following various insults, blockade of different VGCC types have been shown to be neuroprotective, through decrease of Ca^{2+} influx. In EAE, VGCCs were observed to be expressed on axons within inflammatory demyelinated lesions (Kornek et al., 2001). Bepridil-treated animals (a non-specific VGCC blocker) ameliorated EAE disease severity through reduced inflammation and axonal pathology (Brand-Schieber et al., 2004). Specifically, the N-type blocker ω-conotoxin was shown to reduce EAE disease severity and protect axons in both the optic nerves and the spinal cord. In optic nerves, this blocker significantly decreased the signal intensity of Mn^{2+}-

enhanced MRI, indicating a reduction in Ca^{2+} in optic nerve tissue. The same blocker significantly decreased intra-axonal Ca^{2+}, detected *in vivo* using a Ca^{2+} sensitive dye (Gadjanski et al., 2009). In the optic nerve crush model, application of the L-/N-type channel blocker amlodipine and a T-type channel blocker ameliorated intra-axonal Ca^{2+} elevation (Knöferle et al., 2010). Application of the PhTx3-4 spider toxin, targeting both N- and P/Q-types, was neuroprotective in the retina following IVI of NMDA, and was particularly effective in decreasing RGC loss (Binda et al., 2016). On isolated RGCs, application of VGCC blockers decreased initial Ca^{2+} influx, following glutamate receptor stimulation (Hartwick et al., 2008).

- **PMCA** is a transport protein existing as four isoforms, PMCA1-4, derived from different genes and modified further by alternative splicing (Carafoli, 1997). PMCA is considered to be a channel with high Ca^{2+} sensitivity but a low capacity for Ca^{2+} extrusion (Brini & Carafoli, 2011). Thus, it appears to operate well during physiological conditions where intracellular calcium levels are low. In hippocampal neurons following glutamate-induced apoptosis, PMCA was shown to be cleaved by caspases leading to further Ca^{2+} increases and a subsequent switch from apoptotic to necrotic cell death (Schwab et al., 2002). Different levels of PMCA types were found expressed on retinal cells, with dominant PMCA2 and PMCA3 expression on RGCs (Krizaj et al, 2002). In EAE spinal cords, decreased levels of PMCA2 mRNA were implied to contribute to neuronal loss (Nicot et al., 2003).
- **NCX** plasma membrane family includes three types NCX1-3, denoting three different genes that encode them (Annunziato, 2013). NCX is considered to be a channel of low Ca^{2+} sensitivity but high capacity for Ca^{2+} extrusion (Brini & Carafoli, 2011). Thus, it requires high Ca^{2+} levels for activation, but then functions very efficiently – suggesting that, unlike the PMCA, this pump may function best during pathophysiological conditions. NCX functioning is dependent on the net electrochemical gradient across the plasma membrane and can operate in two modes, Ca^{2+} entry (forward) or Ca^{2+} exit (reverse) mode. "The Ca^{2+} entry mode of exchange is usually identified as an internal Na^{+}-dependent Ca^{2+} influx and an external Ca^{2+}-dependent, ouabain-insensitive Na^{+} efflux. The Ca^{2+} exit mode of exchange is defined operationally as an external Na^{+}-dependent Ca^{2+} efflux and an internal Ca^{2+}-dependent ouabain and tetrodotoxin - insensitive Na^{+} influx" (Blaustein & Lederer, 1999). The discovery of NCX was preceded by experiments in which Na^{+} and Ca^{2+} competition across the plasma membrane could not be explained without the existence of a new channel with the aforementioned physiological properties. In the 1960s, the existence of such a channel was proposed in different tissues such as cardiac muscle (Glitsch et al., 1970) and invertebrate neurons (Baker et al., 1969). Due to its co-dependence on intra- and extra-cellular Ca^{2+} and

Na^+, NCX was seen as a double-edged sword when it comes to neuronal protection. In normal physiological conditions, synaptic activity or axonal depolarization, it is assumed to work in its forward mode, extruding Ca^{2+} together with the PMCA from the neuronal cytosol. However, in neuronal cultures following glutamate stimulation, NCX reverse mode of action was observed (Hoyt et al., 1998; Bano et al., 2005; Araujo et al., 2007; Brittain et al., 2012). In cerebral ischemia (Formisano et al., 2013) or following IVI of NMDA (Inokuchi et al., 2009), NCX was observed to contribute to neuronal loss. In EAE, NCX Ca^{2+}-driven influx was connected with NaV channel co-expression along damaged axons (Craner et al., 2004b). When it comes to NCX blockers, there are two blockers commonly used capable of predominantly targeting its reverse operation: KB-R7943, which has the limitation that it does not distinguish between different NCX types, and also has been shown to affect mitochondrial function (Brustovetsky et al., 2011); SEA0400, however, is assumed to affect predominantly the NCX1 type (Matsuda et al., 2001), with fewer off-target effects. Systemic application of SEA0400 leads to RGC protection following IVI of NMDA and ischemia-reperfusion (Inokuchi et al., 2009).

1.5.1 The role of Ca^{2+} in apoptosis

Deregulation of intracellular Ca^{2+} homeostasis shapes the response of cellular effectors, such as endoplasmic reticulum (ER) and mitochondria, which can lead to activation of both pro- and anti-apoptotic pathways (Pinton et al., 2008).

Ca^{2+}-mediated ER stress, which results in protein misfolding and consequently apoptotic cell death, can be initiated by both Ca^{2+} depletion and overload of ER Ca^{2+} pools. This may happen following changes in the Ca^{2+} transport systems (sarco-ER Ca^{2+} ATPase and Ins(1,4,5)P3 receptors). Prolonged ER stress eventually leads to the enhancement of caspase-12 activity, present on the ER membrane, which is cleaved (activated) by m-calpains. Once activated, caspase-12 acts on effector caspases to induce apoptosis (Nakagawa et al., 2000). ER proteins are also reported to interact with the Bcl-2 family of proteins which are the key regulators of apoptotic cell death (Baffy et al., 1993).

The relationship between Ca^{2+} deregulation and mitochondria in the process of apoptosis can be two-sided. Mitochondria are capable of sequestering high amounts of intracellular Ca^{2+} under (patho)physiological conditions in spite of the low affinity of their transporters. The close proximity of mitochondria to ER and plasma membrane enables activation of their transporters following high micro-domain Ca^{2+} increases (Pinton et al., 1998; Thor et al., 1984). That is why mitochondria were mostly seen as an anti-apoptotic factor in Ca^{2+} mediated apoptosis. The main role of mitochondria in the process of apoptosis is connected to the permeabilization of the outer mitochondrial membrane, release of cytochrome c and further activation of effector caspases. In this process, Ca^{2+} increase

does not play a direct role (Carafoli, 2002). However, in pro-apoptotic settings, mitochondrial Ca^{2+} increases via Ins(1,4,5)P3 receptors promotes the opening of the transition permeability pore (PTP) and further induces the release of cytochrome c (Szalai et al., 1999; Crompton, 1999).

Finally, many Ca^{2+}-activated cytosolic factors are involved in the process of apoptosis: calcineurin, nitric oxide synthase, endonucleases, phospholipases and proteases (Orrenius et al., 20003). Ca^{2+} influx through ion-specific channels or following Na^{+} influx and subsequent reverse function of NCX (Baruskova et al., 2012; Staal et al., 2010) can activate calpains (Ma et al., 2013; Yang et al., 2013). Cellular substrates of calpain include many cytoskeleton proteins such as ankyrin, spectrin, NFs, ion channels and some caspases involved in apoptotic cell death (Goll et al., 2003).

1.5.2 Apoptotic and Ca^{2+} dependent modulation of actin cytoskeleton

Under normal physiological conditions, the actin network is in a dynamic balance between assembly and disassembly. There are several mechanisms involved in regulating this balance: tread-milling, severing and whole filament destabilization (Brieher et al., 2013). However, in the case of cell injury these mechanisms can become over-pronounced resulting in irreversible actin network disassembly.

Mounting evidence indicates that actin is at the same time both a sensor and a mediator of apoptosis (Desouza et al., 2012; Franklin-Tong & Gourlay, 2008). The extent of actin and microtubule cytoskeleton damage was shown to be a good predictor of the activated cell death pathways: apoptosis or necrosis (Adamec et al., 2001). In human neutrophil cultures, following induction of apoptosis, actin monomer cleavage was observed following Ca^{2+} increase and calpain activation (Brown et al., 1997). During apoptosis, activated caspases were also found to induce G-actin cleavage. Caspase-cleaved products of G-actin include N-terminal actin, 32 kDa (fractin) and 15 kDa (tActin) fragments (Sokolowski et al., 2014; Utsumi et al., 2003). In oligodendroglial progenitor cells, fractin was found to be not only a morphological apoptotic marker but also to have a functional role in apoptotic signalling (Schulz et al., 2009).

Actin network stability was shown to be affected through F-actin disassembly following intracellular Ca^{2+} increase (Neely and Gesemann, 1994; Furukawa et al., 1995) and NMDA receptors stimulation (Halpain et al., 1998). At the same time, F-actin stability affects, via a feed-forward loop, Ca^{2+}-permeable channels. In addition, F-actin inhibited the function of isolated PMCA from human erythrocytes, whilst G-actin and/or short oligomers caused its activation (Vanagas et al., 2013). Cardiac NCX1 attachment to the plasma membrane is also directed via F-actin, and channel reverse mode of action was observed to be dependent on the actin network polymerization state (Condrescu & Reeves, 2006). F-actin depolymerisation was found to reduce Ca^{2+} influx following NMDA receptor stimulation (Rosenmund & Westbrook, 1993). This implies that the actin cytoskeleton is, besides

mediating channel docking and support, also an active regulator of Ca^{2+} dynamics through modulating channel permeability properties.

Following Ca^{2+} increases, F-actin disassembly can be mediated, amongst other pathways, via the Ca^{2+}-dependent actin-severing protein, gelsolin. Gelsolin was found to be a Ca^{2+}-induced anti-apoptotic factor (Harms et al., 2004). In genetically manipulated mice that lacked gelsolin, following excitotoxic NMDA receptor stimulation, increased Ca^{2+} influx was reported (Furukawa et al., 1997). Having this in mind, gelsolin might be seen as a protective factor during apoptotic Ca^{2+} increases. However, gelsolin itself is targeted and cleaved by caspases, and the resultant cleaved product, N-terminal gelsolin, was observed to correlate with morphological changes associated with apoptosis (Kothakota et al., 1997).

In the case of iAON, early calpain activation was shown to correlate with increased Ca^{2+} levels in the retina as indicated by Mn^{2+}-enhanced MRI, followed by subsequent calpain and calcium changes in the optic nerves (Hoffmann et al., 2013). This opens many questions concerning “primary” neurodegenerative events in axonal loss during AON. A current hypothesis could be that a primary retinal insult resulting in retinal Ca^{2+} increases with subsequent calpain activation and degradation of components of the actin cytoskeleton (as indicated by spectrin degradation - Hoffmann, et al., 2013), in turn may spread anterogradely to the optic nerves through a dysregulation of actin-controlled mechanisms, further contributing to axonal damage.

1.6 Summary

In summary, ON in MS patients and AON in BN rats share several features in common, including RGC degeneration. To date, these degenerative processes and their causes are not fully clear but there are evidences that an initial insult might originate within the retina (or the optic nerve head). This primary insult could come from BRB disruption and retinal signals that could activate pro-inflammatory microglial phenotype and disturb astrocyte-synapse function. This primary retinal injury would be independent from later retinal retrograde damage coming from injured axons following inflammatory lesions formation in the optic nerve. The early retinal pathology in MS is supported by the observation of retinal RNFL thinning in the eyes of MS patients lacking any clear optic nerve pathology (Saidha et al., 2011; Walter et al., 2013). In AON, a role for Ca^{2+} in these initial changes has been highlighted through both MRI and Ca^{2+} imaging experiments (Gadjanski et al., 2009; Hoffmann et al., 2013). In addition, the role of the Ca^{2+}-activated protease, calpain, whose activity correlates with the timing of Ca^{2+} elevation, has been demonstrated by pharmacological inhibition (Hoffmann et al., 2013). Calpain is known to target structural components involved in axonal transport and the maintenance of cytoskeletal integrity, and disturbances in these

compartments have been suggested based on the visualization of βAPP accumulation in damaged axons, disturbed axonal ultrastructure as seen by electron microscopy, and breakdown of the actin-anchoring protein, spectrin. It remains to be determined whether a primary retinal insult can account for the observable pathology, particularly with respect to the optic nerve, and which Ca^{2+}-activated cascade are involved in the mediation of RGC degeneration. Understanding of these early processes in AON may allow for neuroprotective strategies to be developed with translational potential to reduce the burden on MS patients caused by on-going neurodegeneration which can continue even during immunomodulatory handling.

2 The aim of the study

Neurodegeneration in MS correlates with neurological disability in MS patients. Some features of pathological mechanisms behind immune-mediated neuronal loss can be predicted based on MRI and tissue autopsy. However precise mechanisms cannot be answered without the use of animal models and *in vitro* studies. AON was shown to be a suitable model for investigating neurodegenerative processes assumed to be involved in MS ON. Adaptive, humoral and innate arms of the immune system are activated in this model. Prior to inflammatory demyelinating lesions in the optic nerve, retinal deterioration with early RGC loss has also been observed (Hobom et al., 2004; Fairless et al., 2012).

The aim of this study is to address questions regarding early RGC loss and axonal damage. In AON, axonal loss was detected following BBB disruption and infiltration of inflammatory cells in the optic nerve parenchyma accompanied by demyelination. This primary axonal injury can retrogradely induce secondary RGC death which could explain retinal pathology following inflammation of the optic nerve. However, early RGC loss and ultrastructural axonal changes were observed prior to optic nerve pathology and these might initiate axonal injury prior to inflammatory driven demyelination (Fairless et al., 2012). These early changes are timed with increases in retinal Ca^{2+} and activation of the Ca^{2+}-activated protease, calpain (Hoffmann et al., 2013). Since calpain is known to target structural components involved in axonal transport and the maintenance of cytoskeletal integrity, we wish to determine whether such changes occur and how they might fit into the Ca^{2+}-activated cascades potentially involved in RGC degeneration. To address this, the following questions will be investigated:

1) are axonal transport deficits detectable during AON in optic nerves?
2) is the mechanism of glutamate excitotoxicity involved in early RGC loss and cytoskeleton changes?
3) is there a change in the expression of channels involved in Ca^{2+} homeostasis?

3 Methods

3.1 Animals

Female BN rats (8 - 10 weeks old; 140 – 160 g) were used in all EAE experiments. Sprague Dawley (SD) rat pups at postnatal day seven or eight (P7 - 8) were used for *in vitro* experiments for primary RGC cultures. All animals were purchased from Charles River (Sulzfeld, Germany) and kept under environmentally controlled pathogen-free conditions with free access to food and water. Animal experiments were performed according to the relevant laws and institutional guidelines of Baden-Württemburg.

3.2 MOG-EAE induction and animal scoring

BN rats were immunised with whole recombinant rat MOG (a kind gift of Prof Christine Stadelmann, Dept. of Neuropathology, University of Göttingen; Fairless et al., 2012). Immunization emulsion contained 1:1 ratio of 100 µg MOG in phosphate-buffered saline (PBS, Sigma-Aldrich, St. Louis, Missouri, USA) and complete Freund's adjuvant (Sigma-Aldrich) containing 200 µg of heat-inactivated *Mycobacterium tuberculosis* H37RA (Difco Microbiology, Lawrence, Kansas, USA). Rats were anaesthetized with 5% isoflurane inhalation and injected intradermally at the tail with 200 µl of immunization emulsion. Rats were observed daily for clinical signs of EAE. The grading system used to score neurological symptoms is presented in Table 3.2.

Immunized animals were kept until the desired time point in the induction (iAON) or clinical (cAON) stage of the disease course. Animals with signs of severe ataxia or having a score of 3.5 or greater were sacrificed.

score	clinical symptoms
0.5	*distal tail paresis*
1	*complete tail paralysis*
1.5	*complete tail paresis and mild hind leg paresis*
2	*unilateral severe hind leg paresis*
2.5	*bilateral severe hind limb paresis*
3	*complete bilateral hind limb paralysis*
3.5	*complete bilateral hind limb paralysis and paresis of one front limb*
4	*complete paralysis (tetraplegia), moribund state, or death*

Table 3.2 Grading scale of neurological symptoms in BN MOG-EAE.

3.3 Retina excitotoxicity model – IVI of glutamate

In order to induce a primary retinal insult, healthy BN rats received IVI of glutamate. During injections, animals were kept under anaesthesia by inhalation of 5% isoflurane. In total 100 nmoles of glutamate (4 µl of 25 mM glutamate (Sigma-Aldrich) in saline) was injected intravitreally using a patch pipette attached via a plastic tube filled with saline to a 10 µl Hamilton syringe over the course of 5 minutes. 24 hours following IVI of glutamate, animals were sacrificed by ketamine/xylazine overdose. Retina and optic nerves were further processed dependent on experimental design.

3.4 IVI of cholera toxin subunit B-Alexa Fluor 488 conjugate

In order to investigate axonal transport deficits during the course of AON, an IVI of 4 µl of 0.1% Cholera Toxin subunit B conjugated to Alexa Fluor 488 (CTB – A488; Molecular Probes, Thermo Fisher Scientific Inc., Waltham, Massachusetts, USA) in sterile PBS was performed. 24 hours following the injection, animals were sacrificed by ketamine/xylazine overdose, perfused, and retinas with attached optic nerves were dissected and processed for longitudinal sections.

3.5 Isolation and culture of primary RGC

To investigate the physiology of RGCs independent of other retinal cells, a modified primary RGC isolation procedure was established. Our approach consisted of combining two previously reported techniques: MACS RGC isolation kit (MACS Miltenyi Biotec GmbH, Bergisch Gladbach, Germany) and panning protocol (Barres at al., 1989). The first part of the protocol - removal of negative cells with MACS RGC isolation kit gave a very low yield of RGCs and was replaced with a negative panning protocol as described in Barres et al. The second part of the protocol, positive selection for RGCs was performed with a MACS RGC isolation kit according to their instructions. For each preparation, five to seven SD pups P7-8 were decapitated, eyes were removed and retinae dissected followed by brief storage in room temperature (RT) Earle's balanced salt solution with Ca^{2+} and Mg^{2+} (EBSS; Gibco, Carlsbad, California, USA). The protocol is summarized below:

1) Retina digestion and panning preparation

For tissue digestion, EBSS was removed and **papain mix** was added to collected retinas for 10-15 minutes at 37°C. Following digestion, the tube was centrifuged for 1-2 minutes at 1000g, the papain mix was completely removed and cells were re-suspended in 4 ml **LoOvo mix**. After 2 minutes centrifugation at 1000g, **LoOvo mix** was removed and cells re-suspended in a further 6 ml of **LoOvo mix** with added anti-rat macrophage antibody (1:75, Wak – chemie Medical GmbH, Germany) and incubated for 10 minutes at RT. Following centrifugation for 5 minutes (1000g; RT), cells were re-suspended in 10 ml **panning buffer** for the negative panning selection procedure.

- **Papain mix** consisted of 10 ml pre-heated Dulbecco's phosphate-buffered saline (DPBS, Sigma-Aldrich) rewarmed to 37°C with 165 Units of papain (Cellsystems GmbH, Troisdorf, Germany). Following heating to ease mixing, 2 µg L-cysteine (Sigma-Aldrich) was added to activate papain. Afterwards, the papain mix was filtered through 0.45 µm filters (Merck

Millipore, Billerica, Massachusetts, United States) and 100 µl DNase (10000 U/ml in EBSS; Sigma-Aldrich) was added.

- **LoOvo mixture** consisted of 10% LoOvo stock in DPBS. LoOvo stock consisted of 1.5% bovine serum albumin BSA (Sigma-Alrich) with 1.5% ovomucoid (a trypsin inhibitor; Roche Holding AG, Basel, Switzerland) adjusted to pH 7.4.
- **Panning buffer** consisted of 0.04% BSA in DPBS with 1% insulin (from bovine pancreas, 0.5 mg/ml; Sigma-Aldrich).

2) Negative selection with panning protocol

Preparation of panning plates: Two Petri dishes (150 mm diameter; Corning Falcon, Tewksbury, USA) were incubated overnight, each with 20 ml 50 mM Tris – HCl (Sigma-Aldrich), pH 9.5, containing anti-rabbit IgG (H+L) antibody (1:400, Dianova GmbH, Hamburg, Germany). The next day, before tissue collection, antibody was removed and 20 ml of 0.2% BSA in DPBS was added to each of the panning plates and left at RT.

Following tissue preparation, 0.2% BSA was removed from both panning plates. Cells in 10 ml of panning buffer were filtered through a 30 µm cell strainer (Miltenyi Biotec GmbH), followed by incubation on the first panning plate for 30 minutes at RT, with gentle shaking of the plate every 10 minutes. Following incubation, after which most of the unwanted microglia/macrophage cells were attached to the bottom of the dish, the cell suspension was filtered again through a 30 µm cell strainer and poured on the second subtraction plate for another 20 minutes at RT. Following this step, the cell suspension was again collected from the subtraction plate and filtered for the last time through a 30 µm cell strainer and centrifuged for 10 minutes (1000g; RT).

3) Positive selection of RGCs with MACS RGC isolation kit

Shortly, following centrifugation, cells were incubated with CD90.1 antibody attached to magnetic MACS beads in 5% DPBS. Positive selection was done following manufacturer's instructions (Rat retinal ganglion cell isolation kit; Miltenyi Biotec GmbH).

Following centrifugation for 5 minutes at 1000 g, supernatant was discarded and the pellet containing RGCs was re-suspended in **RGC medium (RGM)**. Cell number was determined using a haemocytometer, before seeding cells on PLL-coated glass coverslips (VWR, Radnor, Pennsylvania, USA). Cells were seeded on ø 13 mm in 24 well plates or ø 25 mm in 35 mm dishes, depending on experiment design, and maintained in RGM.

- **Sato's medium** consisted of Neurobasal medium (Gibco) supplemented with 0.2% holo-Transferrin human (Sigma-Aldrich), 0.2% BSA (Sigma-Aldrich), 0.025% progesterone (2.48

mg/ml (ethanol); Sigma-Aldrich), 0.016% putrescine, 1% sodium-selenite (0.4 mg/ml (Neurobasal medium); Sigma-Aldrich).

- **RGM** consisted of Neurobasal medium (Gibco) supplemented with 1% Sato's medium, 1% insulin (form bovine pancreas, 0.5 mg/ml; Sigma), 1% Na-pyruvate (100 mM; Sigma), 2% L-glutamine (2 mM; Sigma-Aldrich), 1% Pen-Strep (10,000 U/mL; Gibco), 1% triiodothyronine (T3, 15nM; Sigma-Aldrich), 0.1% N-acetyl-L-cysteine (3 mg/ml; Sigma, USA), 2% B27 (B27 Supplement x 50; Gibco), 0.1% ciliary neurotrophic factor (CNTF, 10 µg/ml; PeproTech Inc., USA), 0.1% brain derived neurotrophic factor (BDNF, 50 µg/ml; Tebu-bio GmbH, Germany), 0.1% forskolin (10 mM; Sigma). In some experiments, 1:1 media mix of Neurobasal and Dulbecco's modified Eagle's medium (DMEM; GIbco) was used to obtain 290-300 mOsm osmolarity. If Neurobasal medium alone was used, sucrose was added to obtain the desired osmolality. RGCs were kept for two to four days *in vitro* (DIV 2 - 4) before they were used in different experiments. To check the viability of RGCs under *in vitro* conditions, some cultures were kept for up to three weeks. In some experiments, acutely isolated RGCs were needed. In this case, RGCs were processed immediately after the isolation.

RGCs were also isolated from adult BN rats with different disease duration. In this case, the isolation method was the same as for pups RGC isolation, except for the following changes: all reagents were scaled down since only 2 animals were used per preparation; negative panning selection was done in smaller Petri dishes (100 mm diameter; Corning Falcon); and the amount of CD90.1 antibody used for positive selection was decreased appropriately (1:2, compared to the original protocol). In these experiments, RGCs were used acutely, in order to not lose their disease phenotype and because RGCs isolated from adult animals do not recover under *in vitro* conditions as well as RGCs isolated from P7-8 pups.

3.6 Tissue collection and processing

3.6.1 Retinal whole-mounts

For investigating numbers of RGCs an antibody against the RNA-binding protein with multiple splicing (Rbpms; Abcam PLC, Cambridge) was used, a relatively novel RGC marker (Rodriguez et al., 2014). 24 hours following IVI of glutamate or at certain time points during EAE, BN rats were euthanized by inhalation of 5% isoflurane followed by decapitation and removal of the whole eyes from the eye sockets. Following dissection, vitreous body and pigment epithelia removal, retinas were mounted on nitrocellulose membranes (Membrane Filter Black, white grid; GE Healthcare Life Sciences

Watman™, Chicago, Illinois, USA) with the RGC layer uppermost. Following tissue mounting, retinal whole-mounts were immediately processed for antibody labeling (see Section 3.8).

3.6.2 Preparation of frozen tissue sections

At relevant time points during the disease course, animals were sacrificed by overdose i.p. injection of 20% ketamine (1.2 ml/kg) and 2% xylazine (0.6 ml/kg) and perfused via the aorta with 4% paraformaldehyde (PFA). Eyes still connected to the optic nerves were dissected and kept overnight in 4% PFA for additional tissue fixation and washed in PBS. After 12 hours in PBS, tissue was transferred into 30% sucrose (Applichem GmbH, Darmstadt, Germany) in PBS overnight for dehydration and cryoprotection. On the next day, tissue was put into plastic base moulds containing Cryoblock embedding medium (Medite, Burgdorf, Germany) and frozen using cold isopentane (Acros Organics BVBA, Geel, Belgium), cooled with liquid nitrogen. Frozen blocks were kept at -80°C prior to cutting. Four or eight µm thick longitudinal and 0.5 µm cross sections were cut using a cryostat (Leica, Wetzlar, Germany) at -20°C. Sections were transferred to SuperFrost® Plus microscope slides (Thermo Scientific, Waltham, Massachusetts, USA) and kept at -20°C prior to staining.

3.7 Histopathology

3.7.1 Luxol Fast Blue

To illustrate the presence and extent of demyelination, 4 and 8 µm frozen longitudinal ON sections were stained with Luxol Fast Blue (LFB). Pre-cut samples were taken from -20°C and kept at RT to thaw and dry. Following defrosting, slides were rehydrated by washing them three times for 5 minutes in PBS. Afterwards, they were incubated overnight in 0.1% LFB solution (Solvent blue 38, Sigma-Aldrich) at 60°C. The next day slides were cooled to RT and put in 90% alcohol. Each slide was put individually into 0.05% lithium carbonate solution (Sigma-Aldrich) until the colour of the tissue changed to turquoise, put in 70% ethanol and rinsed in tap water. Afterwards, the slides were put in periodic acid (Sigma-Aldrich) for 10 minutes followed by 5 minutes in running tap water. The slides were then incubated for 30 minutes in Schiff´s reagent (Sigma-Aldrich) and left under running tap water for 5 minutes for the blue colour to develop. In a final step, slides were counterstained with haematoxylin, dehydrated and mounted with Roti® - Histokitt II (Carl Roth, Karlsruhe, Germany).

3.7.2 Bielschowsky´s Silver Impregnation

To determine the extent of axonal loss ON longitudinal sections were stained with Bielschowsky´s silver impregnation. Sections were thawed and rehydrated and afterwards incubated in 20% silver nitrate solution (Carl Roth) for 20 mins. Slides were then transferred to distilled water (dH2O). Ammonia (VWR) was added dropwise to the silver nitrate solution until it became clear. The slides were then transferred in the clear solution for 20 mins in the dark. Afterwards the developer was added dropwise until the tissue became brown. The stain was fixed with 2% sodium-thiosulfate (Sigma-Aldrich) for 2 mins. Finally, the sections were dehydrated and mounted with Roti® - Histokitt II.

3.8 Immunofluorescent staining – general protocol

Microscope slides with tissue were taken from -20°C and kept at RT to thaw and dry. Sections were rehydrated by washing three times for 5 minutes in PBS (referred to further in text as a washing step). Antigen retrieval if needed was done by heat – induced using 0.2% citrate buffer at pH 6.0 previously preheated to around 90°C. Slides were immersed in boiling buffer and kept until the temperature dropped to 70°C. This was performed two times and the third time slides were kept in the buffer until it cooled down to RT. Afterwards the washing step was repeated. Nonspecific antibody binding was prevented by incubation of slides in blocking buffer (containing 10% normal goat/rabbit serum in 0.1% PBS Tween 20, PBS-Tw) for 1 hour at RT. Appropriate primary antibody was diluted in the blocking buffer and slides were incubated overnight at 4°C. The next day, after a washing step, slides were incubated with appropriate secondary antibody conjugated with fluorescent dye for 1 hour at RT. After final washing, slides were mounted with anti-fade Vectashield Mounting Medium (Vector laboratories, Burlingame, California, USA) with or without 4', 6-diamidino-2-phenylindole (DAPI; cell nuclei visualization) and covered with glass cover slips. A detailed list of the blocking buffers, primary and secondary antibodies used are given in Table 3.8.1 and Table 3.8.2.

For double immunofluorescence staining, two differently raised primary antibodies were used (eg. mouse and rabbit). Slides were incubated simultaneously with a mix of two different primaries and, subsequently, the mixture of appropriate secondary antibodies conjugated with different fluorophores.

For all immunostaining procedures, appropriate negative controls were used where the primary antibody was omitted.

Fluorescent microscopy and image acquisition was performed using either a conventional Eclipse 80i microscope (Nikon; Shinagawa, Tokyo, Japan) or a LSM 700 confocal microscope (Zeiss).

Antibody	Company	Sub-type	Dilution	Blocking buffer	Antigen retrieval
Neurofilament light (NFL)	Millipore, Billerica, Massachusetts, USA	Rabbit polyclonal	1:500	10% NGS/ 0.1% TBS-Tw	Citrate buffer pH 6.0
Myelin basic protein (MBP)	Sigma-Aldrich	Rabbit polyclonal	1:300	10% NGS/ 0.1% TBS-Tw	Citrate buffer pH 6.0
Kinesin (KIN)	Chemicon International Inc., USA	Mouse monoclonal	1:800	10% NGS/ 0.1% TBS-Tw	Citrate buffer pH 6.0
Alzheimer Precursor Protein A4, a.a. 66-81 of APP (βAPP)	Millipore, Billerica, Massachusetts, USA	Mouse monoclonal	1:1000	10% NGS/ 0.1% TBS-Tw	Citrate buffer pH 6.0
Synaptophysin (SYN)	Millipore, Billerica, Massachusetts, USA	Mouse monoclonal	1:800	10% NGS/ 0.1% TBS-Tw	Citrate buffer pH 6.0
RNA-binding protein with multiple splicing (Rbpms)	Abcam, Cambridge, Great Britain	Mouse polyclonal	1:500	10% NGS/ 0.3% TBS-Tr	-
Brain-specific homeobox/POU domain protein 3A (Brn3a)	Abcam, Cambridge, Great Britain	Rabbit monoclonal	1:200	10% NGS/ 0.3% TBS-Tr	-
Anti-Neurofilament Marker (SMI312)	Covance	Mouse IgG1 cocktail	1:1000	10% NGS/ 0.3% TBS-Tr	-
Sodium-calcium exchanger 1 (NCX1)	Swant, Switzerland	Rabbit polyclonal	1:200	10% NGS/ 0.3% TBS-Tr	-

Table 3.8.1 List of primary antibodies used for immunofluorescent staining.

Antibody	Company	Sub-type	Conjugate	Dilution
Goat anti-mouse	Jackson labs/Dianova, West Grove, Pennsylvania, USA	IgG	**Cy3**	1:400
Goat anti-mouse	Invitrogen	IgG	**Alexa 488**	1:400
Goat anti-rabbit	Jackson labs/Dianova	IgG	**Cy3**	1:400
Goat anti-rabbit	Invitrogen	IgG	**Alexa 488**	1:400
Rabbit anti-goat	Invitrogen	IgG	**Alexa 488**	1:400
Goat anti-rat	Vector laboratories	IgG	**Biotin**	1:200

Table 3.8.2 List of secondary antibodies used for immunofluorescent staining.

3.8.1 Immunocytochemistry

Previously isolated cells in culture, seeded on 13 mm covers slips in 24 well plates, had culture medium removed prior to careful washing with ice cold PBS. Cells were then fixed with 4% PFA for 10 minutes and washed with 0.02% PBS-Tween 20 (PBS-Tw; Sigma-Aldrich). Cell permeabilization was performed with different detergents depending on the antigen of interest. For staining of cytoplasmic antigens, cells were treated with 0.1% PBS-Tw for 10 mins at RT whereas for the detection of nuclear antigens 0.1% PBS-Triton X-100 (PBS-Tr) was used. Following permeabilization and washing step, nonspecific binding was blocked by incubation with 10% NGS in 0.1% PBS-Tw for 30 minutes at RT. Following blocking, cells were incubated overnight at 4˚C with the appropriate primary antibody diluted in blocking buffer. The next day, following washing step, cells were incubated with a fluorescent conjugated secondary antibody for 1 hour at RT. After final washing, coverslips were mounted on glass slides with mounting medium containing DAPI.

3.8.2 Immunofluorescent staining retinal whole–mounts

Immediately after mounting retinas on nitrocellulose membranes in PBS, they were fixed with ice cold 4% PFA for 10 minutes and afterwards washed in PBS. For the purpose of improving penetration of the primary antibody, permeabilization was performed with 0.3% PBS-Tr for 10 minutes at RT. Following blocking for 1 hour at RT (blocking buffer contained 10% NGS in 0.3% PBS-Tr.), retinas were incubated overnight at 4˚C with the Rbpms primary antibody (1:500) in blocking buffer. The next day, following washing, retinas were incubated with Alexa – 488 conjugated secondary antibody for 1 hour at RT. After final washing, retinas were mounted on glass slides with mounting medium containing DAPI. To determine RGC cell densities, four different areas were taken from each of four retinal segments. These areas were aligned longitudinally, from optic nerve head to the outer retinal rim, and pictures were taken using a conventional Eclipse 80i microscope (Nikon) at 20 x magnification, as shown in Figure 3.8.3.1. ImageJ free software (https://imagej.nih.gov/ij/) was used to quantify RGC density in each of the sixteen chosen areas. Using an implemented grid function, eight 0.01 mm^2 squares were used per area (avoiding blood vessels) and in each square RGCs were counted using an ImageJ cell counting plug-in. All retinal whole-mounts were quantified in a blinded manner. The final result represented the RGC cell density per mm^2 for an individual retina, as averaged across the whole retinal whole-mount.

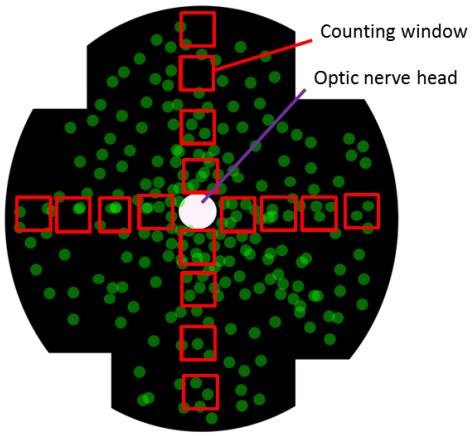

Figure 3.8.3.1 Graphical representation of retinal whole-mount. Green dots represent $Rbpms^+$ RGCs. Red squares represent the positioning of areas of each retina used for RGC quantification.

3.9 Terminal deoxynucleotidyl transferase dUTP nick end labelling (TUNEL) assay

A commonly used technique for the labelling of apoptotic cells is the TUNEL assay. This method involves the identification of fragmented DNA through covalent addition of labelled deoxyuridine triphosphate (dUTP) by the enzyme deoxynucleotidyl transferase (TdT; Gavrieli et al., 1992). This assay was performed on frozen optic nerve sections. After rehydration in PBS, sections were treated with proteinase K (20 µg/ml; Roche) for 5 mins at RT. Endogenous peroxidases were inactivated with 3% H_2O_2 followed by rinsing in Tris buffer (10 mM Tris-HCl, pH 8.0; Carl Roth). Sections were equilibrated in TUNEL dilution buffer (TDB; Roche) for 10 mins at RT. The TUNEL reaction was performed in TDB containing TdT (0.15 U/µl; Promega, Madison, Wisconsin, USA) and biotin-16-dUTP (10 µM; Roche) for 60 min at 37°C. A positive control was performed by pre-treating sections with DNase I (3 U/ml; Roche) and a negative control was performed by omitting biotin-16-dUTP from the TUNEL reaction. The reaction was terminated by washing sections in saline sodium citrate solution (30 mM $Na_3C_6H_5O_7$ containing 300 mM NaCl; both from Sigma-Aldrich) for 15 mins. After rinsing in PBS, non-specific binding sites were blocked with 2% BSA-PBS for 20 mins at RT. Sections were then rinsed in PBS and incubated with the same blocking solution containing streptavidin–Alexafluor 488 or 555 conjugate (1:700; Molecular Probes/Thermo Fisher) for 30 mins at 37 °C. After rinsing with PBS, sections were mounted using anti-fade mounting medium containing DAPI for visualisation of cell nuclei and quantified under the Nikon Eclipse 80i microscope with 20 x magnifications.

3.10 Preparation of tissue lysates

At desired time points during the course of EAE or 24 hours following IVI of glutamate, rats were sacrificed by decapitation after inhalation of 5% isoflurane. Optic nerves were dissected and mechanically homogenized in a glass homogenizer (Kontes, Vineland, New Jersey, USA) with ice cold lysis buffer containing cOmplete Protease Inhibitor Cocktail® (Roche, Mannheim, Germany). To further disrupt the integrity of the tissue, lysates were sonicated for 5 seconds. Cell debris was pelleted at 13000 rpm at 4°C for 15 minutes. Supernatants were collected and kept at -80°C prior to use.

The total protein concentration in the sample was determined using a bicinchoninic acid (BCA) assay (Pierce, Rockford, Illinois, USA) following the instructions provided by the manufacturer.

3.10.1 Western blotting

The expression of different proteins during the course of the disease was examined by Western blotting. Lysates containing 30 µg of total protein was diluted in 2x sample buffer (Anamed Elektrophorese, Groß-Bieberau, Germany) and incubated at 95°C for 10 minutes. Samples were loaded onto a 4–20 % gradient Mini-PROTEAN® TGX Stain-Free™ Precast gels (BioRad, Hercules, California, USA). Proteins were separated by sodium dodecyl sulfate polyacrylamide gel electrophoresis (SDS-PAGE) for 1 hour and 20 mins at 120 V in a running buffer containing 25 mM Tris Base (Carl Roth), 190 mM glycine (Sigma) and 0.1% SDS (Carl Roth). Following electrophoresis, the semi-dry blotting technique using Trans-Blot® Turbo™ Transfer System (BioRad) was used for protein transfer to a polyvinylidene difluoride (PVDF) membrane (BioRad). Different blotting settings (provided by the transfer system) were utilized depending on the molecular weight of the protein investigated. The membrane was incubated in blocking buffer containing 5% milk (Skim milk powder; Sigma) or 5% BSA in 0.1% TBS-Tw, depending on the antibody used, for 1 hour at RT. Following the blocking step, the membrane was incubated in the same blocking buffer with addition of the appropriate primary antibody overnight at 4°C. On the following day, the membrane was washed in TBS-Tw and incubated with the corresponding HRP-conjugated secondary antibody for 1 hour at RT. A list of different blocking agents and primary/secondary antibodies is given in Table 3.10.1. Following the washing step, the membrane was incubated with the ECL Prime reagent (Amersham, USA) for one minute and imaged using the ChemiDoc™ XRS+ Imaging System (BioRad).

The expression of the protein of interest in the sample was normalized to the expression of the house-keeping protein Glyceraldehyde 3-phosphate dehydrogenase (GAPDH, Millipore). A minimum of 3 samples per time point were used in the final quantification for each protein. Quantification of the results was performed using ImageJ free software with the implemented plug-in for Western blot quantification.

Protein	Company	Blocking buffer	Primary antibody dilution	Secondary antibody
Fractin	Millipore, Billerica, Massachusetts, USA	5% milk 0.1% TBS-T	1:1000	Donkey anti-rabbit HRP-conjugated, 1:5000
Gelsolin	Abcam, Cambridge, Great Britain	5% milk 0.1% TBS-T	1:1000	Donkey anti-goat HRP-conjugated, 1:5000
GAPDH	Millipore, Billerica, Massachusetts, USA	5% milk 0.1% TBS-T	1:2500	Sheep anti-mouse HRP-conjugated, 1:5000

Table 3.10.1. Combination of different blocking agents and primary/secondary antibodies for Western blotting. All secondary antibodies were purchased from Amersham (Buckinghamshire, GB).

3.10.2 Globular versus filamentous actin ratio assay

Actin network dynamics were evaluated during the course of disease using the globular versus filamentous actin ratio assay (G/F-actin ratio) on optic nerve lysates. Tissue preparation and protocol was followed to detail as given in the manual of G-actin / F-actin In Vivo assay kit (Cat. #BK037; Cytoskeleton Inc., Denver, Colorado, USA). Briefly, optic nerve lysates were collected in F-stabilization buffer and ultra-centrifuged at 100,000g, 37°C for 1h. In all the experiments, an Optima Max – E ultracentrifuge (Beckmann Coulter Inc., Brea, California, USA) with TLA – 55 FixedAngleRotor (Beckmann Coulter) was used and samples were prepared in 1.5 ml ultracentrifuge tubes (Microfuge® Tube Pollyallomer; Beckmann Coulter). Following ultra-centrifugation, supernatant was carefully removed (G-actin fraction) while the pellet was re-suspended in F-actin depolymerizing buffer (F-actin fraction). Following sample preparation, the protocol for Western blotting was identical to the one used for normal tissue lysates. G/F-actin ratio was calculated as the ratio of globular versus filamentous actin band intensity using the ImageJ application for Western blot quantification.

3.11 Live dead assay

To evaluate the quality of primary RGC cultures and cytotoxic effects of 24 hour glutamate treatment, ethidium homodimer 1 (EthD-1) was used (Molecular Probes, Thermo Fisher Scientific) was used. EthD-1 is a high-affinity nucleic acid stain that is weakly fluorescent until bound to DNA and emits red fluorescence. It cannot cross the intact plasma membrane of live cells. Briefly, media was carefully removed from cultured RGCs (~5.000 cells seeded on 13 mm coverslips) before washing with PBS. Cells were then incubated in 0.5 µm EthD-1 in PBS (250 µl) for 15 minutes at RT. Afterwards, coverslips were mounted without washing on glass slides with mounting medium containing DAPI and immediately examined on a conventional Eclipse 80i microscope (Nikon). Cells were imaged with 20x magnification and six different areas of interest were taken (four on the outer rim and two in the centre of seeded cells) and counted using ImageJ free software with a cell counting plug-in. Results were expressed as the percentage of healthy cells (detected by the absence of EthD-1^{+} labelling and round DAPI positive nuclei) compared to the total counted cells (live and dead together) in all experimental settings.

3.12 Ca^{2+} imaging

Ca^{2+} dynamics of RGCs after glutamate receptor stimulation was addressed using ratio-metric Fura-2 (Molecular Probes, Life Technologies) Ca^{2+}-imaging. RGCs, seeded on 25 mm diameter glass coverslips (~5.000 cells per cover slip), were incubated with 5 ng/µl of Fura-2 (1 µg/ul in DMSO; Molecular Probes, Life Technologies) in RGM for 20 minutes on 37°C. Following incubation, cells were washed in basic Fura-2 imaging solution (FIS; Table 3.10.1) for 5 minutes and transferred to an imaging chamber (Attofluor® Cell Chamber; Molecular Probes, Invitrogen) with the appropriate imaging solution (Table 3.9.1). Cells were recorded using the Nikon Total Internal Reflection Fluorescence (TIRF) microscope but in wide-field epifluorescence mode. A helium lamp with excitation filters for 340 and 380 nm wavelengths and an emission filter of around 510 nm was used for illumination, and data was recorded using a Hamamatsu Ocra AG camera (Model C4742-80-12AG). Ten to thirty cells were captured in the field of view imaged with a 20x objective (Nikon S Fluor 20x NA 0.75 (working distance 1.0 mm), corrected for 0.17 mm coverslips (= type #1.5)). A Nikon Perfect Focus System (PFS3) was included, that continuously determined the distance to the coverslip, readjusting it if required, for instance because of thermal drift. For live cell imaging, the system was equipped with an on-stage incubation chamber (TokaiHit) for controlling the temperature, CO_2 concentration and humidity. Care was taken during the imaging process to prevent

bleaching and photo-toxicity by choosing the shortest possible excitation times (200/60 ms for 340/380 nm wavelengths) and the least frequent data sampling rate (every 2 seconds in short 5 – 10 minutes experiments; every 30 seconds in 1-1.30 hour experiments).

Treatment experiments were performed by adding 300 µl of amount of imaging solution (10 mM HEPES, 5 mM glucose, 120mM NaCl, 2.8 mM KCl, 3mM $CaCl_2x2H_20$, 20.4 mM sucrose) with different stimulators or blockers (Figure 3.12). This large addition volume allowed rapid distribution of the added compounds. All additions were performed by hand using a 1 ml pipette, with care taken to not cause any additional pressure on the cells that might affect Ca^{2+} dynamics).

The fluorescence images were converted into ratio-metric (340/380 nm) data with imaging software Nikon NIS 4.13. Briefly, region of interests (ROIs) around each cell body were automatically selected, corrected for the background signal and processed further for 340/380 nm ratio values.

All Ca^{2+} imaging experiments were performed at the Nikon Imaging Center Heidelberg (http://nic.uni-hd.de/).

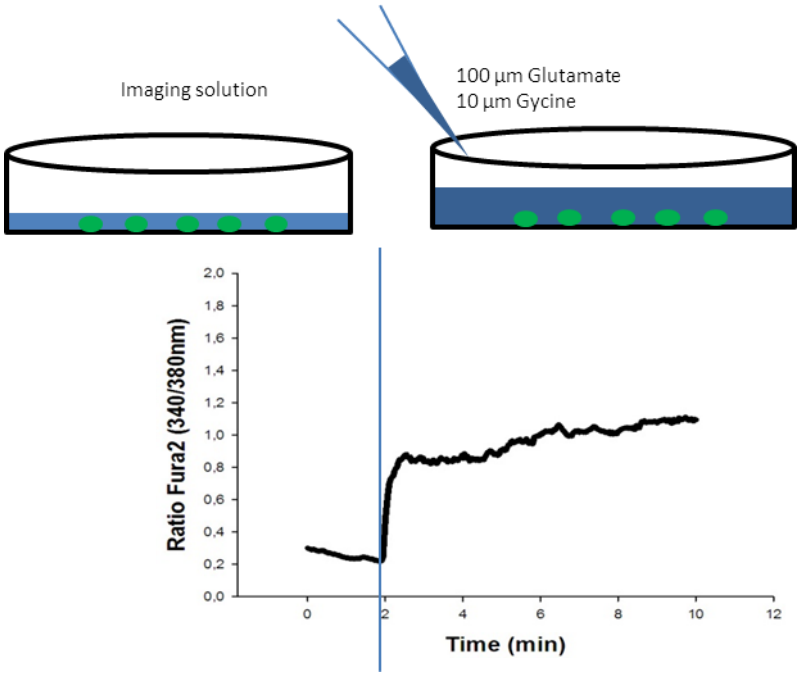

Figure 3.12 Graphical representation of RGC Fura-2 ratio-metric Ca^{2+} imaging. Green dots represent RGCs on a 25 mm glass coverslip mounted in the imaging chamber.

3.13 Quantitative Real Time - Polymerase Chain Reaction (qRT-PCR)

Total RNA was isolated from RGCs of adult BN rats and P7-8 pups SD rats using an RNAeasy Mini Kit (Qiagen, Hilden, Germany) according to the manufacturer's instructions. Total amount of RNA and dsDNA was measured on Qubit®2.0 fluorometer (Thermo Fisher Scientific) with Qubit®2.0 RNA Assay Kit and Qubit®2.0 dsDNA HS Assay Kit (Thermo Fisher Scientific). To generate the desired cDNA pool from RNA templates, Transcriptor high fidelity cDNA synthesis kit (Roche, Germany) was used. qRT-PCR was performed on an ABI 7000 thermal cycler with SYBR Green PCR Mastermix (Applied Biosystems, Waltham, Massachusetts, USA). All samples were analysed in duplicate. All primers used in the qPCR experiments were designed using online NCBI Primer BLAST tool (https://blast.ncbi.nlm.nih.gov/Blast.cgi; Table 3.11) and whenever possible separated by at least one intron on the genomic DNA to exclude amplification of genomic DNA. PCR reaction products were controlled by including no-RT-controls, by omission of templates and by melting curve analysis. The analyses of relative gene expression data gene was determined using the $2^{-[\Delta\Delta Ct]}$ method by comparison of threshold values, normalized to a house-keeping gene, in this case glyceraldehydes-3-phosphate dehydrogenase (GAPDH).

Rat Genes	NCBI Reference	qPCR primers
Sodium Calcium Exchanger 1 (NCX 1)	Kuroda et al., 2013.	F:GTGTTTGTCGCTCTTGGAACCTC R: CGTTGCTTCCGGTGACATTG
Sodium Calcium Exchanger 2 (NCX 2)	NM_078619.1	F: TGGAGGGAGCAGTTTTTAGA R: CATCACGTAGTCAAAGCAGG
Sodium Calcium Exchanger 3 (NCX 3)	NM_078620.2	F: CTGGAAGCTAAGGGGAATCG R: CTCTGCTCGAAGACCATTCA
Calcium ATPase 1 (PMCA 1)	NM_053311.1	F: AGGTGTGGAGAAGAAGGGA R: GCCCATGACTTGTTTCTTCC
Calcium ATPase 2 (PMCA 2)	NM_012508.5	F: CACCATCTCACTGGCCTATT R: CTTGTAGTGGACATCACCGA
Calcium ATPase 3 (PMCA 3)	NM_133288.1	F: GCTCCATGACGTAACCAATC R: TACGGAATGCTTTCACCACT
Glutamate ionotropic receptor AMPA type subunit 1 (Gria 1)	NM_031608.1	F: ACTCAAGCGTCCAGAATAGG R: CCACACAGTAGCCCTCATAG
Glutamate ionotropic receptor AMPA type subunit 2 (Gria 2)	NM_001083811.1	F: GGTACGACAAAGGAGAGTGC R: TTTGCCACCTTCATTCGTTT
Glutamate ionotropic receptor AMPA type subunit 4 (Gria 4)	NM_001113184.1	F:TACGACAAAGGAGAATGTGGCA R: GCCGCCAACCAGAATGTAG
Glutamate ionotropic receptor NMDA subtype 1 (Grin 1)	NM_001270602.1	F: GCGTCTGGTTTGAGATGATG R: ATAGGACAGTTGGTCGAGGT
Glutamate ionotropic receptor NMDA subtype 2a (Grin 2a)	NM_012573.3	F: AGTGGTCTATCAACGAGCAG R: TGATTCCTGTCTCCACGAAG
Glutamate ionotropic receptor NMDA subtype 2b (Grin 2b)	NM_012574.1	F: CAGCATTCCTACGACACCTT R: ATGAATCGGCCCTTGTCTTT
Calcium voltage – gated channel subunit alpha -1A (Cacna 1A)	NM_012918.3	F: CACCGAGTTTGGGAATAACT R: AAAGTCCAGAGGAGAATGCG
Calcium voltage – gated channel subunit alpha -1C (Cacna 1C)	NM_012517.2	F: GATTGTTGTGGGTAGCATTGT R: GGGAGAGCATTGGGTATGTT
Calcium voltage – gated channel subunit alpha -1B (Cacna 1B)	NM_001195199.1	F: GGTGGCATTTGCATTCTCAG R: CAGTCAAACACAGCCTTGAG
glyceraldehydes – 3 – phosphate dehydrogenase (GAPDH)	NM_017008.4	F: CAGGGCTGCCTTCTCTTGTG R: TGGTGATGGGTTTCCCGTTG

Table 3.13 Primers used for qRT-PCR analyses. NCBI reference number is added next to the self-designed primer pairs using NCBI primer BLAST tool.

3.14 MK801 and SEA0400 treatment studies during iAON

In order to investigate the role of NMDA activation during iAON on RGC loss and actin axonal network changes, MOG-immunized animals received IVI of 4 nmoles MK801 (4 µl of 1mM MK801-maleate (Sigma-Aldrich) diluted in sterile-filtered saline) on day 4 and again on day 7 post-immunization (day 4 p.i. and day 7 p.i.). Control animals received the corresponding IVI of 4 µl saline. In order to investigate the role of NCX1 in early RGC loss and actin axonal cytoskeleton changes, the NCX reverse-mode blocker SEA0400 (ApexBio; Houston, Texas, USA) was used. EAE animals received IVI of 4 nmoles SEA0400 (4 µl of 1mM SEA0400) in 1% DMSO in sterile-filtered saline) on day 4 p.i. and day 7 p.i. Control animals received the corresponding IVI of 4 µl 1% DMSO in saline. Following both treatments, retinas were further prepared for whole-mounting followed by Rbpms-staining to determine RGC cell density, and optic nerves were used for the G/F-actin assay.

3.15 Statistical analyses

All data are presented as their mean values ± standard error of the mean (SEM). All data analyses were done using SigmaPlot 12.5 software. Where two experimental groups were compared, if data were normally distributed (as assessed by the Shapiro-Wilk test), statistical significance was assessed by two-tailed Student's t-test. If data failed the Shapiro-Wilk test, statistical significance was assessed by Mann-Whitney rank sum test. Where more than two groups were compared in normally distributed data (as assessed by the Shapiro-Wilk test), one way analysis of variance (ANOVA) combined with post hoc Dunnett's method was used for comparing multiple experimental groups versus controls. If data failed the Shapiro-Wilk test, Kruskal-Wallis one way analysis of variance on ranks followed by Dunn's method was used for comparing multiple experimental groups versus controls. Three levels of significance were defined: * p value ≤ 0.05 was considered significant, ** p value ≤ 0.01 was considered strongly significant; *** p value ≤ 0.001 was considered highly significant.

4 Results

4.1 Disease course

Following immunization with MOG, rats were scored daily for the appearance of neurological EAE deficits – see Methods, chapter 3.2). The average day of onset of EAE was between days 12 and 14 post immunization (p.i.; n = 24; Figure 4.1.A), with symptoms appearing as early as day 11 p.i.. Simultaneously with the onset of EAE, identified by the development of neurological symptoms indicative of spinal cord lesions, animals develop autoimmune optic neuritis (AON) with high incidence. AON is typically characterised histopathologically by the presence of inflammatory demyelinating lesions in the optic nerves accompanied by axonal loss (Fairless et al., 2012; Figure 4.1.B).

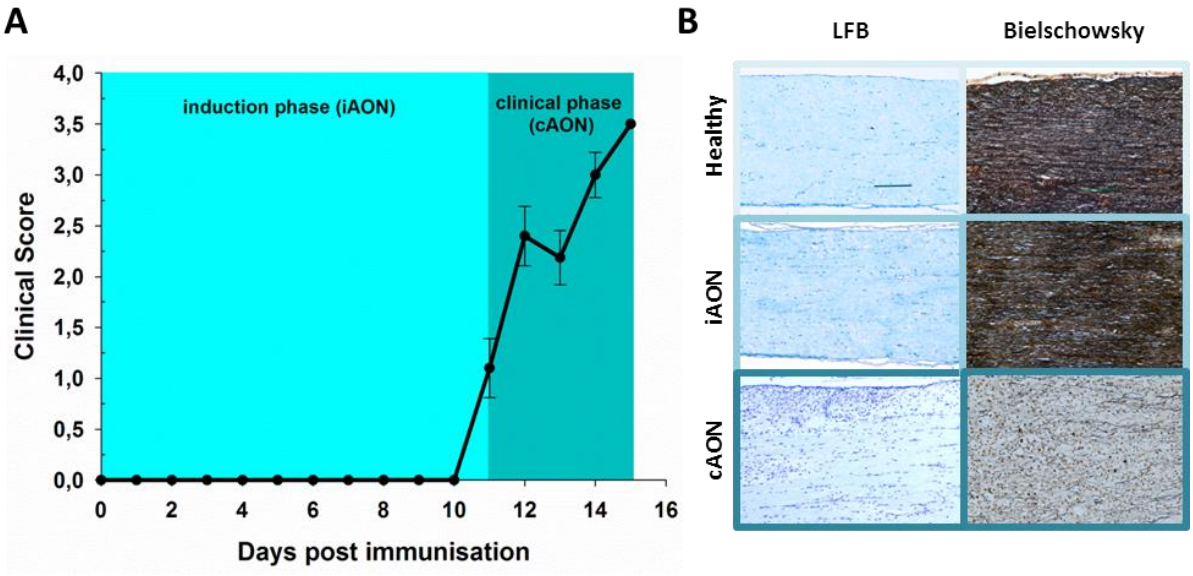

Figure 4.1. Time-course of MOG-EAE and AON. (A) Neurological score of rats following immunisation with MOG, as assessed by clinical spinal cord deficits typical of EAE. The timing of clinical EAE onset correlates strongly with the onset of autoimmune optic neuritis (AON; Fairless et al., 2012); and thus the pre-clinical phase is considered as the induction phase of AON (iAON), and the period of neurological deficit is considered the clinical phase of AON (cAON). Average onset of cAON is on day 12 post immunazation (n = 24 animals). **(B)** Representative images showing demyelination (LFB) and axonal loss (Bielschowsky) in the optic nerve in cAON phase, illustrating that the histopathological hallmarks of AON correlate with the disease stages identified by EAE clinical impairment. Scale bars 100 µm.

4.2 Early RGC loss detection with the anti-Rbpms immunostaining of retinal whole-mounts

RGC loss was previously shown to start during the iAON in BN rats by retrograde labelling with Fluorogold (Fairless at al., 2012.). This finding was re-evaluated in this study using immunofluorescent staining of retinal whole-mounts with an antibody against Rbpms, a novel selective marker for RGCs (Rodriguez et al., 2014). For the purposes of this study, RGC cell densities in healthy versus day 10 p.i. (late stage of iAON) animals were compared (Figure 4.2.A). In healthy animals, the average number of Rbpms-positive RGCs per mm^2 (2391 ± 45) was significantly higher compared to that in iAON animals (2191 ± 32, p = 0.0003; Figure 4.2.B).

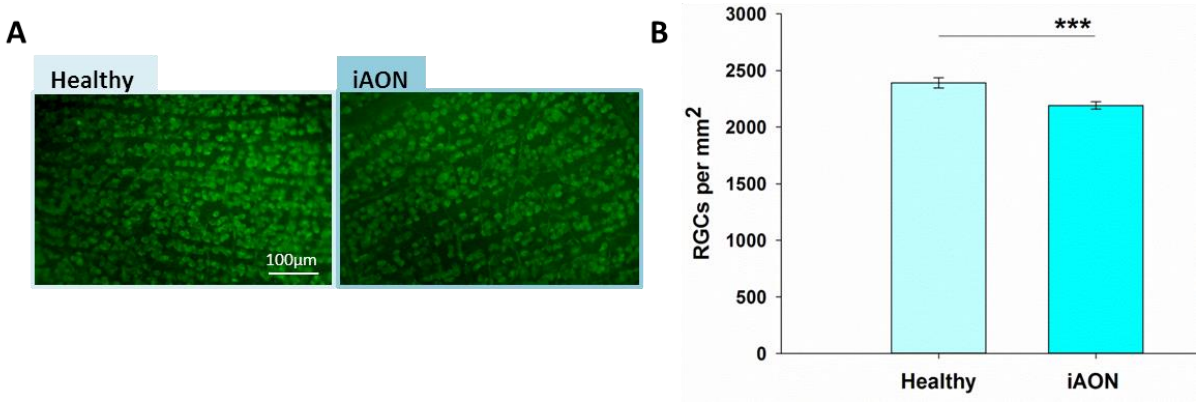

Figure 4.2. Anti-Rbpms staining confirming early RGC loss during iAON. (A) Representative retinal whole-mounts stained with Rpbms antibody in healthy and iAON animals. **(B)** RGC cell density is significantly decreased in retinas during iAON compared to healthy retinas (n = 3 healthy animals, 6 retinas; n = 4 iAON animals, 8 retinas; *** p ≤ 0.001, Student's t-test).

4.3 Axonal transport deficits during AON

Previous studies of neurodegeneration in AON have hinted at the potential for an axonal transport deficit during the induction disease phase due to the identification of calpain-mediated degradation of spectrin within the optic nerve (Hoffmann et al., 2013), and also disturbances in the ultrastructural integrity of optic nerve axons (Fairless et al., 2012). In order to address potential axonal transport deficits during AON, immunofluorescence staining was performed against different proteins involved in the machinery of transportation: anterograde transport "motor" protein - kinesin (kin), synaptic vesicle "cargo" protein - synaptophysin (syn) and the axonal stress and transport failure marker - beta-amyloid precursor protein (βAPP). Co-staining with myelin basic protein marker (MBP) was used

to check the myelination status of axons and, together with cell nuclei labelling with DAPI, aided the identification of inflammatory demyelinating lesions. Specificity of accumulated transport proteins within RGC axons was confirmed with double staining against neurofilament light protein (NFL).

4.3.1 Axonal transport profile in the ONH

The ONH is the area where RGC axons are naturally unmyelinated (Figure 4.3.1), and has been suggested to be an area of potential vulnerability to injuries such as glaucoma (Chidlow et al., 2008; Cherecheanu et al., 2013) and AON (Fairless et al., 2012). For instance, during iAON the ONH was the area of the optic nerve with the greatest microglial activation (Fairless et al., 2012). Thus, the identification of axonal transport deficits might be more apparent within this potentially vulnerable area. In addition, although a previous investigation of βAPP in the optic nerve did not identify any areas of accumulation prior to cAON onset (Fairless et al., 2012), this was performed only on cross sections from the distal optic nerve, and thus could have missed key areas. Following immunostaining for axonal transport protein accumulation, clusters of immunoreactivity could be seen in cAON (Figure 4.3.1.1.C.i-iii; Figure 4.3.1.2.C.i-iii), where it correlated with regions of cellular density indicated by DAPI labelling, demonstrating areas of inflammatory infiltration. However, accumulation of axonal transport proteins within the ONH was not observed during iAON (Figure 4.3.1.1.B.i-iii; Figure 4.3.1.2.B.i-iii).

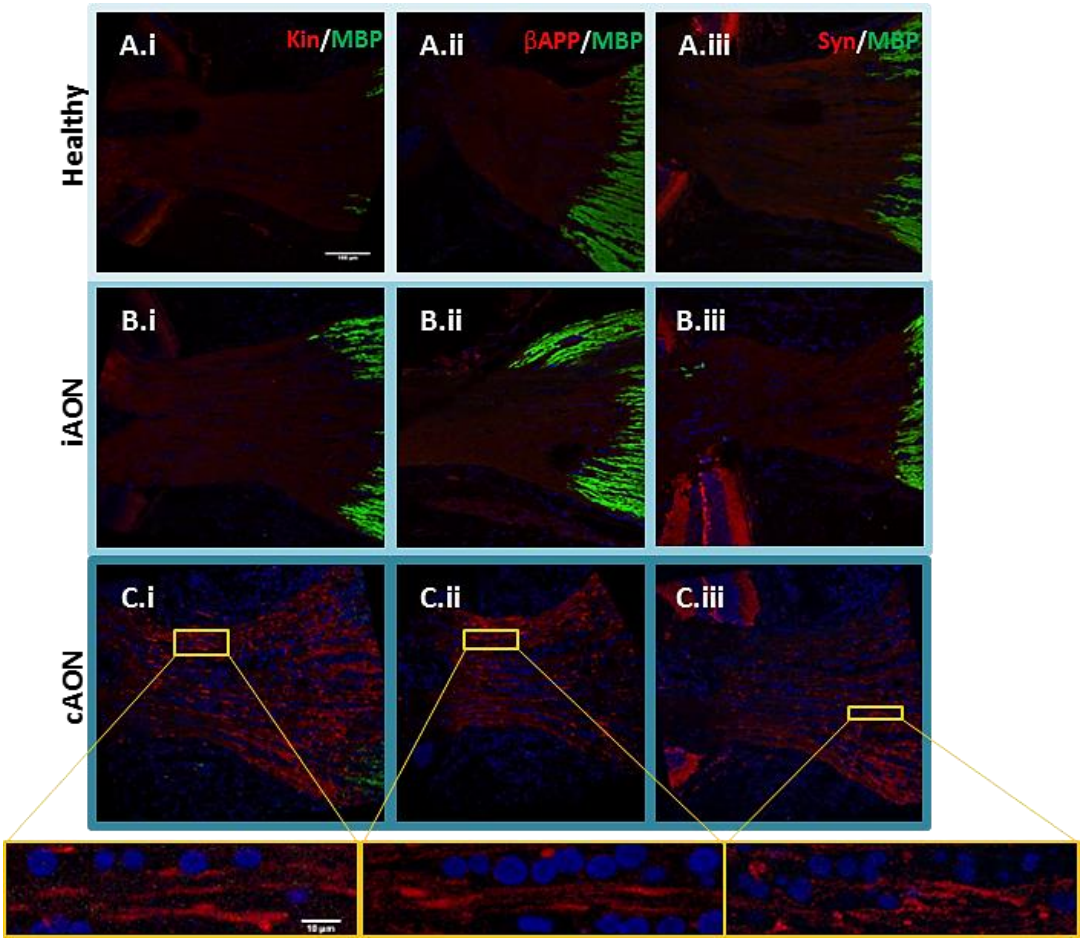

Figure 4.3.1.1 Axonal transport deficits in the ONH are observed with the onset of cAON. ONH could be identified as the unmyelinated retro-bulbar region of the optic nerve, as seen with MBP staining (green). Accumulation of axonal transport proteins (Kin (A-C.i), βAPP (A-C.ii), Syn (A-C.iii); red) was visible with the appearance of hyper-cellularity due to infiltration of immune cells, as indicated by DAPI staining (blue), in the proximal optic nerve part. Bottom row represents enlarged areas marked with yellow rectangles in panel above (C.i-iii; n = 6 animals per time point investigated; scale bars 100 µm, insert 10 µm).

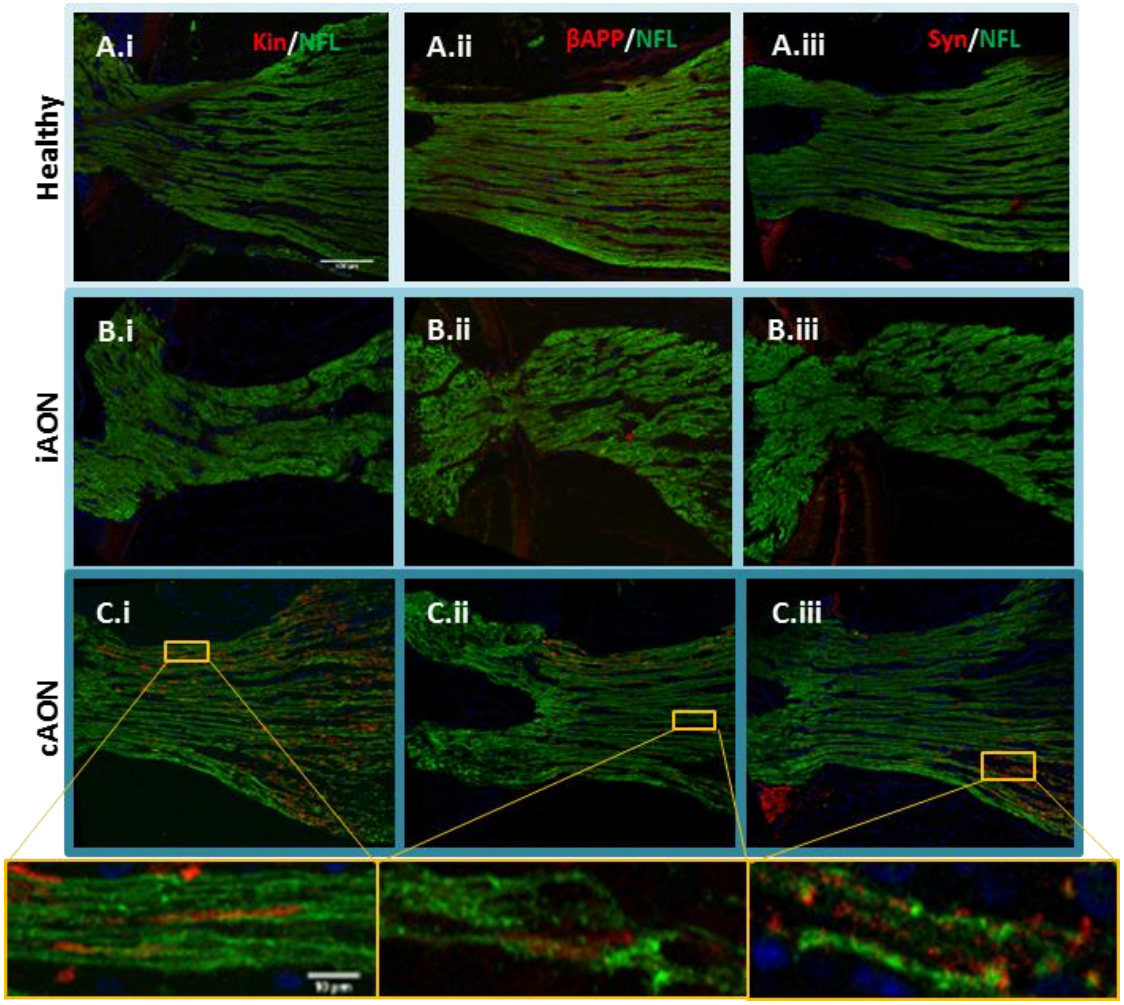

Figure 4.3.1.2. Transport markers accumulate within RGC axons in the ONH with the onset of cAON. ONH axons are visualized using the anti-NFL antibody (green). Accumulation of transport proteins (Kin (A-C.i), βAPP (A-C.ii), Syn (A-C.iii); red) were localized to NFL labeled axons in the proximal optic nerve part. . Bottom row represents enlarged areas marked with yellow rectangles in panel above (C.i-iii; n = 6 animals per time point investigated; scale bars 100 µm, insert 10 µm).

4.3.2 Axonal transport profile in the distal optic nerve

In parallel with the ONH, more distal regions of the optic nerve where RGC axons are fully myelinated (Figure 4.3.2.1) were also investigated for evidence of axonal transport protein accumulation. As was seen in the ONH, during cAON there was evidence of transport protein accumulation (Figure 4.3.2.1.C.i-iii; Figure 4.3.2.2.C.i-iii), but this was not seen during iAON. Interestingly, accumulation of βAPP was present within and in the vicinity of inflammatory demyelinated lesions, in both myelinated and demyelinated axons on optic nerve cross-sections (Figure 4.3.2.3.A). The same was observed for the accumulation of Syn (Figure 4.3.2.3.B).

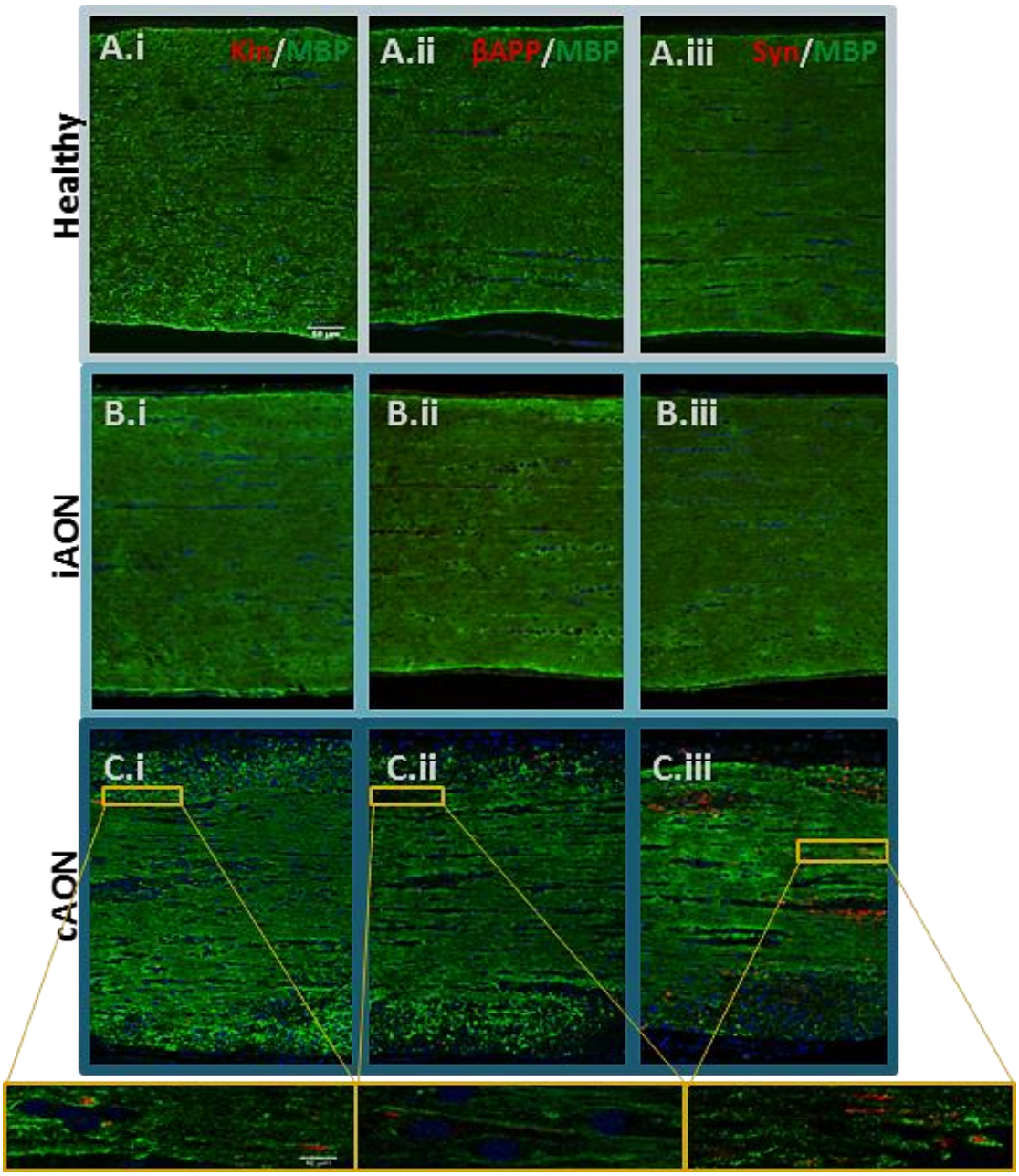

Figure 4.3.2.1. Axonal transport deficits in the optic nerve are observed with the onset of cAON. (A) Distal part of the optic nerve consists of myelinated RGC axons, as seen with MBP staining (green). No accumulation of axonal transport proteins (Kin (A-C.i), βAPP (A-C.ii), Syn (A-C.iii); red) is visible prior the onset of inflammatory demyelination (areas of increased DAPI positive nuclei). Bottom row represents enlarged areas marked with yellow rectangles in panel above (C.i-iii; n = 6 per time point; scale bars 100 µm, insert 10 µm).

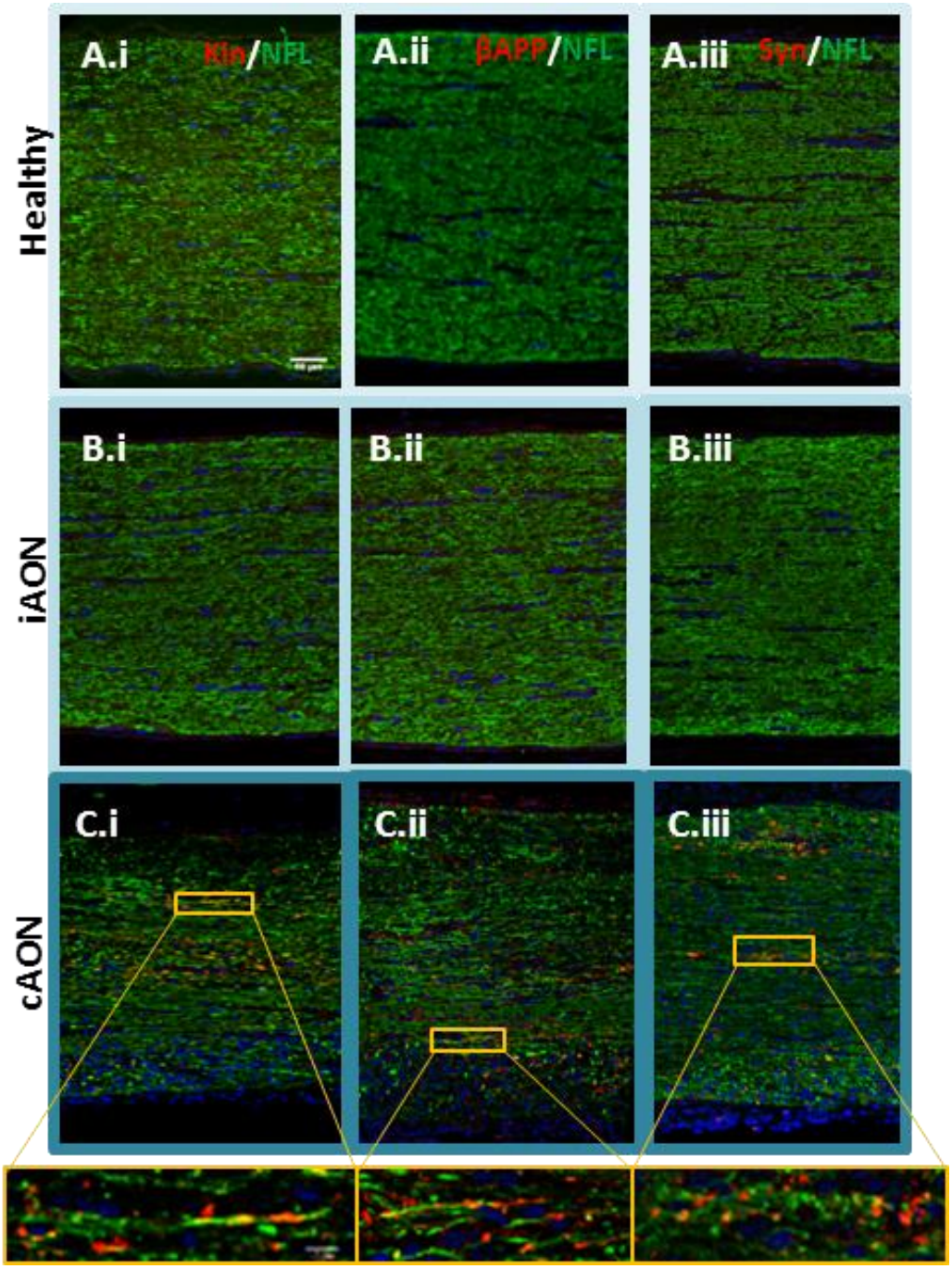

Figure 4.3.2.2. Transport markers accumulate within RGC axons in optic nerves with the onset of cAON. In the distal part of the optic nerve accumulation of axonal transport proteins (Kin (A-C.i), βAPP (A-C.ii), Syn (A-C.iii); red) localize to NFL positive axons (green) prior the onset of inflammatory demyelination (areas of increased DAPI positive nuclei). Bottom row represents enlarged areas marked with yellow rectangles in panel above (C.i-iii; n = 6 per time point; scale bars 100 µm, insert 10 µm).

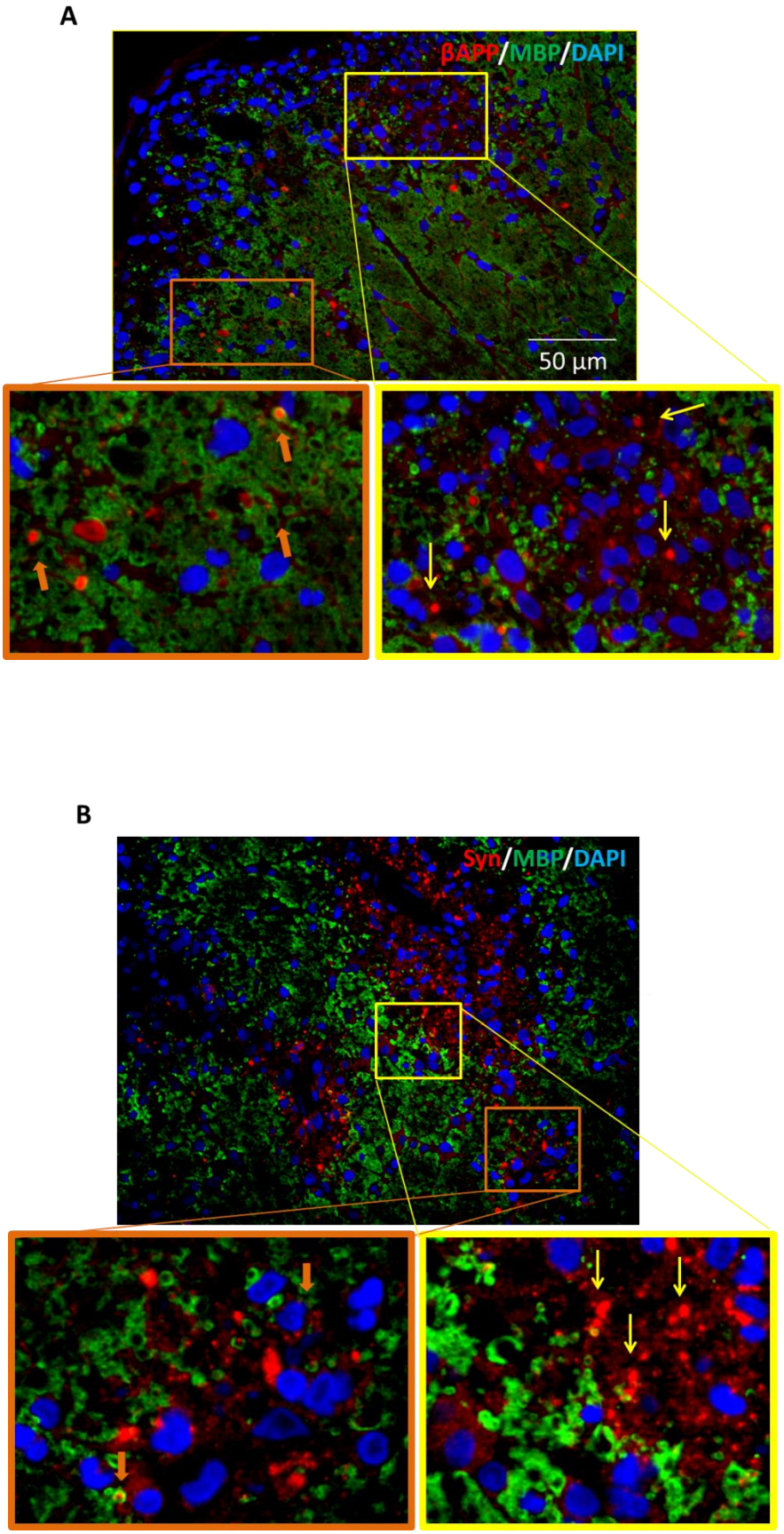

Figure 4.3.2.3. Optic nerves cross-sections profile of transport proteins accumulation in cAON. (A) βAPP (red) was visible in both myelinated (orange square insert, thick arrows) and unmyelinated (yellow square insert, open arrows) axons. **(B)** Syn (red) was visible in both myelinated (orange square insert, thick arrows) and demyelinated (yellow square insert, open arrows) axons following the onset of cAON (n = 3; scale bar 50 µm).

4.3.3 Cholera Toxin B subunit A488-conjugate for detection of axonal transport deficits during AON

In addition to determining areas of transport protein accumulation to identify axonal transport deficits, cholera toxin B-subunit (CTB), a common tracer used to map out axonal projections can also be used (Abbott et al., 2013). CTB conjugated to Alexa 488 was injected into the vitreous body of the eye, and left for 24 hours to be transported along the RGC axons in an anterograde direction. The ONH was then assessed for evidence of CTX-A488 accumulation. In the iAON ONH (Figure 4.3.3.A.i), the initial axonal projections were heavily labelled with CTX-A488, but this was not different in appearance to that of the healthy ONH (Figure 4.3.3.B.i). In contrast, during cAON, areas of CTXB-A488 accumulation was seen in both the initial and distal regions of the optic nerve (Fig. 4.3.3.C.i-ii), where it correlated with the borders of infiltrated lesions (see Fig. 4.3.3.C.ii insert), representing regions of axonal damage where axons had not been totally lost.

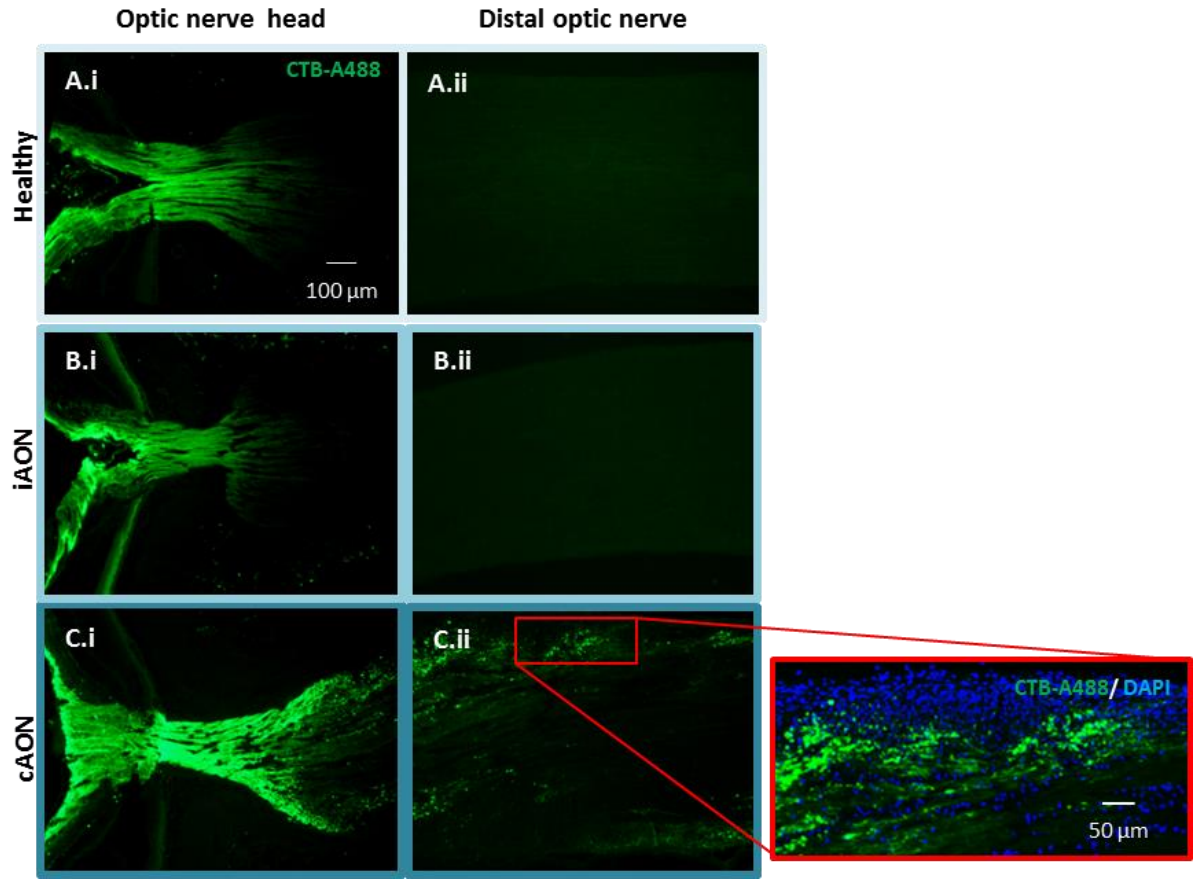

Figure 4.3.3. CTB-A488 accumulation is associated with inflammatory lesions following the onset of cAON. No change in labeling pattern of CTB-A488 was seen between healthy and iAON 24 hours following intravitreal injection of the tracer **(A.i-ii; B.i-ii)**. After the onset of cAON, CTB-A488 was detected within inflammatory lesions **(C.ii)**. Insert shows an inflammatory lesion co-stained with DAPI (n = 3 per time point; scale bars 100 µm, insert 10 µm).

4.4 Actin network profile in optic nerves during AON

4.4.1 G/F-actin ratio is increased along the course of AON

The actin network has been shown to be both a sensor and a mediator in the process of apoptotic cell death (Desouza et al., 2012; Franklin-Tong & Gourlay, 2008). Knowing that RGC loss during AON was confirmed to be mostly of apoptotic nature (Fairless et al., 2012) accompanied by retinal and optic nerve Ca^{2+} increases (Hoffmann et al., 2013), the status of the RGC axonal actin network was next addressed. This was achieved using a sedimentation assay allowing the ratio of globular to fibrous actin to be assessed (the G/F-actin ratio). This ratio was significantly elevated already during iAON (0.88 ± 0.20) when compared to healthy animals (Figure 4.4.1; 0.38 ± 0.09, p = 0.04). The same was observed in animals at the onset of cAON (1.20 ± 0.22, p = 0.011 compared to the healthy animals).

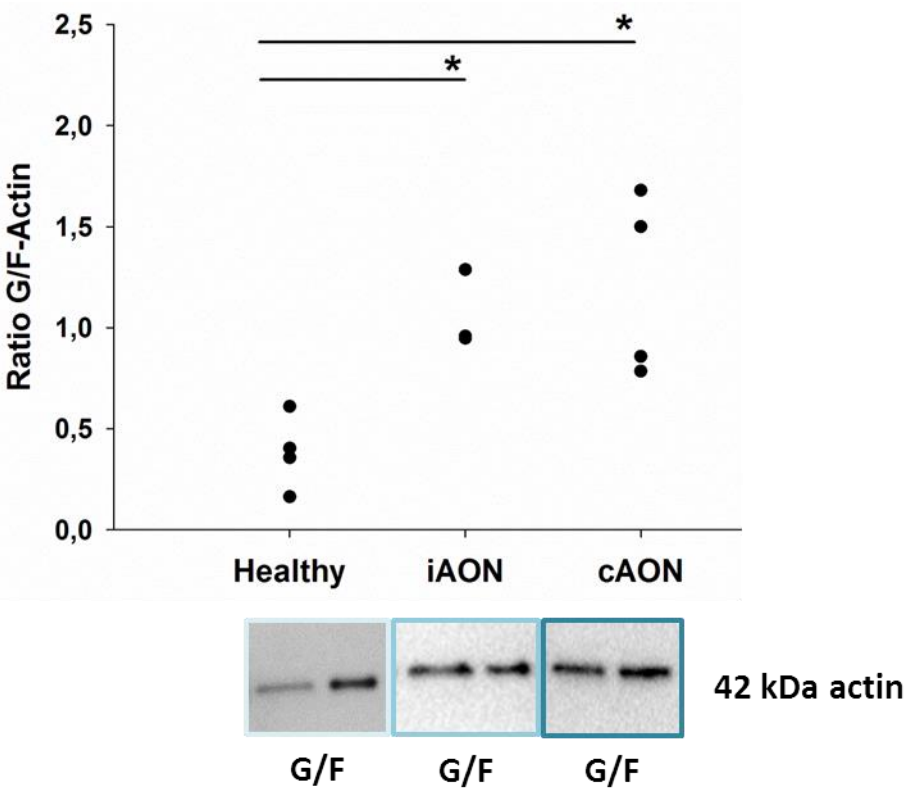

Figure 4.4.1. Actin network disassembly during AON. The G/F-actin ratio increases in the optic nerve during disease progression. This increase in ratio is detectible starting from the iAON (* $p < 0.05$, one way ANOVA with post hoc Dunnett's multiple comparison test; n = 4 animals per time point).

4.4.2 Expression of proteins associated with actin cytoskeleton changes during AON

Considering that changes in the actin network were observed during AON in the optic nerve, the expression of proteins implicated in actin network dynamics that are affected in the process of apoptosis by caspases, gelsolin (a mediator of F-actin disassembly) and fractin (a G-actin monomer cleavage product), were investigated by Western blot.

The expression of these proteins was found to be changed during AON. There was a statistically significant decrease of gelsolin levels in both iAON (0.55 ± 0.05, $p = 0.014$) and cAON (0.34 ± 0.06, $p < 0.001$) when compared to healthy animals (0.77 ± 0.07, Figure 4.4.2.A). Conversely, there was a significant accumulation of the G-actin cleaved product fractin in optic nerves from both iAON (0.48 ± 0.07, $p = 0.012$) and cAON (0.64 ± 0.09, $p < 0.001$), when compared to healthy animals (0.17 ± 0.04; Figure 4.4.2.B).

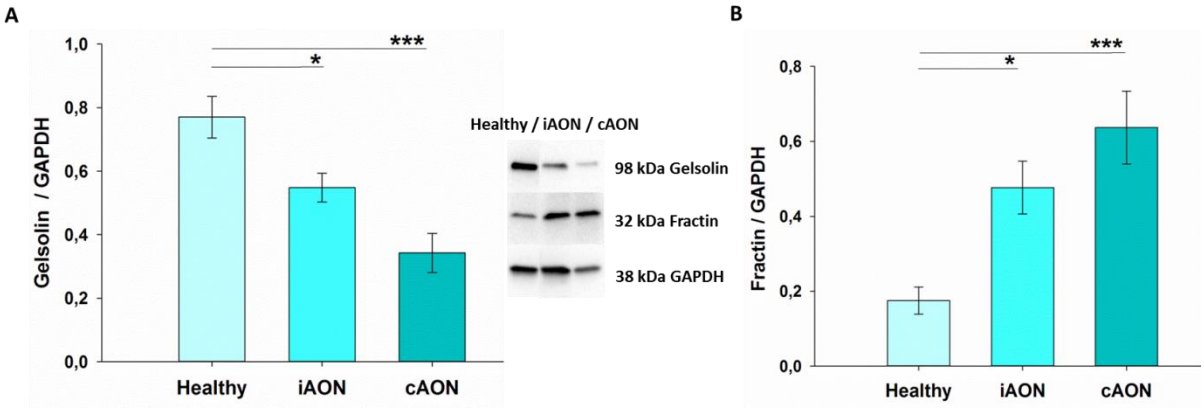

Figure 4.4.2. F-actin severing protein gelsolin and G-actin are both affected during AON. (A) Gelsolin levels decrease during AON. **(B)** Fractin levels are increased during AON. (* $p < 0.05$; *** $p \leq 0.001$, ANOVA with post hoc Dunnett's multiple comparison test; n = 6 animals per time point).

4.5 Intravitreal injection of glutamate as a model of primary RGC loss

Intravitreal injection (IVI) of excessive levels of different glutamate receptor agonists has long been known to induce the loss of RGCs and their axons in the optic nerve (Luo et al., 2001; Chidlow et al., 2008). The phenomenon of glutamate excitotoxicity is suspected to play a role in the animal model of AON since

the initial RGC loss correlates with increased Ca^{2+} levels in the retina (Hoffmann et al., 2013). In addition, minocycline treatment was shown to reduce retinal glutamate levels during iAON (Maier et al., 2007). In order to examine this hypothesis, naive BN rats following IVI with 100 nmoles of glutamate were examined 24 hours later to determine if it resulted in optic nerve and retina alterations similar to those observed during AON.

4.5.1 RGC loss following IVI of glutamate

Anti-Rbpms immunostaining was used in order to quantify the density of surviving RGCs following the injection of glutamate (Figure 4.5.1.A). The density of RGCs in glutamate-injected retinas (1931 ± 75 RGC per mm^2) was found to be significantly decreased compared to control animals receiving IVI of saline (2217 ± 54 RGC per mm^2, p = 0.013). In addition, RGC loss was confirmed by TUNEL assay (Figure 4.5.1.B). $TUNEL^+$ cells were also found in other retinal layers (inner and outer nuclear layers) similar to what was observed in retinas from animals with AON (Fairless et al., 2012).

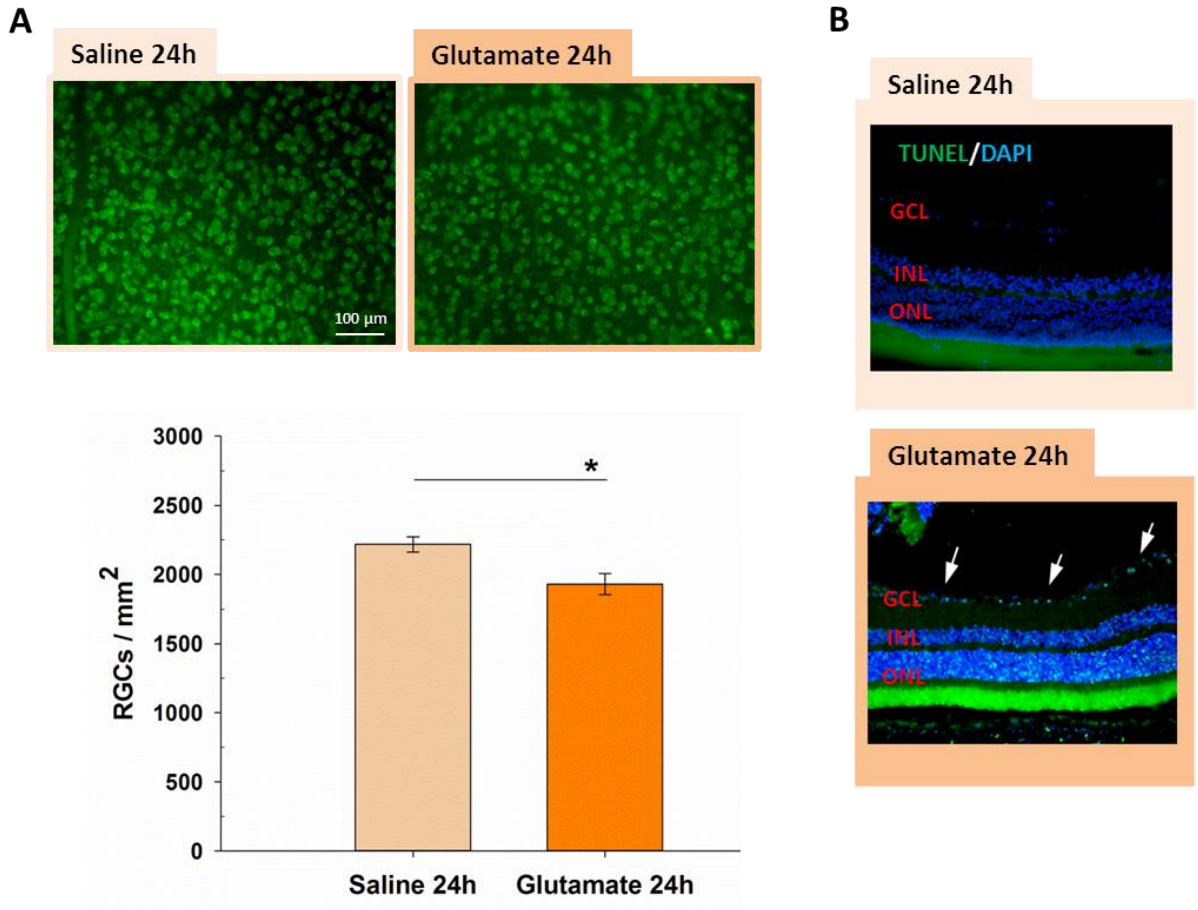

Figure 4.5.1. Intravitreal glutamate injection leads to RGC loss. (A) Retinal whole-mount stained with the Rpbms antibody 24h following intravitreal injection of saline or glutamate. In the glutamate injected retinas, RGC numbers were significantly reduced compared to the saline injected (n = 4 animals / 8 retinas; * p < 0.05, Student t-test). **(B)** $TUNEL^+$ cells were found only in retinas of animals that received the IVI of glutamate (white arrows point at TUNEL positive cells in ganglion cell layer-GCL; inner nuclear layer-INL; outer nuclear layer-ONL).

4.5.2 Axonal transport profile following IVI of glutamate

Immunofluorescent staining of optic nerve sections was performed in order to investigate whether IVI of glutamate would cause the failure of axonal transport. The accumulation of proteins involved in axonal transport (Kin, Syn, βAPP), which would be indicative of its failure, was not observed 24 hours following IVI of glutamate neither in the ONH (Figure 4.5.2.A), nor in the distal segment of the optic nerve (Figure 4.5.2.B).

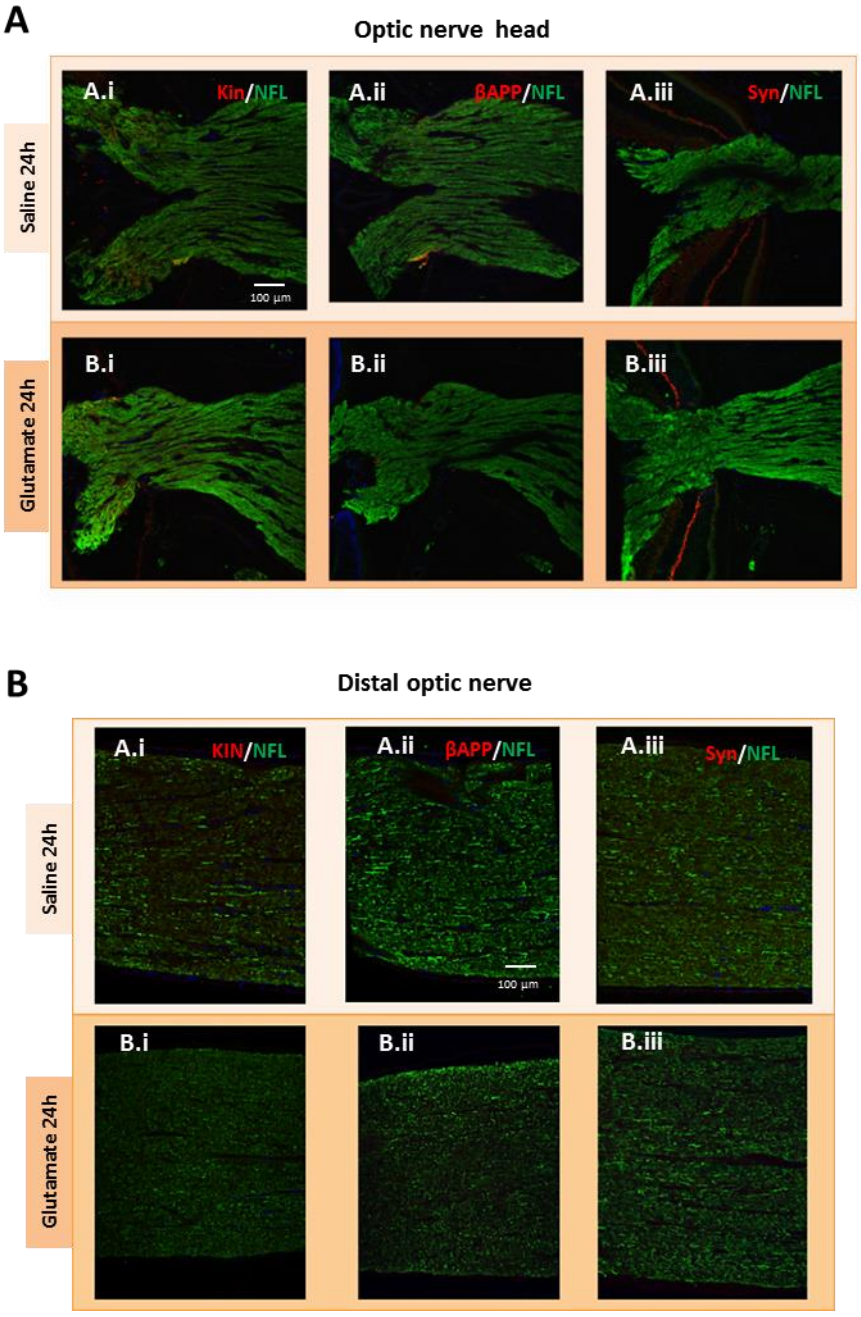

Figure 4.5.2. Axonal transport deficits are not detected 24 hours following IVI of glutamate. No visible accumulation of axonal transport proteins (Kin (A-B.i), βAPP (A-B.ii), Syn (A-B.iii); red)was detected 24 hours following intravitreal injection of glutamate in the ONH **(A)** or along the optic nerve **(B)** (n = 3 per time point).

4.5.3 G/F-actin ratio is increased in optic nerves following IVI of glutamate

G/F-actin assay was used in order to investigate whether IVI of glutamate affects the actin cytoskeleton in a similar way to that observed in AON. The G/F-actin ratio was found to be significantly increased in animals injected with glutamate (1.75 ± 0.47, p = 0.011; Figure 4.5.3) when compared to saline injection (0.53 ± 0.08). Again, this was similar to that observed in animals with AON, compared to healthy ones (Figure 4.4.1).

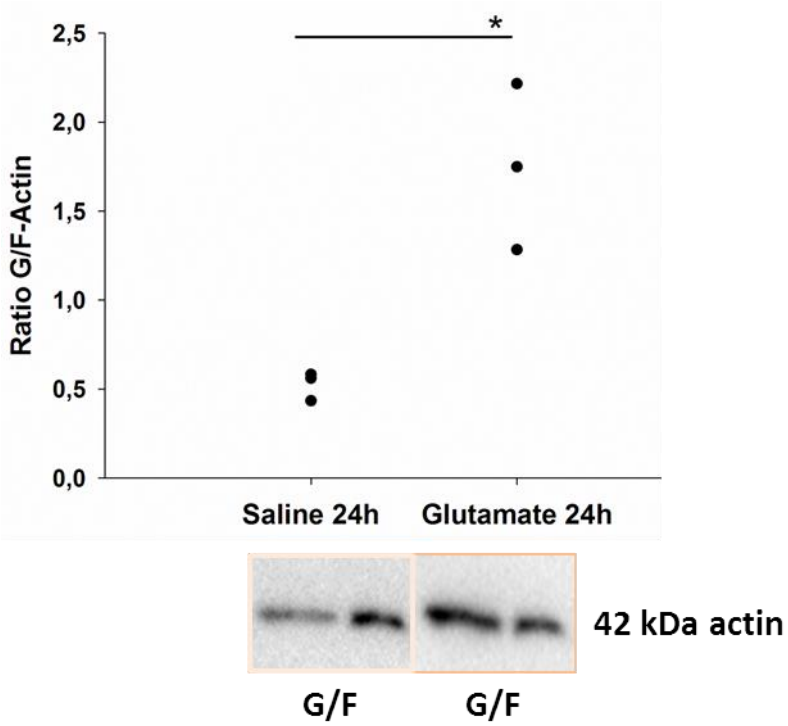

Figure 4.5.3. IVI of glutamate affects the organization of the optic nerve actin network. An increase in the G/F-actin ratio is detectible in optic nerves 24 hours following the IVI of glutamate (n = 3, *p ≤ 0.05, compared to saline injected animals, Student's t-test).

4.6 Blockade of the NMDA receptor protects RGCs and reverses actin network changes in the optic nerve during iAON

In order to confirm if NMDA glutamate receptors are involved in early RGC loss and changes in the optic nerve actin network during iAON, IVI of NMDA-receptor blocker MK801 (dizocilpine) was performed. MK801 was chosen since it is a use-dependent and prolonged blocker that exerts stable effects for some time after the drug has been washed out (Huettner & Bean, 1988; McKay et al.,

2013). Since the G/F actin ratio was altered during iAON in a similar way to IVI of glutamate, the next question was whether glutamate receptor blockade would therefore reduce these observed alterations. Previously, it was shown that systemic application of MK801 was neuroprotective during AON (Sühs et al., 2014). However, this neuroprotective effect in the retina may have been observed because of the overall change in EAE progression after systemic blocker application. In this study, IVI of MK801 was applied in order to affect only AON progression and therefore reduce retinal deterioration. Animals received IVI of MK801 twice during iAON: at day 4 p.i., a day prior to the earliest reported RGC loss (Fairless et al., 2012) and repeated at day 7 p.i. to ensure prolonged blocker effect. Animals were sacrificed at late stage iAON, day 10 p.i.. The density of surviving RGCs was significantly elevated in the MK801 treatment group (2331 ± 34 RGC per mm^2, p = 0.0005) compared to the control saline group (2136 ±27 RGC per mm^2, Figure 4.6.1.A) during iAON.

G/F-actin assay was used in combination with MK801 treatment. Following IVI of MK801, the G/F-actin ratio was significantly decreased (0.25 ± 0.04, p = 0.016), compared to the saline injected animals (0.82 ± 0.17). In addition to restoring the G/F-actin ratio to values found in healthy optic nerves (Fig. 4.4.1), MK801 treatment during iAON also led to changes in the expressional changes in both gelsolin and fractin in optic nerves. Gelsolin levels in MK801-treated animals were significantly increased (0.70 ± 0.04) compared to saline-treated animals (0.43 ± 0.03, p = 0.0005) during iAON. Levels of fractin were significantly decreased following IVI of MK801 (0.12 ± 0.03) when compared to saline-injected animals (0.32 ± 0.03, p = 0.002).

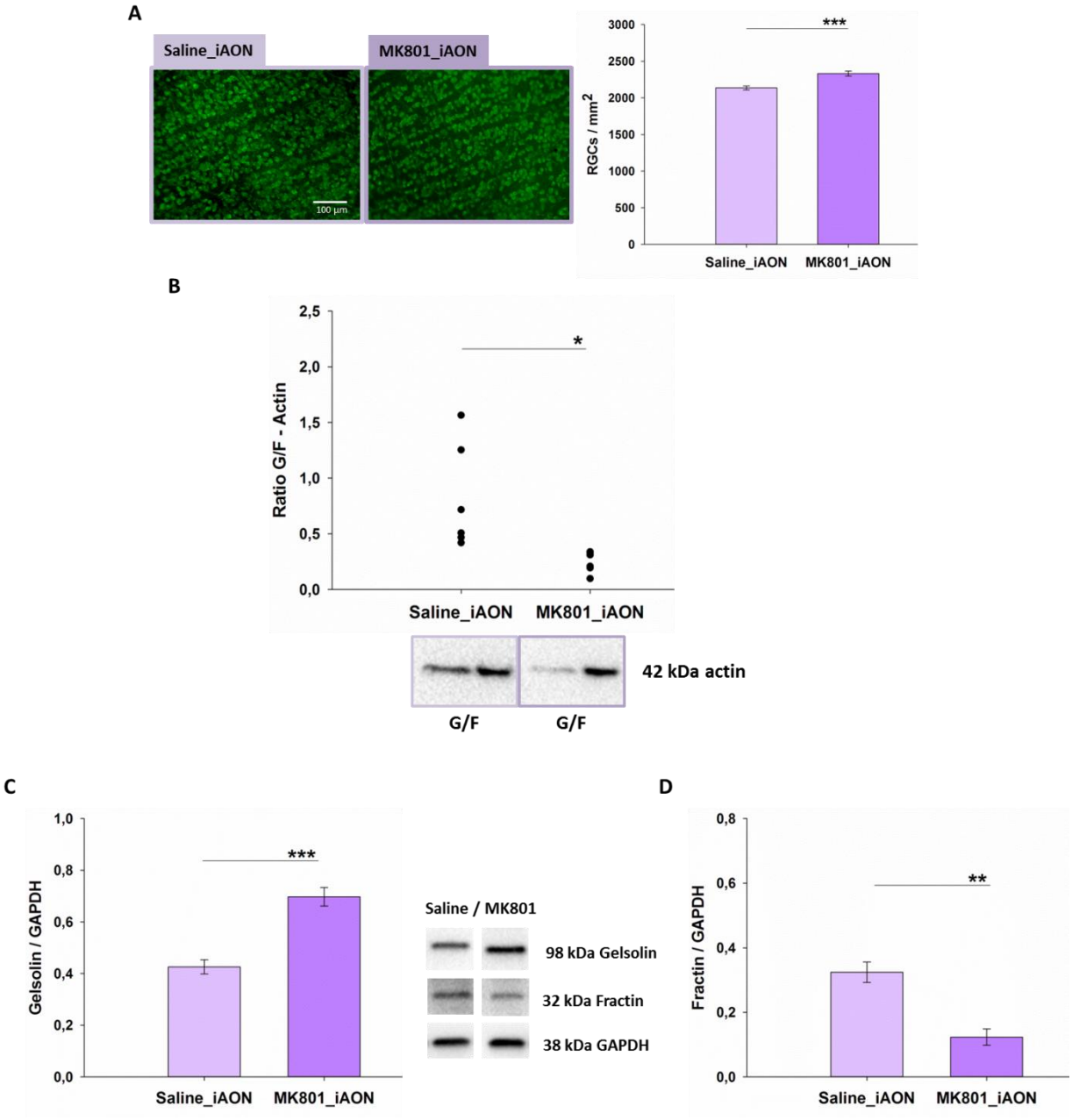

Figure 4.6. IVI of MK801 in the early phase of iAON is neuroprotective. (A) The density of RGCs is significantly increased following MK801 treatment compared to the control saline group during iAON (n = 4 animals /8 retinas per group; *** $p < 0.001$, Student t-test). **(B)** The G/F-actin ratio is decreased following IVI of MK801 when compared to saline-injected animals (n = 6 animals per group, *$p < 0.05$, Student t-test). MK801 treatment leads to a significant increase of gelsolin **(C)** and a decrease of fractin **(D)** in the optic nerve when compared to control animals (n = 5 for saline and n = 4 animals for MK801 treatment, ** $p \leq 0.01$, *** $p < 0.001$, Student's t-test).

4.7 mRNA expression of Ca^{2+}-permeable channels in RGC is regulated during the course of AON

The treatment with NMDA receptor blockers (see previous chapter) as well as previous works (Gadjanski et al., 2009; Hoffmann et al., 2013; Sühs et al., 2014) highlighted the importance of Ca^{2+} dynamics in the pathophysiology of AON. Taking this into consideration, qRT-PCR on acutely isolated RGCs (two hours following euthanasia of animals, thus representing physiology of RGCs at the time of isolation) was used in order to investigate whether channels involved in Ca^{2+} dynamics are differentially expressed during AON. NCX1 and PMCA3 were found to be significantly up-regulated during iAON while the L-type VGCC, and subunits of the NMDA (Grin2b) and AMPA (GluR1) receptors were up-regulated during cAON (Table 4.7).

Calcium related channels	Healthy Mean ± SE (x 10^{-3})	iAON Mean ± SE (x 10^{-3}) (p value to Healthy)	cAON Mean ± SE (x 10^{-3}) (p value to Healthy)
Sodium-Calcium Exchanger			
NCX1	5.0 ± 0.6	**7.6 ± 0.9** (**p < 0.05**)	7.3 ± 0.1
NCX2	3.2 ± 0	3.6 ± 0.6	3.8 ± 0.7
NCX3	0.92 ± 0.2	1.1 ± 0.2	1.2 ± 0.2
Calcium Pump			
PMCA1	10.7 ± 0.7	12 ± 1	17 ± 2
PMCA2	15 ± 1	21 ± 3	17 ± 1
PMCA3	7 ± 1	**17 ± 4** (**p < 0.05**)	10 ± 1
Voltage Gated Calcium Channel			
Cacna1a (P/Q-type)	17 ± 3	14 ± 2	20 ± 3
Cacna1b (N-type)	0.08 ± 0.02	0.10 ± 0.02	0.10 ± 0.03
Cacna1c (L-type)	0.46 ± 0.03	0.59 ± 0.04	**0.71 ± 0.05** (**p ≤ 0.01**)
NMDA receptor			
Grin1a	30 ± 7	31 ± 3	37 ± 1
Grin2	4.76 ± 0.07	5 ± 1	4.5 ± 0.6
Grin2b	1.6 ± 0.2	1.4 ± 0.4	**2.9 ± 0.3** (**p < 0.05**)
AMPA receptor			
GluR1	3.4 ± 0.5	4.2 ± 0.4	**5.6 ± 0.6** (**p < 0.05**)
GluR2	4.2 ± 0.4	3.9 ± 0.4	5.2 ± 0.1
GluR4	4.5 ± 0.4	4.9 ± 0.5	6.4 ± 0.8

Table 4.7. Screening of Ca^{2+} related channel expression in RGCs acutely isolated at different time points during AON. Data were analyzed with the 2−[ΔΔCt] method, with GAPDH as the internal control (n = 6 for healthy and iAON; n = 5 for cAON). The values presented in the table are coefficients with 10^{-3} base. The expression of channels during iAON and cAON was compared to healthy values using the one way ANOVA with post hoc Dunnett's multiple comparison test (NCX1, Cacna1c, Grin2b, GluR1) and Kruskal-Wallis test on ranks followed by Dunn's multiple comparison test (PMCA3).

4.8 Utilization of primary RGC cultures for studying Ca^{2+} responses following glutamate stimulation

The primary RGC culture was used as an *in vitro* model to study Ca^{2+} dynamics following glutamate receptor stimulation. The culture conditions used in this study were established previously by Barres et al., 1998. RGC medium (RGM, see chapter 3.5) includes BDNF, CNTF and forskolin previously described to provide best conditions for RGC viability (Meyer-Franke et al., 1995). However, the presence of growth factors might interfere with glutamate-induced neuronal excitotoxicity (Melo et al., 2013).In this study, we first tested if it would be possible to take them out of the RGM. In the case they were kept in RGM, RGCs underwent neurite extension within two weeks, as observed with immunostaining for pan-axonal marker (SMI312; Figure 4.8.A). In the case BDNF, CNTF and forskolin were omitted from the medium, cells viability was significantly decreased after two days *in vitro* (56 ± 1%) compared to the cells kept in RGM (45 ± 3%, p = 0.03; Figure 4.8.B). This decline in cell viability without BDNF, CNTF and forskolin in RGM progressed further after four days *in vitro* (55 ± 3%) compared to the cells in RGM (27 ± 3, p = 0.002; Figure 4.8.C). Considering this, RGM was used for cultivation of primary RGCs in all experiments.

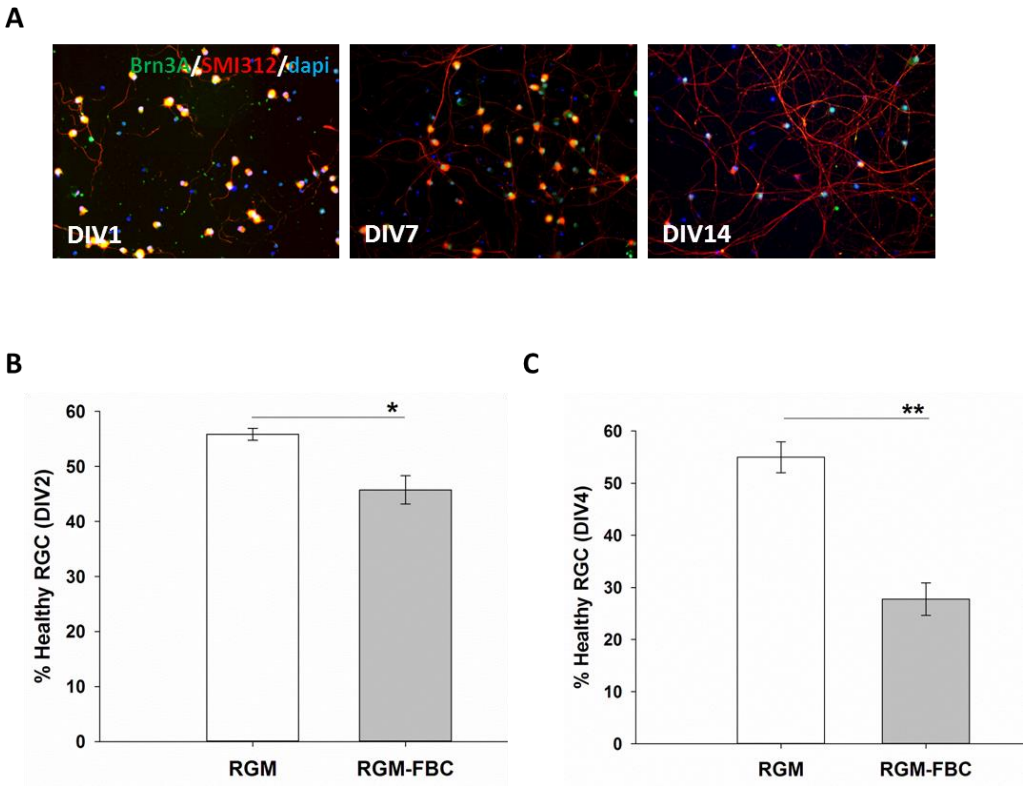

Figure 4.8. RGC viability is dependent on BDNF, CNTF and forskolin. (A) Examples of RGC differentiation at different time points in the RGM. This was true only in the case RGCs were kept in RGM. Live dead assay on isolated RGCs in different medium conditions after two **(B)** and four **(C)** days *in vitro* was significantly decreased (RGM: full mediumRGM-FBC: full medium without forskolin, BDNF and CNTF; n = 4, * $p < 0.05$, ** $p \leq 0.01$, DIV2-Mann-Whitney Rank Sum Test, DIV4-Student's t-test).

4.8.1 Primary RGC culture is not prone to glutamate excitotoxicity

Glutamate excitotoxicity is one of the proposed mechanisms of neurodegeneration in the retina under different pathological conditions (see chapter 1.9.2). The question of glutamate excitotoxicity in cultivated RGCs has been controversial since previously published works gave conflicting results with regard to whether RGCs were susceptible to glutamate excitotoxicity in culture (Ullian et al., 2004; Hartwick et al., 2008). In order to investigate the viability of primary RGC culture following prolonged exposure to toxic levels of glutamate, a cell toxicity assay was performed using EthD1 labelling. Cells were exposed to 100 µM glutamate and 10 µM glycine (NMDA receptor co-agonist) in RGM over the course of 24 hours (Figure 4.8.1.A). There was no significant difference observed between the numbers of healthy RGCs in the control versus the glutamate-treated group (Figure 4.8.2.B).

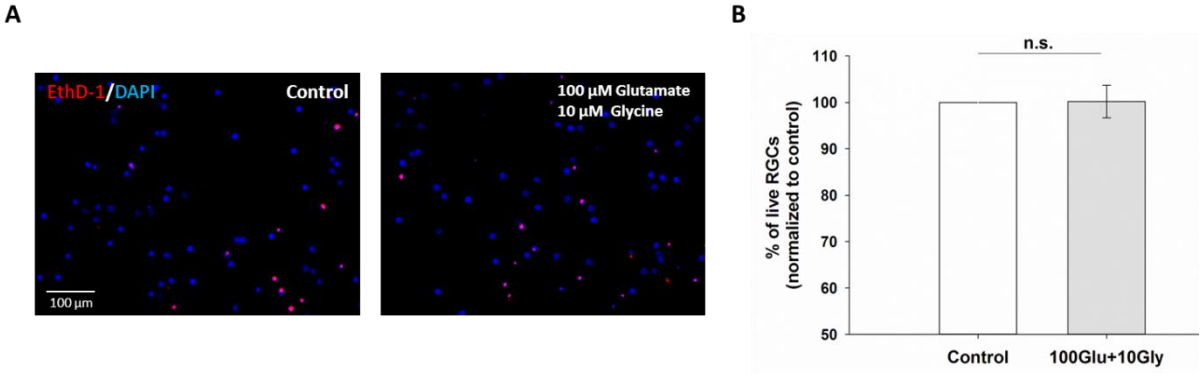

Figure 4.8.1. RGC invulnerability to glutamate excitotoxicity. (A) Cell toxicity assessment of isolated RGCs in control conditions (left) and 24 hours following glutamate exposure (right). Dying cells are labeled with EthD-1 (red) and have shrunken nuclei. **(B)** The percentage of dead cells compared to the total cells counted (number of DAPI-positive cells – both healthy and shrunken) was not changed following RGC exposure to glutamate (n = 6 experiments; Student's t-test).

4.8.2 Ca^{2+} dynamics in primary RGCs following glutamate receptor stimulation

In order to investigate Ca^{2+} dynamics following glutamate receptor stimulation of primary RGCs, ratio-metric Fura-2 Ca^{2+} imaging was used. Glutamate receptors were stimulated by addition of different agonists in the imaging solution: glutamate and glycine, NMDA or AMPA. In control experiments, only imaging solution was added (Figure 4.8.2.A). Agonist application induced an initial Ca^{2+} response, which was greatest for co-application of glutamate and glycine, followed by NMDA, and then AMPA (Fig. 4.8.2.B.iii). This is expected since glutamate stimulates both NMDA and AMPA

receptors and NMDA receptors have a greater permeability coefficient for Ca^{2+} than AMPA receptors (Traynelis et al., 2010). Cells were then maintained for between 1 and 1.5 hours in order to observe the phenomenon of delayed calcium deregulation (DCD), considered to be an essential factor leading to cell death (Budd & Nicholls, 1996; Tymianski et al., 1993). Only a few cells underwent DCD (Figure 4.8.2.A, traces in red) irrespective of the agonist they were exposed to (glutamate and glycine 4.2%, n = 5/119; NMDA 0.85%, n = 3/352; AMPA 1%, n = 2/216). Interestingly, this was also observed under control conditions (6%, n = 5/85).

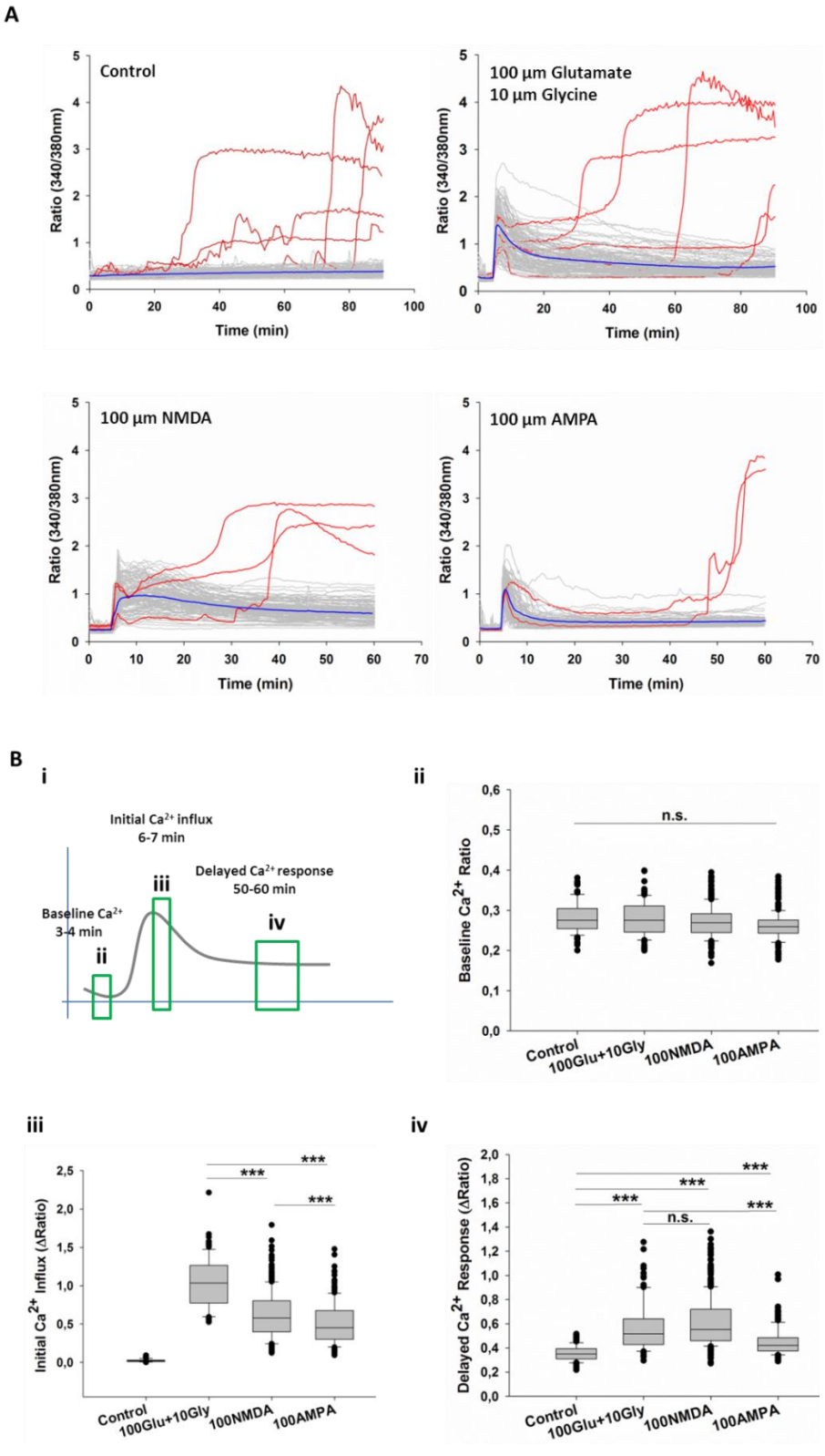
A
Control
100 µm Glutamate
10 µm Glycine
100 µm NMDA
100 µm AMPA
Ratio (340/380nm)
Time (min)
B
i
Initial Ca2+ influx
6-7 min
Delayed Ca2+ response
50-60 min
Baseline Ca2+
3-4 min
ii
iii
iv
ii
Baseline Ca2+ Ratio
n.s.
iii
Initial Ca2+ Influx (ΔRatio)
iv
Delayed Ca2+ Response (ΔRatio)
***
n.s.
Control
100Glu+10Gly
100NMDA
100AMPA

Figure 4.8.2. RGC Ca^{2+} dynamics following glutamate receptor stimulation. (A) Ca^{2+} dynamics of isolated RGCs after treatment with different glutamate receptor agonists (addition 5 mins into recording) over 70-90 min. Ca^{2+} traces of individual RGCs are shown in grey, except for those that later underwent DCD, which are shown in red. The blue line represents the average response of RGCs not undergoing DCD **(B.i)** Scheme representing time points at which individual traces were used for quantification in B.ii-iv. **(B.ii)** Baseline Ca^{2+} levels were equivalent prior to agonist stimulation in all four experimental groups. **(B.iii)** Ca^{2+} increase was the highest in RGCs exposed to glutamate and glycine. **(B.iv)** Prolonged glutamate receptor stimulation led to a significant increase in intracellular Ca^{2+} when compared to control non-stimulated cells. Experimental groups were compared either to control or to glutamate-glycine treated group using Kruskal-Wallis test on ranks followed by Dunn's multiple comparison test and Mann-Whitney Rank Sum Test in the case only two groups were compared (n.s. - not significant, *** $p < 0.001$).

4.8.3 Role of NCX in Ca^{2+} dynamics following glutamate stimulation of RGCs

The role of NCX in Ca^{2+} intracellular extrusion/influx following glutamate receptors stimulation has been already addressed in several studies on isolated CNS neurons (Bano et al., 2005; Araujo et al., 2007), but so far not on isolated RGCs. NCX1 channel expression on RGCs was observed with immunocytochemistry (Figure 4.8.3.1.A). In addition, mRNA levels of NCX1 were increased in cultured RGCs (Figure 4.8.3.1.B), as well as in RGCs isolated from iAON (Table 4.7). NCX essentially has two modes of action: in physiological conditions it is assumed to work predominantly in forward - mode, extruding Ca^{2+} from the cell together with PMCA. However, in the conditions of high intracellular Na^{+} levels, it may act to bring more toxic Ca^{2+} into the cell (Stys et al., 1997). In order to test if NCX contributes to intracellular Ca^{2+} increase following glutamate receptor stimulation the NCX reverse-mode blocker SEA0400 (2-[4-[(2,5-difluorophenyl)methoxy]phenoxy]-5-ethoxyaniline) was used. This blocker is considered to be the most potent and specific NCX reverse-mode blocker with a high specificity for the NCX1 isoform (Matsuda et al., 2001).

The effect of SEA0400 on Ca^{2+}-dynamics following glutamate-glycine stimulation was investigated using ratio-metric Fura-2 Ca^{2+} imaging (Figure 4.8.3.2). In control experiments, only the imaging solution was added at the second and fifth minute into recording (n = 190 cells). After beginning of recording, cells were either pre-treated with/without NCX blocker (10 nM, n = 216; 100 nM n = 196; 1 µM, n = 148) 3 minutes prior to addition of glutamate-glycine (Fig 4.8.3.2.A). Application of different concentrations of SEA0400 alone to the imaging solution did not affect basal Ca^{2+} levels on isolated RGCs (Figure 4.8.4.B.i). However, once glutamate-glycine stimulation was applied, immediately (Figure 4.8.4.B.ii., red circles) and a few minutes later (Figure 4.8.4.B.ii, black diamonds), Ca^{2+} levels were significantly lower if cells were pre-treated with SEA0400. In both cases the magnitude of the Ca^{2+} decrease was found to be dependent on the concentration of SEA0400 (Figure 4.8.4.B.ii).

A

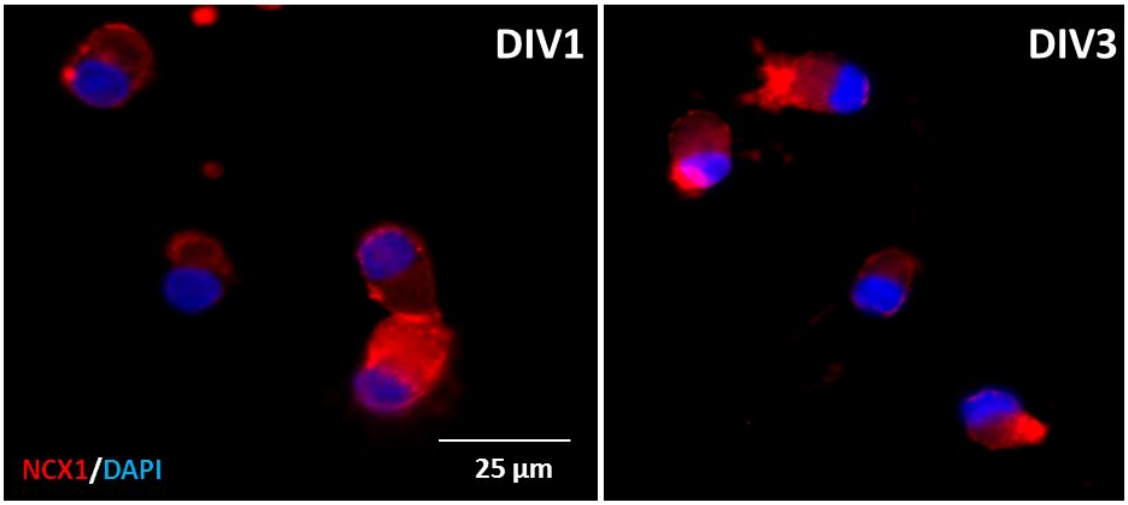

B

Calcium related channels	Acute RGCs Mean ± SE (x 10^{-3})	DIV3 RGCs Mean ± SE (x 10^{-3}) (p value to acute)
Sodium-Calcium Exchanger		
NCX1	9 ± 1	22.3 ± 0.5 **(p = 0.0003)**
NCX2	9 ± 2	6 ± 1
NCX3	2.0 ± 0.2	0.7 ± 0.1 **(p = 0.002)**

Figure 4.8.3.1 NCX1 expression on P7-8 isolated RGCs. (A) NCX1 staining of isolated RGCs following one (DIV1) and three days (DIV3) in culture. **(B)** qRT-PCR of NCX isoforms expression were analyzed with the $2^{-[\Delta\Delta Ct]}$ method, with GAPDH as the internal control (n = 3). The values presented in the table are coefficients with 10^{-3} base. The expression of NCX in acutely isolated and RGCs in culture after three days were compared using the one way ANOVA with post hoc Dunnett's multiple comparison test.

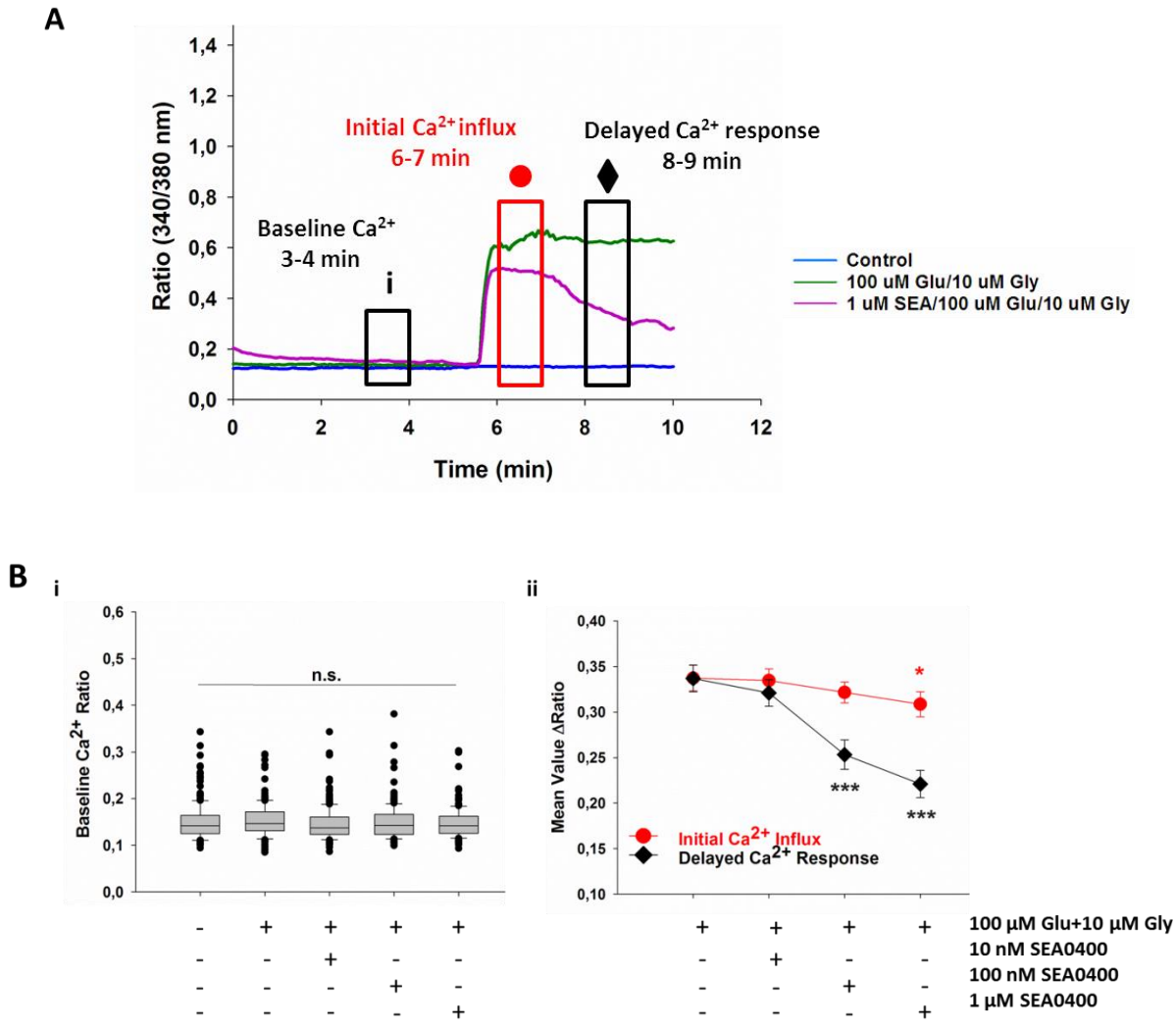

Figure 4.8.3.2 SEA0400 reduces the Ca^{2+} increase following glutamate receptor stimulation of isolated RGCs. (A) Representative example traces of control experiments (blue); glutamate-glycine stimulation (green); SEA0400 blocker application prior to glutamate-glycine addition (purple). Rectangles represent time points at which individual traces were used for quantification. **(B.i)** Baseline Ca^{2+} levels were not changed following SEA0400 addition into the imaging solution. **(B.ii)** The increase of Ca^{2+} following glutamate-glycine addition (5^{th} minute into recording) was dependent on concentration of SEA0400. Levels of Ca^{2+} recorded several minutes (8-9 mins) following glutamate-glycine addition were also dependent on the SEA0400 concentration present in the imaging solution. Levels of Ca^{2+} following glutamate-glycine stimulation is stable for 5 min following addition while they decrease when cells were pre-treated with SEA0400. Experimental groups were compared using Kruskal-Wallis test on ranks followed by Dunn's multiple comparison test (n.s. - not significant, * $p < 0.05$, *** $p < 0.001$).

4.9 Treatment study with NCX1 receptor blocker SEA0400 in AON

In chapter 4.6, a possible role for Ca^{2+} in the process of RGC loss in iAON was supported by the protective effect of MK801 application. It was therefore of interest to see whether NCX also played a role in the process of iAON-associated RGC degeneration, perhaps acting downstream of glutamate activation. In order to address this question, application of the NCX reverse-mode blocker SEA0400 in a disease setting was made.

Intravitreal application of SEA0400 during the early iAON was performed in the same way as with the MK801 treatment: at day 4 p.i., a day prior to the earliest reported RGC loss (Fairless et al., 2012) and at day 7 p.i. to ensure prolonged blockade. Animals were sacrificed in late stage iAON, day 10 p.i.. IVI of SEA0400 did not show any protective effect on RGC survival in treated (2150 ± 23 RGC per mm^2, Figure 4.9.A) versus control (2111 ± 32 RGC per mm^2) animals. Similarly, in the optic nerve, the actin G/F-actin ratio in SEA0400-treated animals (1.2 ± 0.2, Figure 4.9.B) was not different compared to control saline-injected animals (1.5 ± 0.2). Similar results were observed following IVI of glutamate where co-application of SEA0400 had no effect (data not shown).

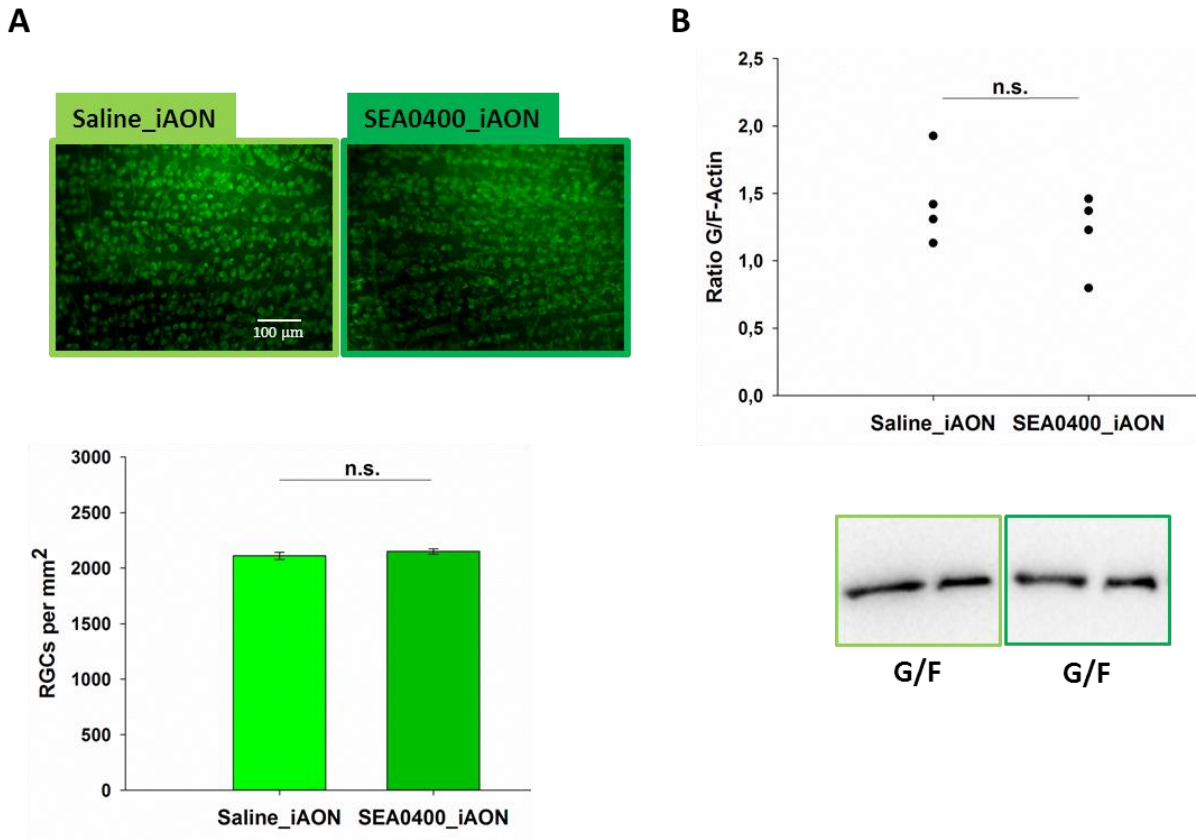

Figure 4.9. SEA0400 treatment during iAON did not show neuroprotective effects during iAON. **(A)** The density of $Rbpms^+$ RGCs was not significantly different in control compared to SEA0400-treated animals (n = 6, n.s. - not significant; Student t-test). **(B)** Also, the optic nerve G/F-actin ratio remained unchanged irrespective of treatment with SEA0400 (n = 4 per, n.s. – not significant, Student's t-test).

5 Discussion

5.1 Anti-Rbpms staining can be used for detection of RGC loss in iAON

Retinal degeneration is connected with many ophthalmological and systemic neurodegenerative diseases including glaucoma, age-related macular degeneration, retinitis pigmentosa, cancer and autoimmune diseases, including MS (Balendra et al., 2015). In MS, ON is a common first sign of disease development (Balcer, 2006). The appearance of BBB disruption and inflammatory demyelinated lesions in the optic nerve is accompanied by retinal degeneration (Roed et al., 2005; Green et al., 2010; Syc et al., 2012; Kupersmith et al., 2016). However, changes in the retina, observed by ganglion and inner retinal layers have also been observed in the eyes of some MS patients irrespective of the presence of ON (Saidha et al., 2011; Walter et al., 2013). These findings, together with the detection of GM lesions in the cortex and axonal changes in the NAWM initiated the research of neurodegenerative processes in MS irrespective of primary demyelination (Haines et al., 2011).

There is a variety of techniques available for the assessment of RGC loss in different experimental models. Genetically modified animals with fluorescently labelled RGC-specific markers, such as Thy1, can be used for the *in vivo* detection of retinal degeneration (Leung et al., 2008). Specific labelling of apoptotic RGCs can be performed with an annexin V-based method - Detection of Apoptotic Retinal Cells (DARC; Guo & Cordeiro, 2008) or with the use of a small cell-permeable caspase-activated imaging probe CapQ (Galvao et al., 2013). One of the most widely used methods is retrograde labeling of RGCs by the injection of lipophilic dyes into the superior colliculi. One of these dyes, Fluoro-gold, is assumed to label cells by crossing cell membranes in its uncharged form but ultimately is trapped within lysosomes and endosomes by a favourable pH gradient (Wessendorf, 1991). RGCs can also be quantified in retinal whole-mounts and sections with the use of RGC-specific antibodies, such as Brn3a (Nadal-Nicolás et al., 2012: Lanz et al., 2017) and Rbpms (Rodriguez et al, 2014) or with nonspecific, pan-neuronal antibodies such as NeuN (Wang et al., 2005; Dijk et al., 2007).

However in different models of optic nerve and retinal injury, the extent of RGC loss can vary significantly depending on the technique used. The loss of RGCs might be over- or underestimated due to the specificity of the method used for labelling. For example, Fluoro-gold was shown to spread into amacrine cells (Abdel-Majid et al., 2005) and in the case of retinal injury even into microglia/macrophages via phagocytosis (Heiduschka et al., 2010; Mead et al., 2014). By counting only the number of cells in the ganglion cell layer, one can overestimate the number of RGCs, due to

the presence of displaced amacrine cells and astrocytes, which can comprise up to 50% of the total cell population in this layer (Perry, 1981; Mead & Tomarev, 2016). On the other side, several RGC-specific antibodies can also lead to erroneous interpretations of RGC loss, since they only label a sub-population of the RGCs - an issue that is commonly overlooked (Sanes & Masland, 2015). For example, Brn3a-specific labelling has been shown to underestimate RGC number in the rodent retina (Nadal-Nicolás et al., 2015).

Fluoro-gold has been used previously in the BN-AON model where it was proven to be sensitive enough to detect the RGC loss in iAON (Hobom et al., 2004; Fairless et al., 2012). However, this method is time costly - animals need to be injected at least a week prior to MOG immunization to avoid any possible axonal retrograde transport deficits in the optic nerve that would affect vesicular tracer transport to the RGC bodies. Also the method itself is invasive – surgical procedure needs to be performed in order to inject the tracer into the areas of the brain that are targeted by RGC axonal projections (superior colliculi). Finally, RGC quantification needs to be performed soon following retinal removal because of the fast bleaching properties of Fluoro-gold. In this study, a relatively novel antibody against Rbpms was used to label RGCs. Rpbms as an RGC-specific marker was suggested a decade ago following a study on the gene expression profile of RGCs (Piri et al., 2006). It has been shown to be superior to Fluoro-gold since it does not label disperse amacrine cells and, is stable following injury unlike Brn3a (Rodriguez et al, 2014).

In the present study, Rbpms staining was specific and sensitive enough to confirm RGC loss during iAON (Figure 4.2). The total density of RGCs per mm^2 was decreased around 10% in iAON compared to healthy animals. In a previous study by our group using the same BN-AON model, it was reported that Fluoro-gold labelling revealed an RGC loss of about 20% at the same disease stage compared to healthy animals (Fairless et al, 2012). This discrepancy in RGC loss might come from differences in the total RGC number counted. In healthy animals, total RGC number per mm^2 following Fluoro-gold labelling was reported to be 2046 ± 208 (Fairless et al., 2012) compared to the 2391 ± 45 cells per mm^2 found in this study with anti-Rbpms antibody. Lower RGC loss in the case of Rbpms staining could be due to the fact that in this case all RGCs are counted, while in the case of Fluoro-gold only the populations of RGCs whose axons terminate in the superior colliculi are being quantified. It could be possible that within Fluoro-gold labelled RGCs there are sub-populations of cells that are particularly vulnerable to pathological signals during iAON. This would explain why in the case of Rbpms staining, when all RGCs are taken into account, the Fluoro-gold sub-populations contribute less in overall RGC count statistics. For example, following optic nerve crush it was observed that largest RGC types, alpha-RGCs (αRGCs), survive preferentially but not exclusively following such kind of injury (Duan et al., 2015). The other possibility might be that Fluoro-gold heavily labelled amacrine

cells as well, and that 10% higher increase in what is supposedly RGC loss comes from those retinal interneurons.

5.2 Axonal transport deficits do not precede RGC loss during iAON

One of the possible mechanisms that have been proposed to contribute to MS neurodegeneration is impairment of axonal transport (Lingor et al., 2012). Recent studies have shown that axonal transport deficits are observed following the onset of inflammatory demyelination in both optic nerves (Lin et al., 2014) and spinal cords (Sorbara et al., 2014) of EAE mice.

The primary cause of early RGC loss in AON is currently still unknown. One of the proposed mechanisms could be axonal transport deficits as suggested in the model of glaucoma. In this model, axonal transport deficits were observed prior to RGC loss in the retina (Chidlow et al., 2011). In the ONH, RGC axons are naturally unmyelinated which makes them potentially more vulnerable to harmful influences. In our model, disruptions in the BBB in the ONH and BRB together with the activation of microglia in both compartments were observed during iAON (Fairless et al., 2012). It could be hypothesized that activated microglia might damage axons through production of ROS/RNS leading to mitochondrial damage and increased axonal Ca^{2+} (see chapter 1.5). Downstream of this Ca^{2+} increase, axonal transport deficits and axonal cytoskeleton network might then be disturbed, leading to and axonal swellings.

In the present study, both the ONH and distal parts of the optic nerve were inspected for axonal transport defects during AON. Our hypothesis was that if the axons were damaged prior to RGC bodies, axonal transport accumulation would be visible due to normal protein production but obstructed within stressed axons, as was suggested in the animal model of glaucoma (Chidlow et al., 2011). However, if the primary damage would be to the RGC bodies in the retina, this might impair protein production and thus have an invisible effect further downstream in the optic nerve axons. Accumulation of axonal transport markers was observed only after the onset of the cAON, in both the ONH (Figure 4.3.1.1-2) and in the distal optic nerve (Figure 4.3.2.1-3). Along the optic nerve, accumulation of transport proteins was detected only within areas of inflammatory lesions. This was also confirmed by similar observations following IVI of CTB-A488 (Figure 4.3.3), whose transport is known to be dependent on intact microtubules (Abbott et al., 2013). In the example cases of Syn and βAPP (Figure 4.3.2.3), protein accumulation was visible in both myelinated and demyelinated axons within inflammatory lesion. This implies that disruption of microtubule-associated transport might be an early event in axonal degeneration. Transport can be halted by inflammatory mediators (eg.

ROS/RNS), commonly found in high levels within inflammatory lesions, that could pass through the myelin barrier, damage mitochondria and initiate Focal Axonal Degeneration (Nikic et al., 2011). Following demyelination, transport deficits might be initiated due to axonal cytoskeleton restructuring (de Waegh & Brady 1990, Brady et al. 1999) and a lack of metabolic support by oligodendrocytes (Saab et al., 2013; Fünfschilling et al., 2016). This was confirmed in different genetically modified mouse strains lacking the major structural proteins of CNS myelin. These animals developed a late-onset, slowly progressing axonopathy and axon degeneration (Griffiths et al. 1998, Yin et al. 1998, Lappe-Siefke et al. 2003).

Considering that deficits in axonal transport were not observed during iAON, even in the area of the ONH, they are presumably not the underlying cause of the early RGC loss. In addition, IVI of glutamate which leads to primary RGC loss did not cause any observable disturbances in axonal transport (Figure 4.5.2) and thus mirrored the observations obtained during iAON that primary RGC degeneration does not result in visible axonal transport deficits.

It should be noted that the technique used in this study to characterize axonal transport (immunohistochemistry) also has limitations. Although care was taken to cover as much of the ON area as possible, it could be that some parts of the tissue were not examined. It might also be that in the iAON phase, axonal transport is not obstructed, but only slowed down or more frequently paused. Also another drawback of immunohistochemistry is that it provides a pathological image frozen in time which could pose a problem while studying highly dynamical processes such as axonal transport. In a recent study, mitochondria and peroxisomes were traced *in vivo* using two-photon imaging of EAE mice spinal cords (Sorbara et al., 2014). Persistent arrest of organelles was only seen within inflamed spinal cords. However, in the NAWM, within totally preserved axons, transport of mitochondria was affected in another way. There was no permanent accumulation of these organelles, but the duration of stops was significantly increased, particularly in the retrograde direction. Although it was not discussed in that study, mitochondrial arrest could be connected with intra-axonal Ca^{2+} increases. Mitochondrial motility is decreased following a rise in axonal Ca^{2+} (Rintoul et al., 2003; Yi et al., 2004). This could also be the case in iAON where an increase in the optic nerve Ca^{2+} has been reported (Hoffmann et al., 2013).

5.2 Actin cytoskeleton as a marker of axonal stress in AON

Inflammatory-driven demyelination in ON is not present during the iAON disease phase (Figure 4.1; Fairless et al, 2012). However, examination of the optic nerve ultrastructure by electron microscopy

at this disease stage revealed shrunken axons and the appearance of vacuoles in the peri-axonal space despite normal-appearing myelin sheaths (Fairless et al., 2012). This indicated that there could be some axonal destruction prior to the demyelination process. In previous work of our group, it has already been shown that in iAON there is an increased level of the calpain-specific 147 kDa spectrin break-down product. Calpain activity correlated with the detection of increased Ca^{2+} levels within AON as detected by MEMRI (Hoffmann et al., 2013).

Besides spectrin, the axonal sub-membrane cytoskeleton is composed of different adaptor proteins (ankyrins) and the actin network (Bennett & Gilligan, 1993). Since spectrin is an anchoring protein between plasma membrane channels and the axonal cytoskeleton via actin filaments, we wanted to address whether the actin network is also affected in iAON. The G/F-actin ratio in the optic nerve, providing information on the dynamics of the actin network, was observed to increase starting from iAON (Figure 4.4.1). This finding implies that axonal cytoskeleton re-organization precedes the axonal transport deficits that were detected later on during the cAON disease stage. The observed G/F-actin ratio could be the consequence of an upstream trigger of RGC apoptosis. This is supported by the evidence of the G/F-actin ratio increase following primary retinal insult, IVI of glutamate (Figure 4.5.1-3).

Since it was hypothesized that actin network restructuring might be due to Ca^{2+}-dependent actin binding proteins, one of the villin family proteins, gelsolin was investigated. This protein has been reported to have an anti-apoptotic role following a rise of intracellular Ca^{2+}, which might suggest that the observed G/F-actin ratio change might be a feed-back mechanism by which the axons are coping with the intra-axonal Ca^{2+} increase, presumably by modulating Ca^{2+}-permeable plasma membrane channel activity (see chapter 1.11). When cells then enter the process of apoptotic death, gelsolin is cleaved by activated caspases. In this study it was observed that the 98 kDa (full protein) gelsolin levels decrease starting during iAON (Figure 4.4.2.A).

Another actin-remodeling phenomenon associated with apoptosis is caspase-3-induced cleavage of the actin G-monomer (see chapter 1.11). In our model, starting during iAON, fractin levels were significantly increased compared to healthy animals (Figure 4.4.2.B). Both the changes observed regarding gelsolin and fractin levels are in agreement with the previous report that the RGC loss which begins during iAON and progresses with the onset of cAON is apoptotic in nature (Fairless et al., 2012).

In conclusion, the axonal actin network is affected early on during AON and, together with the spectrin cleavage previously observed, they may be the initiators of the axonal ultra-structural changes. Further on, these intra-axonal changes could be reflected in functional visual deficits and

disruptions of axo-myelin synapses at the Nodes of Ranvier where first irregularities have been observed during iAON (Aleksandar Stojic, PhD thesis 2016).

5.4 NMDA glutamate receptor is involved in RGC neurodegeneration during iAON

One of the neurodegenerative mechanisms assumed to be involved in MS pathology is glutamate excitotoxicity. In the context of neuro-inflammation, inflammatory cells are a potential source of extracellular glutamate through the cysteine/glutamate anti-porter Xc (Pampliega et al., 2011). Activated monocytes and microglia/macrophages have been reported to potentially be the main sources of glutamate in MS, based on findings from the EAE model (Evonuk et al., 2015). Glutamate released from monocytes might also activate glutamate receptors expressed on endothelial cells (Krizbai et al., 1998; Sharp et al., 2003; Andras et al.,2007), facilitating their infiltration and subsequent CNS inflammation. Altered glial glutamate uptake and release via glutamate transporters might also initiate synaptic glutamate increases in MS patients (Domercq et al., 2005; Werner et al., 2001). In axons, vesicular release of glutamate at the axo-myelinic synapse is also possible (Micu et al., 2016). Once extracellular glutamate is increased, overstimulation of metabotropic- and ionotropic-glutamate receptors might lead to prolonged Ca^{2+} increases and finally neuronal cell death (Dong et al., 2009). In EAE models, different glutamate receptors agonists have been shown to ameliorate EAE disease severity and progression: NMDA-receptor blockers, MK801 and memantine (Bolton & Paul, 1997; Sühs et al., 2014), and the AMPA-receptor blocker NBQX (Pitt et al., 2000; Smith et al., 2000), reduced neurological deficits and neurodegeneration. In BN-AON, there have been indications of the role of glutamate in retinal degeneration. Glutamate levels and RGC loss in the retina were ameliorated after systemic application of minocycline, already in iAON (Maier et al., 2007).

In this present study, IVI of glutamate was used in order to investigate the extent of injury that an increase in retinal glutamate could cause, to both RGC bodies and axons. Twenty four hours following IVI of glutamate, both RGC loss (Figure 4.5.1) and the G/F-actin ratio in the optic nerve (Figure 4.5.3) were of similar values as observed during the iAON disease stage. This change in actin network dynamics preceded any accumulation of axonal transport proteins, a sign of axonal transport deficit, or the appearance of axonal swellings (Figure 4.5.2). Similar observations have been made in a rat glaucoma model, where the axonal cytoskeleton within the retina, including F-actin, were disturbed before any RNFL thickness changes could be detected (Huang et al., 2011).

Recognizing that a glutamate-induced retinal insult results in the similar RGC loss and axonal responses as in iAON, a treatment study - blockade of retinal NMDA glutamate receptors (with MK801) during iAON - was performed.

MK801 (dizocilpine) has been used in different applications - as an anticonvulsant (Wong et al., 1986), an antipsychotic (Hunt et al., 2015) and a neuroprotector (Yoles et a., 1997; Berman & Murray, 1996). It is established that MK801 is a specific antagonist of the NMDA glutamate receptor that is effective once NMDA receptors are open (Huettner & Bean, 1988; Halliwell et al., 1989), i.e. it is use-dependent. It is considered to be a prolonged, irreversible blocker, though it has been shown that the blockade efficiency depends on channel activity and Mg^{2+} ion presence (McKay et al., 2013). The effect of MK801 treatment in iAON was visible in both retina and optic nerves. The density of RGCs in late iAON was significantly increased following IVI of MK801 compared to saline-injected control animals (Figure 4.6.A). In addition, the optic nerve G/F-actin ratio was significantly decreased in MK801-treated eyes (Figure 4.6.B), and correlated with the gelsolin increase (Figure 4.6.C) and fractin decrease (Figure 4.6.D) compared to control eyes.

NMDA receptor stimulation following IVI of NMDA in the retina has been known to induce RGC loss (Munemasa et al., 2006; Bai et al., 2013; Sakamoto et al., 2010; Manabe & Lipton, 2003). Molecular changes involved in retinal injury downstream of NMDA receptor stimulation in addition to direct Ca^{2+} influx through the NMDA receptor pore are diverse: activation of other Ca^{2+} permeable plasma membrane channels, e.g. VGCCs (Melena & Osborne, 2001), mobilization of intracellular Ca^{2+} stores (Lei et al., 1992), pro-apoptotic activation of c-Jun N-terminal kinase and p38 mitogen-activated protein kinase (Munemasa et al., 2005), activation of RhoA pathway (Kitaoke et al., 2004), etc. However, based on our previous report on calpain activity (Hoffmann et al., 2013), prolonged intracellular Ca^{2+} increase following NMDA receptor activity and Ca^{2+}-mediated injury appears to be the relevant mechanism. In addition, it remains to be investigated to what extent the silencing of NMDA receptors expressed on RGCs alone contributes to their protection, particularly since MK801 effect could also mediate more indirect effects. For example, it has been reported that increased extracellular glutamate affects BBB permeability via NMDA receptor stimulation (Sharp et al., 2003; Andras et al., 2007; Vazana et al., 2016). MK801 application might have reversed BRB induced damage by decreasing influx of fibrin (Davalos et al., 2012) or pro-inflammatory cytokines from T-cells detected within the choroid in iAON (Fairless et al., 2012). For example, MK801 might have also affected the BRB permeability (known to be disrupted in iAON; Fairless et al., 2012) by acting on endothelial NMDA receptors, and in that way reduced potential harmful blood components and cytokines leakage into the retina (Vazana et al., 2016; Kusaka et al., 1999).

5.3 Invulnerability of RGCs to glutamate excitotoxicity *in vitro*

In order to investigate downstream mechanisms of glutamate-induced RGC loss, a primary RGC culture was established based on the protocol first described by Barres et al., 1998. The phenomenon of glutamate excitotoxicity was historically first reported in the retina (Lucas & Newhouse, 1957). Since then, it was observed in different neuronal populations throughout the CNS and is shown to be involved in the majority of neurodegenerative diseases (Lipton & Rosenberg, 1994). *In vitro* studies on different CNS neuronal populations, such as cortical (Chinopoulos et al., 2004), spinal (Tymianski et al. 1993) and cerebellar granule neurons (Bano et al. 2005), all confirmed glutamate-induced cell death in about 60 -80% of cells accompanied by the phenomenon of delayed Ca^{2+} deregulation (DCD). However, RGCs which are undoubtedly prone to glutamate-mediated cell death *in vivo* (see chapter 5.2) were reported to be only weakly susceptible to glutamate excitotoxicity (Hartwick et al., 2008) or not vulnerable at all (Ullian et al., 2004) in culture.

In this present study, the purity of seeded RGCs was 80-90%, less than compared to the original isolation method where the purity was reported to be around 99%. Within 24 hours, a portion of these cells died as observed by EthD1 labelling. The vast majority of surviving cells had large nuclei with extending neurites, morphologically characteristic of RGCs but not of other retinal cell types (Figure 4.8.A). The presence of forskolin (an external substitute for cyclic adenosine monophosphate; cAMP), BDNF and CNTF in the culture medium was shown to be essential for cell viability (Figure 4.8.B-C). The necessity for their presence in the culture medium where axotomized RGCs are kept, has been already reported (Meyer-Franke et al., 1998). The beneficial effect on RGC survival following axonal transection was seen if cAMP was pharmacologically increased in the presence of growth factors (Shen et al., 1999; Hellström et al., 2011). This protective effect in isolated RGCs is attributed to co-operation between cAMP and growth factors in rapid recruitment of tyrosine kinase receptor B (TrkB) to the plasma membrane (Meyer-Franke et al., 1998).

RGC loss was not observed in response to 24 hour treatment with glutamate-glycine, in our defined culture conditions (Figure 4.8.1). In order to visualize if the absence of cell death is reflected in RGC Ca^{2+} dynamics following glutamate receptor stimulation, ratio-metric Fura-2 Ca^{2+} imaging was performed. In these experiments, different glutamate receptor agonists were used (glutamate-glycine, NMDA, AMPA; Figure 4.8.2.A). The intracellular Ca^{2+} increase immediately after the agonist addition was the highest in the case of glutamate-glycine and NMDA stimulation (Figure 4.8.2.B.iii). This implies that, at least in culture, the majority of extracellular Ca^{2+} following RGC stimulation is mediated via NMDA receptors. Delayed Ca^{2+} levels were observed to positively correlate with the initial Ca^{2+} increase (Figure 4.8.2.iv). However, in the vast majority of cells delayed Ca^{2+} levels were

never as high as observed in the few cases when the phenomenon of DCD was observed (Figure 4.8.2.A). Further on, only the cells in which DCD was observed were labelled with annexin V-Alexa Fluor 594 conjugate (author's observation, data not shown).

Expression of different NMDA receptor subtypes have been confirmed in RGC culture (Ullian et al., 2004). However, current influx following NMDA receptor stimulation was shown to be significantly lower compared to the levels recorded in hippocampal cells (Ullian et al., 2004). Besides, the presence of BDNF in the culture media, an anti-apoptotic factor (Almeida et al., 2005; Melo et al., 2013) and modulator of synaptic NMDA receptor activity (Hildebrand et al., 2016), could suppress RGC degeneration following prolonged glutamate receptor stimulation.

5.4 Role of NCX1 in Ca^{2+} dynamics following glutamate receptor stimulation in cultured RGCs

The role of NCX following glutamate receptor stimulation in isolated neuronal cultures has been mostly addressed following AMPA receptor stimulation and in the context of DCD phenomenon (Hoyt et al., 1998; Bano et al., 2005; Araujo et al., 2007; Brittain et al., 2012). One of the hypotheses behind these studies is that DCD starts once a cell is overloaded with intracellular Na^{2+}, and subsequently the new Na^{+} gradient forces the NCX to operate in reverse-mode. This idea originated from studies on isolated axons, where a loss of saltatory conduction, ATP depletion, and re-distribution of Na^{+}/K^{+}-pump, leads to axonal Na^{2+} overload and NCX reverse-mode activity (Stys et al., 1997; Craner et al., 2004a and 2004b).

Data on the expression of Ca^{2+}-related channels in acutely isolated and cultured RGCs showed a significant increase in the level of NCX1 mRNA expression in cultured RGCs (Table 4.8.3). This finding is consistent with the described role of NCX1 in neurite outgrowth (Secondo et al., 2015), a process that is extensive in cultured RGCs (Figure 4.8.A). However, we also wanted to investigate if NCX1 affects RGC Ca^{2+} influx/extrusion following glutamate-glycine stimulation, using the reverse-mode NCX blocker, SEA0400 (Figure 4.9; Matsuda et al., 2001). In parallel with intracellular Ca^{2+} increase, glutamate-glycine stimulation of cultured RGCs induced a significant increase in Na^{+} intracellular levels (author's observation using SBFI ratio-metric Na^{+} dye, data not shown) that might drive NCX into its reverse-mode of action. SEA0400 was added to the imaging solution and subsequently RGCs were stimulated with glutamate-glycine. A dose-dependent decrease in Ca^{2+} responses were observed following glutamate-glycine stimulation of cells pre-treated with SEA0400 (Figure 4.9.C.iv). The reverse-mode blocker SEA0400 was reported to have an IC_{50} value of 30 nM in neurons (Matsuda

et al., 2001) and in data presented here, a significant Ca^{2+} decrease was observed starting from 100 nM SEA0400 concentrations. This observed decrease, though significant, was not as effective as that observed with blockade of VGCCs following glutamate-glycine stimulation (Hartwick et al., 2008). These results suggest the possibility that most NCX1 receptors are either inactive or operate in the forward-mode following glutamate-glycine stimulation of cultured RGCs. This might be explained by the insufficient Na^+ and Ca^{2+} electrochemical gradient across the plasma membrane and also the efficiency of other channels, such as Na^+/K^+ pump, Na^+-voltage channels, VGCCs and PMCAs in dealing with glutamate-glycine-induced depolarization.

5.5 SEA0400 blocker application during iAON did not protect RGCs

The kinetics and the mode of operation of NCX are highly dependent on the experimental conditions of isolated plasma membranes (Blaustein & Lederer, 1999). In the living cell, besides ion concentration inside/outside of the cell and the presence of other plasma membrane channels, intracellular factors additionally affect NCX physiology – either directly, such as cAMP (Menè et al., 1993) or indirectly, such as PKC/PKA pathways that affect Na^+/K^+-pump (Beguin et al., 1994).

Interest in the role of NCX in neurodegenerative mechanisms originated from studies of axonal damage following oxygen deprivation and subsequent failure of Na^+/K^+-pump because of insufficient ATP and further axonal Ca^{2+} increase via axolemal NCX activity (Stys et al., 1992a, 1992b, 1993; Waxman et al., 1994). The additional observations that a reduction in Na^+ influx protected axons in a spinal cord injury model, supported the role of NCX in Ca^{2+}-mediated axonal injury (Agrawal & Fehlings, 1996; Hains et al., 2004) and in EAE (Kapoor et al., 2003; Lo et al., 2003; Bechtold et al., 2004).

During iAON, MK801 treatment was shown to be protective of RGCs (see chapter 5.4). One of the possible mechanisms involved in RGC degeneration might be chronic activity of the NMDA receptor, prolonged depolarization, Na^+ influx and NCX reverse-mode of operation. However, application of SEA0400 reverse-mode blocker did not have any protective effect on RGC survival during iAON (Figure 4.9.A). The same was observed in the optic nerve, where no change in the G/F-actin ratio was detected between control and SEA0400 treated groups (Figure 4.9.B). Preliminary experiments following intravitreal co-injection of glutamate and SEA0400 resulted in similar observations where no effects in either RGC survival or the G/F actin ratio decrease compared to IVI of glutamate alone (author's observation, data not shown). Since NCX1 expression was confirmed in adult acutely isolated RGCs (Table 4.7), the treatment inefficiency most probably reflects that NCX1 reverse-mode

of operation is not involved in the potential mechanism of NMDA receptor-mediated RGC loss in iAON. However, it should be taken into consideration that the dose regime was not efficient enough. As presented in this study, SEA0400 was not effective in iAON, but it might still have neuroprotective effects during cAON. In this disease stage, SEA0400 might induce axonal salvage following demyelination, when axonal loss is assumed to be initiated in the similar manner as in the axonal oxidative damage injury discussed above.

5.6 Summary

In summary, the study presented in this thesis was based on observations previously reported in the induction phase in the animal model of the AON - the loss of RGCs and the ultra-structural changes in the axons in the absence of myelin disruption. Both observations correlated with the subtle BRB and BBB leakage as well as the increased microglial activation in the retina and in the ONH (Fairless et al., 2012). In parallel with these findings, Ca^{2+} increase and calpain activity were observed (Hoffmann et al., 2013). Since gross pathology in the optic nerves was not observed during iAON, the hypothesis was that the early neuronal insult, independent of primary demyelination, might originate within areas lacking myelin, that is, the retina and ONH. The possibility that axonal transport deficits accompany the observed ultra-structural changes was based on the potential vulnerability of axons within the ONH. RGC axons are naturally unmyelinated in this part of the optic nerve and are in direct contact with potentially harmful influences. However, axonal transport deficits were not observed during iAON in either the ONH or distal parts of the optic nerve. Furthermore, the rationale was to address macroscopic parameters that would reflect ultra-structural axonal changes (G/F-actin ratio) and to address how they may correlate with RGC loss. In parallel with restructuring of the actin network, the Ca^{2+}-activated actin binding protein gelsolin and also the actin globular monomer were affected starting from iAON. Both of them are shown to be substrates for caspases (Kothakota et al., 1997; Sokolowski et al., 2014) and this further suggested that axonal structural changes are interconnected with apoptotic death pathways initiated in RGCs (Fairless et al., 2012).

Among other possibilities, the origin of RGC loss in iAON was assumed to be connected with the phenomenon of glutamate excitotoxicity. The glutamate intra-retinal increase in iAON may come from the reported BRB leak and reactive glial cells (microglia and astrocytes) in the retina (Fairless et al., 2012). If so, the ionotropic NMDA receptor was suspected to be the most important mediator of RGC loss, predominantly because of its Ca^{2+} permeability and assumption that intracellular Ca^{2+} overload contributes to RGC loss (Hoffmann et al., 2013). In naïve animals, IVI of glutamate was used as a model for retinal glutamate increase. RGC loss and actin structure changes observed in this

model were comparable to the findings in iAON. This observation further initiated a treatment study during iAON with the NMDA receptor blocker MK801. The IVI application of MK801 was shown to be neuroprotective during iAON in both retina, where RGC counts were higher than in the untreated animals, and in optic nerves, where actin network parameters reversed to values comparable to healthy animas (Figure 5.6).

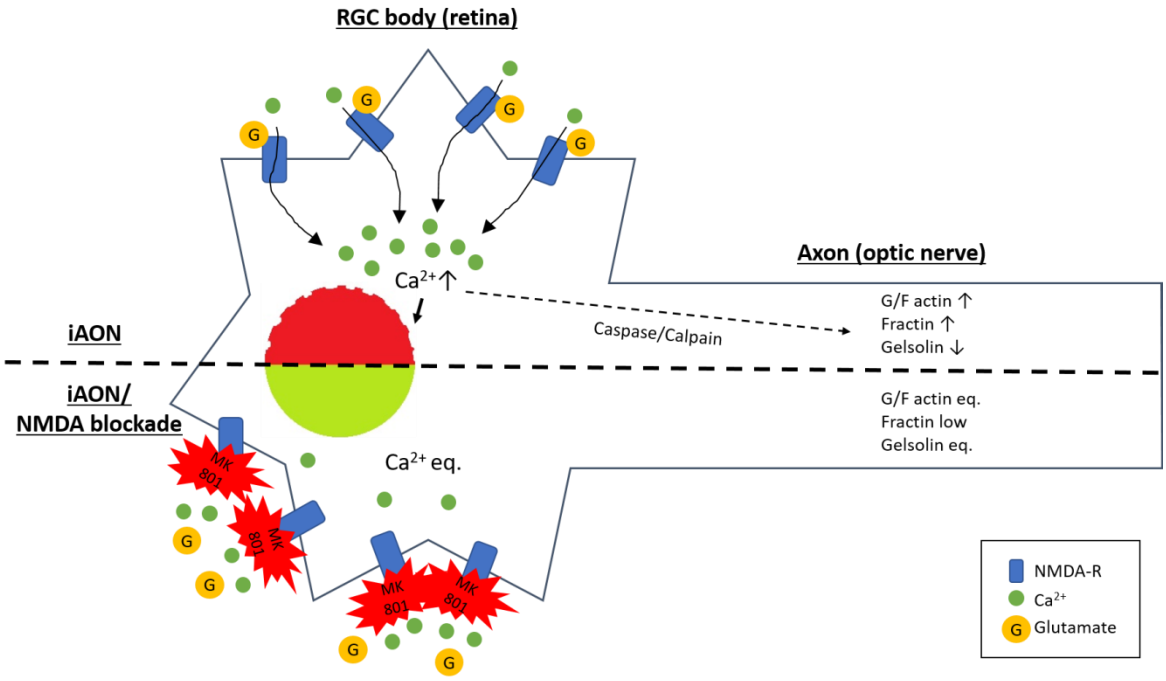

Figure 5.6. MK801 neuroprotection during iAON. Sheme representing MK801 protective effects on RGCs, in possible Ca^{2+}-related manner. Blockade of retinal NMDA receptors increases RGC survival and restores axonal actin network parameters to the levels comparable to healthy animals.

In conclusion, this study provides further evidence that NMDA receptor activity within the visual system contributes to early neurodegeneration of RGCs in AON. Collectively with other studies, there is an emerging consensus that glutamate excitotoxicity plays a role in neuroinflammatory diseases such as MS. This is of great importance, since it is now appreciated that neurodegenerative processes in MS are more widespread than primary demyelination and significantly contributes to on-going and irreversible disability in MS patients. In light of the fact that to date only immunomodulatory treatments are available, with limited neuroprotective effects, the search of neuroprotective therapies should be a major aim for future studies.

References

- Abbott C.J., Choe T.E., Lusardi T.A., Burgoyne C.F., Wang L., Fortune B. (2013) Imaging axonal transport in the rat visual pathway. Biomed Opt Express. 4(2):364-86.
- Abdel-Majid R.M., Archibald M.L., Tremblay F., Baldridge W.H. (2005) Tracer coupling of neurons in the rat retina inner nuclear layer labeled by Fluorogold. Brain Res. 1063: 114-120.
- Adamec E., Yang F., Cole G.M., Nixon R.A. (2001) Multiple-label immunocytochemistry for the evaluation of nature of cell death in experimental models of neurodegeneration. Brain Res Protoc. 7(3):193-202.
- Agrawal S.K., Fehlings M.G. (1996) Mechanisms of secondary injury to spinal cord axons in vitro: role of Na+, Na+/K+-ATPase, the Na+/H+ exchanger, and the Na+/Ca2+ exchanger. J Neurosci. 16:545-552.
- Aizenman E., Frosch M.P., Lipton S.A. (1988) Responses mediated by excitatory amino acid receptors in solitary retinal ganglion cells from rat. J Physiol. 396:75-91.
- Al-Louzi O.A., Bhargava P., Newsome S.D., Balcer L.J., Frohman E.M., Crainiceanu C., Calabresi P.A., Saidha S. (2016) Outer retinal changes following acute optic neuritis. Mult Scler. 22(3):362-72.
- Almeida R.D., Manadas B.J., Melo C.V., Gomes J.R., Mendes C.S., Grãos M.M., Carvalho R.F., Carvalho A.P., Duarte C.B. (2005) Neuroprotection by BDNF against glutamate-induced apoptotic cell death is mediated by ERK and PI3-kinase pathways. Cell Death Differ. 12(10):1329-43.
- Alter M., Kahana E., Loewenson R. (1978) Migration and risk of multiple sclerosis. Neurology 28:1089–93.
- Anderson J.M., Hampton D.W., Patani R., Pryce G., Crowther R.A., Reynolds R., Franklin R.J., Giovannoni G., Compston D.A., Baker D., Spillantini M.G., Chandran S. (2008) Abnormally phosphorylated tau is associated with neuronal and axonal loss in experimental autoimmune encephalomyelitis and multiple sclerosis. Brain 131(Pt 7):1736-48.
- Andras I.E., Deli M.A., Veszelka S., Hayashi K., Hennig B., Toborek M. (2007) The NMDA and AMPA/KA receptors are involved in glutamate-induced alterations of occludin expression and phosphorylation in brain endothelial cells. J Cereb Blood Flow Metab. 27:1431–1443.
- Annunziato L. (2013) Sodium Calcium Exchange: A Growing Spectrum of Pathophysiological Implications. Springer Science+Business Media New York.
- Araujo I.M., Carreira B.P., Pereira T., Santos P.F., Soulet D., Inácio A., Bahr B.A., Carvalho A.P., Ambrósio A.F., Carvalho C.M. (2007) Changes in calcium dynamics following the reversal of the sodium-calcium exchanger have a key role in AMPA receptor-mediated

neurodegeneration via calpain activation in hippocampal neurons. Cell Death Differ. 14(9):1635-46.

- Ascherio A., Munger L.K. (2007a) Environmental Risk Factors for Multiple Sclerosis. Part I: The Role of Infection. Ann Neurol. 61:288–299.
- Ascherio A., Munger L.K. (2007b) Environmental Risk Factors for Multiple Sclerosis. Part II: Noninfectious Factors. Ann Neuro. 61:504–513.
- Bading H. (2013) Nuclear calcium signalling in the regulation of brain function. Nat Rev Neurosci. 14(9):593-608.
- Baffy G., Miyashita T., Williamson J.R., Reed J.C. (1993) Apoptosis induced by withdrawal of interleukin-3 (IL-3) from an IL-3-dependent hematopoietic cell line is associated with repartitioning of intracellular calcium and is blocked by enforced Bcl-2 oncoprotein production. J Biol Chem. 268(9):6511-9.
- Bai N., Aida T., Yanagisawa M., Katou S., Sakimura K., Mishina M., Tanaka K. (2013) NMDA receptor subunits have different roles in NMDA-induced neurotoxicity in the retina. Mol Brain 6:34.
- Baker D., Amor S. (2012) Publication guidelines for refereeing and reporting on animal use in experimental autoimmune encephalomyelitis. J Neuroimmunol. 242(1-2):78-83
- Baker P.F., Blaustein M.P., Hodgkin A.L., Steinhardt R.A. (1969) The influence of calcium on sodium efflux in squid axons. J Physiol. 200(2):431-58.
- Balcer L.J. (2006) Clinical practice. Optic neuritis. N Engl J Med. 354(12):1273-80.
- Balcer L.J., Miller D.H., Reingold S.C., Cohen J.A. (2015) Vision and vision-related outcome measures in multiple sclerosis. Brain 138(Pt 1):11-27.
- Balendra S.I., Normando E.M., Bloom P.A., Cordeiro M.F. (2015) Advances in retinal ganglion cell imaging. Eye (Lond) 29(10):1260-9.
- Bano D., Young K.W., Guerin C.J., Lefeuvre R., Rothwell N.J., Naldini L., Rizzuto R., Carafoli E., Nicotera P. (2005) Cleavage of the plasma membrane Na^+/Ca^{2+} exchanger in excitotoxicity. Cell 120(2):275-85.
- Baranzini S.E., Srinivasan R., Khankhanian P. (2010) Genetic variation influences glutamate concentrations in brains of patients with multiple sclerosis. Brain 133: 2603–11.
- Baranzini S.E., Wang J., Gibson R.A., Galwey N., Naegelin Y., Barkhof F., Radue E.W., Lindberg R.L., Uitdehaag B.M., Johnson M.R., Angelakopoulou A., Hall L., Richardson J.C., Prinjha R.K., Gass A., Geurts J.J., Kragt J., Sombekke M., Vrenken H., Qualley P., Lincoln R.R., Gomez R., Caillier S.J., George M.F., Mousavi H., Guerrero R., Okuda D.T., Cree B.A., Green A.J., Waubant E., Goodin D.S., Pelletier D., Matthews P.M., Hauser S.L., Kappos L., Polman C.H.,

Oksenberg J.R. (2009) Genome-wide association analysis of susceptibility and clinical phenotype in multiple sclerosis. Hum Mol Genet. 18:767–78.

- Barsukova A.G., Forte M., Bourdette D. (2012) Focal increases of axoplasmic Ca2+, aggregation of sodium-calcium exchanger, N-type Ca2+ channel, and actin define the sites of spheroids in axons undergoing oxidative stress. J Neurosci. 32(35):12028-37.
- Bechtold D.A., Kapoor R., Smith K.J. (2004) Axonal protection using flecainide in experimental autoimmune encephalomyelitis. Ann Neurol. 55:607-616.
- Beck R.W., Gal R.L., Bhatti M.T., Brodsky M.C., Buckley E.G., Chrousos G.A., Corbett J., Eggenberger E., Goodwin J.A., Katz B., Kaufman D.I., Keltner J.L., Kupersmith M.J., Miller N.R., Moke P.S., Nazarian S., Orengo-Nania S., Savino P.J., Shults W.T., Smith C.H., Trobe J.D., Wall M., Xing D.; Optic Neuritis Study Group. (2004) Visual function more than 10 years after optic neuritis: experience of the optic neuritis treatment trial. Am J Ophthalmol. 137(1):77-83.
- Beguin P., Beggah A.T., Chibalin A.V., Burgener-Kairuz P., Jaisser F., Mathews P.M., Rossier B.C., Cotecchia S., Geering K. (1994) Phosphorylation of the Na,K-ATPase alpha-subunit by protein kinase A and C in vitro and in intact cells. Identification of a novel motif for PKC-mediated phosphorylation. J Biol Chem. 269(39):24437-45.
- Beirowski B., Nógrádi A., Babetto E., Garcia-Alias G., Coleman M.P. (2010) Mechanisms of axonal spheroid formation in central nervous system Wallerian degeneration. J Neuropathol Exp Neurol. 69(5):455-72.
- Bennett V., Gilligan D.M. (1993) The spectrin-based membrane skeleton and micron-scale organization of the plasma membrane. Annu Rev Cell Biol. 9:27-66.
- Ben-Nun A., Wekerle H. and Cohen I.R. (1981) The rapid isolation of clonable antigen-specific T lymphocyte lines capable of mediating autoimmune encephalomyelitis. Eur J Immunol. 11(3):195-9.
- Berkelaar M., Clarke D.B., Wang Y.C., Bray G.M., Aguayo A.J. (1994) Axotomy results in delayed death and apoptosis of retinal ganglion cells in adult rats. J Neurosci. 14(7):4368-74.
- Berman F.W., Murray T.F. (1996) Characterization of [3H]MK-801 binding to N-methyl-D-aspartate receptors in cultured rat cerebellar granule neurons and involvement in glutamate-mediated toxicity. J Biochem Toxicol. 11(5):217-26.
- Bernstein B.W., Maloney M.T., Bamburg J.R. (2011) Actin and Diseases of the Nervous System. G. Gallo, L.M. Lanier (eds.), Neurobiology of Actin, Advances in Neurobiology 5, 201; Springer Science+Business Media, LLC 2011.
- Billger M., Wallin M., Karlsson J.O. (1988) Proteolysis of tubulin and microtubule-associated proteins 1 and 2 by calpain I and II. Difference in sensitivity of assembled and disassembled microtubules. Cell Calcium 9(1):33-44.

- Binda N.S., Carayon C.P., Agostini R.M., Pinheiro A.C., Cordeiro M.N., Silva M.A., Silva J.F., Pereira E.M., da Silva Junior C.A., de Castro Junior C.J., Guimarães A.L., Gomez M.V. (2016) PhTx3-4, a Spider Toxin Calcium Channel Blocker, Reduces NMDA-Induced Injury of the Retina. Toxins 8(3).
- Bjartmar C., Kidd G., Mörk S., Rudick R., Trapp B.D. (2000) Neurological disability correlates with spinal cord axonal loss and reduced N-acetyl aspartate in chronic multiple sclerosis patients. Ann Neurol. 48(6):893-901.
- Black M.M. (2016) Axonal transport: The orderly motion of axonal structures. Methods in Cell Biology, Volume 131, ISSN 0091-679X, http://dx.doi.org/10.1016/bs.mcb.2015.06.001 © 2016 Elsevier Inc.
- Blaustein M.P., Lederer W.J. (1999) Sodium/calcium exchange: its physiological implications. Physiol Rev. 79(3):763-854.
- Bö L., Dawson T.M., Wesselingh S., Mörk S., Choi S., Kong P.A., Hanley D., Trapp B.D. (1994) Induction of nitric oxide synthase in demyelinating regions of multiple sclerosis brains. Ann Neurol. 36(5):778-86.
- Bö L., Vedeler C.A., Nyland H., Trapp B.D. and Mörk S.J. (2003) Intracortical multiple sclerosis lesions are not associated with increased lymphocyte infiltration. Mult Scler. 9(4):323-31.
- Bolton C1, Paul C. (1997) MK-801 limits neurovascular dysfunction during experimental allergic encephalomyelitis. J Pharmacol Ex Ther. 282(1):397-402.
- Boretius S., Gadjanski I., Demmer I., Bähr M., Diem R., Michaelis T. and Frahm J. (2008) MRI of optic neuritis in a rat model. Neuroimage 41(2):323-34.
- Brady S.T., Witt A.S., Kirkpatrick L.L., de Waegh S.M., Readhead C., Tu P.H., Lee V.M. (1999) Formation of compact myelin is required for maturation of the axonal cytoskeleton. J Neurosci. 19:7278–88.
- Brand-Schieber E., Werner P. (2004) Calcium channel blockers ameliorate disease in a mouse model of multiple sclerosis. Exp Neurol. 189(1):5-9.
- Breij E.C., Brink B.P., Veerhuis R., van den Berg C., Vloet R., Yan R., Dijkstra C.D., van der Valk P., Bö L. (2008) Homogeneity of active demyelinating lesions in established multiple sclerosis. Ann Neurol. 63(1):16-25.
- Brieher W. (2013) Mechanisms of actin disassembly. Mol Biol Cell. (15):2299-302.
- Brini M., Carafoli E. (2011) The Plasma Membrane Ca2+ ATPase and the Plasma Membrane Sodium Calcium Exchanger Cooperate in the Regulation of Cell Calcium Cold Spring Harb Perspect Biol. 3(2): a004168.

- Brink B.P., Veerhuis R., Breij E.C., van der Valk P., Dijkstra C.D., Bö L. (2005) The pathology of multiple sclerosis is location-dependent: no significant complement activation is detected in purely cortical lesions. J Neuropathol Exp Neurol. 64(2):147-55.
- Brittain M.K., Brustovetsky T., Sheets P.L., Brittain J.M., Khanna R., Cummins T.R., Brustovetsky N. (2012) Delayed calcium dysregulation in neurons requires the NMDA receptor and the reverse Na^{+}/Ca^{2+} exchanger. Neurobiol Dis. 46(1):109-17.
- Brown A. (2009) Slow axonal transport. Encyclopedia of Neuroscience 9:1-9.
- Brown S.B., Bailey K., Savill J. (1997) Actin is cleaved during constitutive apoptosis. Biochem J. 323 (Pt 1):233-7.
- Brustovetsky T., Brittain M.K., Sheets P.L., Cummins T.R., Pinelis V., Brustovetsky N. (2011) KB-R7943, an inhibitor of the reverse Na+ /Ca^{2+} exchanger, blocks N-methyl-D-aspartate receptor and inhibits mitochondrial complex I. Br J Pharmacol. 162(1):255-70.
- Budd S.L., Nicholls D.G. (1996) Mitochondria, calcium regulation, and acute glutamate excitotoxicity in cultured cerebellar granule cells. J Neurochem. 67:2282–2291.
- Bull N.D., Chidlow G., Wood J.P., Martin K.R., Casson R.J. (2012) The mechanism of axonal degeneration after perikaryal excitotoxic injury to the retina. Exp Neurol. 236(1):34-45.
- Bullok K., Piwnica-Worms D. (2005) Synthesis and characterization of a small, membrane-permeant, caspase-activatable far-red fluorescent peptide for imaging apoptosis. J Med Chem. 48(17):5404-7.
- Calabrese M., Filippi M., Gallo P. (2010) Cortical lesions in multiple sclerosis. Nat Rev Neurol. 6(8):438-44.
- Calabrese M., Magliozzi R., Ciccarelli O., Geurts J.J., Reynolds R. and Martin R. (2015) Exploring the origins of grey matter damage in multiple sclerosis. Nat Rev Neurosci. 16(3):147-58.
- Calabrese M., Poretto V., Favaretto A., Alessio S., Bernardi V., Romualdi C., Rinaldi F., Perini P. and Gallo P. (2012) Cortical lesion load associates with progression of disability in multiple sclerosis. Brain 135(Pt 10):2952-61.
- Cambron M., D'Haeseleer M., Laureys G. (2012) White-matter astrocytes, axonal energy metabolism, and axonal degeneration in multiple sclerosis. J Cereb Blood Flow Metab. 32:413–24.
- Carafoli E. (1997) Plasma membrane calcium pump: structure, function and relationships. Basic Res Cardiol. 92 Suppl 1:59-61.
- Carafoli E. (2002) Calcium signaling: A tale for all seasons. Proc Natl Acad Sci. USA 99:1115–1122.

- Castegna A., Palmieri L., Spera I. (2011) Oxidative stress and reduced glutamine synthetase activity in the absence of inflammation in the cortex of mice with experimental allergic encephalomyelitis. Neuroscience 185: 97–105.
- Catterall W.A., Perez-Reyes E., Snutch T.P., Striessnig J. (2005) International Union of Pharmacology. XLVIII. Nomenclature and structure-function relationships of voltage-gated calcium channels. Pharmacol Rev. 57(4):411-25.
- Cennamo G., Romano M.R., Vecchio E.C., Minervino C., Della Guardia C., Velotti N., Carotenuto A., Montella S., Orefice G., Cennamo G. (2016) Anatomical and functional retinal changes in multiple sclerosis. Eye (Lond) 30(3):456-62.
- Chalmoukou K., Alexopoulos H., Akrivou S., Stathopoulos P.,Reindl M., Dalakas C.M. (2015) Anti-MOG antibodies frequently associated with steroid – sensitive recurrent optic neuritis. Neurol Neuroimmunol Neuroinflamm. 2(4):e131.
- Charcot JM. (1868) Histologie de la sclérose en plaques. Gazette des hopitaux, Paris 41: 554–55.
- Chen H., Chan D.C. (2005) Emerging functions of mammalian mitochondrial fusion and fission. Hum Mol Genet. 14 Spec No. 2:R283-9.
- Cherecheanu A.P., Garhofer G., Schmidl D., Werkmeister R., Schmetterer L. (2013) Ocular perfusion pressure and ocular blood flow in glaucoma. Curr Opin Pharmacol. 13(1):36-42.
- Chidlow G., Wood J.P., Manavis J., Osborne N.N., Casson R.J. (2008) Expression of osteopontin in the rat retina: effects of excitotoxic and ischemic injuries. Invest Ophthalmol Vis Sci. 49(2):762-71.
- Chinopoulos C., Gerencser A.A., Doczi J., Fiskum G., Adam-Vizi V. (2004) Inhibition of glutamate-induced delayed calcium deregulation by 2-APB and La3+ in cultured cortical neurones. J Neurochem. 91(2):471-83.
- Chiu K., Lam T.T., Ying Li W.W., Caprioli J., Kwong Kwong J.M. (2005) Calpain and N-methyl-d-aspartate (NMDA)-induced excitotoxicity in rat retinas. Brain Res. 1046(1-2):207-15.
- Choi W.D: (1988) Calcium-mediated neurotoxicity: relationship to specific channel types and role in ischemic damage. TINS 11:465–467.
- Clements J.D., Lester R.A., Tong G., Jahr C.E., Westbrook G.L. (1992) The time course of glutamate in the synaptic cleft. Science 258(5087):1498-501.
- Coleman M. (2005) Axon degeneration mechanisms: commonality amid diversity. Nat Rev Neurosci. 6(11):889-98.
- Coleman MP1, Freeman MR. (2010) Wallerian degeneration, wld(s), and nmnat. Annu Rev Neurosci. 33:245-67.

- Collard C.D., Park K.A., Montalto M.C. (2002) Neutrophil-derived glutamate regulates vascular endothelial barrier function. J Biol Chem. 277: 14801–11.
- Compston A. and Coles A. (2008) Multiple sclerosis. Lancet 372(9648):1502-17.
- Condrescu M., Reeves J.P. (2006) Actin-dependent regulation of the cardiac Na^{+}/Ca^{2+} exchanger. Am J Physiol Cell Physiol. 290(3):C691-701.
- Cook N.J., Kaupp U.B. (1988) Solubilization, purification, and reconstitution of the sodium-calcium exchanger from bovine retinal rod outer segments. J Biol Chem. 263(23):11382-8.
- Cordeiro M.F., Guo L., Luong V., Harding G., Wang W., Jones H.E., Moss S.E., Sillito A.M., Fitzke F.W. (2004) Real-time imaging of single nerve cell apoptosis in retinal neurodegeneration. Proc Natl Acad Sci USA 101(36):13352-6.
- Craner M.J., Hains B.C., Lo A.C., Black J.A. and Waxman S.G. (2004a) Co-localization of sodium channel Nav1.6 and the sodium-calcium exchanger at sites of axonal injury in the spinal cord in EAE. Brain 127(Pt 2):294-303.
- Craner M.J., Newcombe J., Black J.A., Hartle C., Cuzner M.L. and Waxman S.G. (2004b) Molecular changes in neurons in multiple sclerosis: altered axonal expression of Nav1.2 and Nav1.6 sodium channels and Na+/Ca2+ exchanger. Proc Natl Acad Sci U S A. 101(21):8168-73.
- Crompton M. (1999) The mitochondrial permeability transition pore and its role in cell death. Biochem J. 341(Pt 2):233-49.
- Cunnea P., Mháille A.N., McQuaid S., Farrell M., McMahon J., FitzGerald U. (2011) Expression profiles of endoplasmic reticulum stress-related molecules in demyelinating lesions and multiple sclerosis. Mult Scler. 17(7):808-18.
- Dahlström A. B., Czernik A. J., Li, J. Y. (1992) Organelles in fast axonal transport. What molecules do they carry in anterograde vs retrograde directions, as observed in mammalian systems? Molecular Neurobiology 6:157e177.
- Dalton C.M., Chard D.T., Davies G.R., Miszkiel K.A., Altmann D.R., Fernando K., Plant G.T., Thompson A.J., Miller D.H. (2004) Early development of multiple sclerosis is associated with progressive grey matter atrophy in patients presenting with clinically isolated syndromes. Brain 127(Pt 5):1101-7.
- Davalos D., Ryu J.K., Merlini M., Baeten K.M., Le Moan N., Petersen M.A., Deerinck T.J., Smirnoff D.S., Bedard C., Hakozaki H., Gonias Murray S., Ling J.B., Lassmann H., Degen J.L., Ellisman M.H. and Akassoglou K. (2012) Fibrinogen-induced perivascular microglial clustering is required for the development of axonal damage in neuroinflammation. Nat Commun. 3:1227.

- De Stefano N., Matthews P.M., Filippi M., Agosta F., De Luca M., Bartolozzi M.L., Guidi L., Ghezzi A., Montanari E., Cifelli A., Federico A., Smith S.M. (2003) Evidence of early cortical atrophy in MS: relevance to white matter changes and disability. Neurology 60(7):1157-62.
- De Vos K.J., Chapman A.L., Tennant M.E., Manser C., Tudor E.L., Lau K.F., Brownlees J., Ackerley S., Shaw P.J., McLoughlin D.M., Shaw C.E., Leigh P.N., Miller C.C., Grierson A.J. (2007) Familial amyotrophic lateral sclerosis-linked SOD1 mutants perturb fast axonal transport to reduce axonal mitochondria content. Hum Mol Genet. 16(22):2720-8.
- De Vos K.J., Grierson A.J., Ackerley S., Miller C.C. (2008) Role of axonal transport in neurodegenerative diseases. Annu Rev Neurosci. 31:151-73.
- de Waegh S., Brady S.T. (1990) Altered slow axonal transport and regeneration in a myelin - deficient mutant mouse: the trembler as an in vivo model for Schwann cell-axon interactions. J Neurosci. 10:1855–65.
- del Pilar Martin M., Cravens P.D., Winger R., Frohman E.M., Racke M.K., Eagar T.N., Zamvil S.S., Weber M.S., Hemmer B., Karandikar N.J., Kleinschmidt-DeMasters B.K. and Stüve O. (2008) Decrease in the numbers of dendritic cells and CD4+ T cells in cerebral perivascular spaces due to natalizumab. Arch Neurol. 65(12):1596-603.
- Desouza M., Gunning P.W., Stehn J.R. (2012) The actin cytoskeleton as a sensor and mediator of apoptosis. Bioarchitecture 2(3):75-87.
- D'Este E., Kamin D., Göttfert F., El-Hady A., Hell S.W. (2015) STED nanoscopy reveals the ubiquity of subcortical cytoskeleton periodicity in living neurons. Cell Rep. 10(8):1246-51.
- Dezawa M., Takano M., Negishi H., Mo X., Oshitari T., Sawada H. (2002) Gene transfer into retinal ganglion cells by in vivo electroporation: a new approach. Micron 33(1):1-6.
- Diamond J.S., Copenhagen D.R. (1993) The contribution of NMDA and non-NMDA receptors to the light-evoked input-output characteristics of retinal ganglion cells. Neuron 11(4):725-38.
- Diamond J.S., Copenhagen D.R. (1993)The contribution of NMDA and non-NMDA receptors to the light-evoked input-output characteristics of retinal ganglion cells. Neuron 11(4):725-38.
- Diaz-Sanchez M., Williams K., DeLuca G.C., Esiri M.M. (2006) Protein co-expression with axonal injury in multiple sclerosis plaques. Acta Neuropathol. 111(4):289-99.
- Diem R., Sättler M.B., Merkler D, Demmer I., Maier K., Stadelmann C., Ehrenreich H. and Bähr M. (2005) Combined therapy with methylprednisolone and erythropoietin in a model of multiple sclerosis. Brain 128(Pt 2):375-85.
- Dijk F., Bergen A.A., Kamphuis W. (2007) GAP-43 expression is upregulated in retinal ganglion cells after ischemia/reperfusion-induced damage. Exp Eye Res. 84:858-67.

- Domercq M., Etxebarria E., Pérez-Samartín A., Matute C. (2005) Excitotoxic oligodendrocyte death and axonal damage induced by glutamate transporter inhibition. Glia 52: 36–46.
- Dong X.X., Wang Y. and Qin Z.H. (2009) Molecular mechanisms of excitotoxicity and their relevance to pathogenesis of neurodegenerative diseases. Acta Pharmacol Sin. 30(4):379-87.
- Duan X., Qiao M., Bei F., Kim I.J., He Z., Sanes J.R. (2015) Subtype-specific regeneration of retinal ganglion cells following axotomy: effects of osteopontin and mTOR signaling. Neuron 85(6):1244-56.
- Dutta R. and Trapp B.D. (2011) Mechanisms of neuronal dysfunction and degeneration in multiple sclerosis. Prog Neurobiol. 93(1):1-12.
- Dziedzic T., Metz I., Dallenga T. (2010) Wallerian degeneration: a major component of early axonal pathology in multiple sclerosis. Brain Pathol. 20:976–85.
- Ebers G.C., Sadovnick A.D., Risch N.J. (1995) A genetic basis for familial aggregation in multiple sclerosis. Canadian Collaborative Study Group. Nature 377(6545):150-1.
- Ebers G.C., Yee I.M., Sadovnick A.D., Duquette P. (2000) Conjugal multiple sclerosis: population-based prevalence and recurrence risks in offspring. Canadian Collaborative Study Group. Ann Neurol. 48(6):927-31.
- Evonuk K.S., Baker B.J., Doyle R.E., Moseley C.E., Sestero C.M., Johnston B.P., De Sarno P., Tang A., Gembitsky I., Hewett S.J., Weaver C.T., Raman C., DeSilva T.M. (2015) Inhibition of system Xc– transporter attenuates autoimmune infl ammatory demyelination. J Immunol. 195: 450–63.
- Fairless R., Williams S.K., Hoffmann D.B., Stojic A., Hochmeister S., Schmitz F., Storch M.K. and Diem R. (2012) Preclinical retinal neurodegeneration in a model of multiple sclerosis. J Neurosci. 32(16):5585-97.
- Ferguson B., Matyszak M.K., Esiri M.M. and Perry V.H. (1997) Axonal damage in acute multiple sclerosis lesions. Brain 120 (Pt 3):393-9.
- Ferreirinha F., Quattrini A., Pirozzi M., Valsecchi V., Dina G., Broccoli V., Auricchio A., Piemonte F., Tozzi G., Gaeta L., Casari G., Ballabio A., Rugarli E.I. (2004) Axonal degeneration in paraplegin-deficient mice is associated with abnormal mitochondria and impairment of axonal transport. J Clin Invest. 113(2):231-42.
- Fischer MT, Sharma R, Lim JL, et al. (2012) NADPH oxidase expression in active multiple sclerosis lesions in relation to oxidative tissue damage and mitochondrial injury. Brain 135 (Pt 3):886–99.
- Fletcher D.A., Mullins R.D. (2010) Cell mechanics and the cytoskeleton. Nature 463(7280):485-92.

- Fliegner K.H. and Liem R.K. (1991) Cellular and molecular biology of neuronal intermediate filaments. Int Rev Cytol. 131:109-67.
- Foo L.C., Allen N.J., Bushong E.A., Ventura P.B., Chung W.S., Zhou L., Cahoy J.D., Daneman R., Zong H., Ellisman M.H., Barres B.A. (2011) Development of a method for the purification and culture of rodent astrocytes. Neuron 71(5):799-811.
- Formisano L., Guida N., Valsecchi V., Pignataro G., Vinciguerra A., Pannaccione A., Secondo A., Boscia F., Molinaro P., Sisalli M.J., Sirabella R., Casamassa A., Canzoniero L.M., Di Renzo G., Annunziato L. (2013) NCX1 is a new rest target gene: role in cerebral ischemia. Neurobiol Dis. 50:76-85.
- Franklin-Tong V.E., Gourlay C.W. (2008) A role for actin in regulating apoptosis/programmed cell death: evidence spanning yeast, plants and animals. Biochem J. 413(3):389-404.
- Fu C.T., Sretavan D.W. (2012) Ectopic vesicular glutamate release at the optic nerve head and axon loss in mouse experimental glaucoma. J Neurosci. 32(45):15859-76.
- Fu L., Matthews P.M., De Stefano N., Worsley K.J., Narayanan S., Francis G.S. (1998) Imaging axonal damage of normal-appearing white matter in multiple sclerosis. Brain 121(Pt 1): 103–13.
- Fujino M., Funeshima N., Kitazawa Y., Kimura H., Amemiya H., Suzuki S. and Li X.K. (2003) Amelioration of experimental autoimmune encephalomyelitis in Lewis rats by FTY720 treatment. J Pharmacol Exp Ther. 305(1):70-7.
- Fünfschilling U., Supplie L.M., Mahad D., Boretius S., Saab A.S., Edgar J., Brinkmann B.G., Kassmann C.M., Tzvetanova I.D., Möbius W., Diaz F., Meijer D., Suter U., Hamprecht B., Sereda M.W., Moraes C.T., Frahm J., Goebbels S., Nave K.A. (2016) Glycolytic oligodendrocytes maintain myelin and long-term axonal integrity. Nature 485:517–521.
- Furukawa K., Fu W., Li Y., Witke W., Kwiatkowski D.J., Mattson M.P. (1997) The actin-severing protein gelsolin modulates calcium channel and NMDA receptor activities and vulnerability to excitotoxicity in hippocampal neurons. J Neurosci. 17(21):8178-86.
- Furukawa K., Smith-Swintosky V.L., Mattson M.P. (1995) Evidence that actin depolymerization protects hippocampal neurons against excitotoxicity by stabilizing [Ca2+]i. Exp Neurol. 133(2):153-63.
- Gadjanski I., Boretius S., Williams S.K., Lingor P., Knöferle J., Sättler M.B., Fairless R., Hochmeister S., Sühs K.W., Michaelis T., Frahm J., Storch M.K., Bähr M., Diem R. (2009) Role of n-type voltage-dependent calcium channels in autoimmune optic neuritis. Ann Neurol. 66(1):81-93.
- Galvao J., Davis B.M., Cordeiro M.F. (2013) In vivo imaging of retinal ganglion cell apoptosis. Curr Opin Pharmacol. 13(1):123-7.

- Ganter P, Prince C and Esiri MM. (1999) Spinal cord axonal loss in multiple sclerosis: a post-mortem study. Neuropathol Appl Neurobiol. 25(6):459-67.
- Garland P., Broom LJ., Quraishe S., Dalton P.D., Skipp P., Newman T.A., Perry V.H. (2012) Soluble axoplasm enriched from injured CNS axons reveals the early modulation of the actin cytoskeleton. PLoS One 7(10):47552.
- Gasser D.L., Newlin C.M., Palm J. and Gonatas N.K. (1973) Genetic control of susceptibility to experimental allergic encephalomyelitis in rats. Science 181(4102):872-3.
- Gelfland J.M., Nolan R., Schwartz D.M., Graves J., Green A.J. (2012) Microcystic macular oedema in multiple sclerosis is associated with disease severity. Brain 135: 1786–93.
- George E.B., Glass J.D., Griffin J.W. (1995) Axotomy-induced axonal degeneration is mediated by calcium influx through ion-specific channels. J Neurosci. 15(10):6445-52.
- Gilmore C.P., Donaldson I., Bö L., Owens T., Lowe J. and Evangelou N. (2008) Regional variations in the extent and pattern of grey matter demyelination in multiple sclerosis: a comparison between the cerebral cortex, cerebellar cortex, deep grey matter nuclei and the spinal cord. J Neurol Neurosurg Psychiatry 80(2):182-7.
- Gilmore C.P., Donaldson I., Bö L., Owens T., Lowe J. and Evangelou N. (2008) Regional variations in the extent and pattern of grey matter demyelination in multiple sclerosis: a comparison between the cerebral cortex, cerebellar cortex, deep grey matter nuclei and the spinal cord. J Neurol Neurosurg Psychiatry 80(2):182-7.
- Glitsch H.G., Reuter H., Scholz H. (1970) The effect of the internal sodium concentration on calcium fluxes in isolated guinea-pig auricles. J Physiol. 209(1):25-43.
- Goll D.E., Thompson V.F., Li H., Wei W., Cong J. (2003) The calpain system. Physiol Rev.
- Goverman J., Woods A., Larson L., Weiner L.P., Hood L. and Zaller D.M. (1993) Transgenic mice that express a myelin basic protein-specific T cell receptor develop spontaneous autoimmunity. Cell 72(4):551-60.
- Graumann U., Reynolds R., Steck A.J., Schaeren-Wiemers N. (2003) Molecular changes in normal appearing white matter in multiple sclerosis are characteristic of neuroprotective mechanisms against hypoxic insult. Brain Pathol. 13: 554–73.
- Green J.A., McQuaid S., Hauser L.S., Allen V.I., Lyness R. (2010) Ocular pathology in multiple sclerosis: retinal atrophy and inflammation irrespective of disease duration. Brain 133; 1591–1601.
- Gregory S.G., Schmidt S., Seth P., Oksenberg J.R., Hart J., Prokop A., Caillier S.J., Ban M., Goris A., Barcellos L.F., Lincoln R., McCauley J.L., Sawcer S.J., Compston D.A., Dubois B., Hauser S.L., Garcia-Blanco M.A., Pericak-Vance M.A., Haines J.L., Multiple Sclerosis Genetics Group (2007)

Interleukin 7 receptor alpha chain (IL7R) shows allelic and functional association with multiple sclerosis. Nat Genet. 39:1083–91.

- Griffiths I., Klugmann M., Anderson T., Yool D., Thomson C., Schwab M.H., Schneider A., Zimmermann F., McCulloch M., Nadon N., Nave K.A. (1998) Axonal swellings and degeneration in mice lacking the major proteolipid of myelin. Science 280(5369):1610-3.
- Guo L., Cordeiro M.F. (2008) Assessment of neuroprotection in the retina with DARC. Prog Brain Res. 173:437-50.
- Haahr S., Plesner A.M., Vestergaard B.F. and Höllsberg P. (2004) A role of late Epstein-Barr virus infection in multiple sclerosis. Acta Neurol Scand. 109(4):270-5.
- Hafler D.A., Compston A., Sawcer S., Lander E.S., Daly M.J., De Jager P.L., de Bakker P.I., Gabriel S.B., Mirel D.B., Ivinson A.J., Pericak-Vance M.A., Gregory S.G., Rioux J.D., McCauley J.L., Haines J.L., Barcellos L.F., Cree B., Oksenberg J.R., Hauser S.L. (2007) Risk alleles for multiple sclerosis identified by a genomewide study. N Engl J Med. 357:851–62.
- Haider L., Simeonidou C., Steinberger G., Hametner S., Grigoriadis N., Deretzi G., Kovacs G.G., Kutzelnigg A., Lassmann H., Frischer J.M. (2014) Multiple sclerosis deep grey matter: the relation between demyelination, neurodegeneration, inflammation and iron. J Neurol Neurosurg Psychiatry. 85(12):1386-95.
- Haines J.D., Inglese M., Casaccia P. (2011) Axonal Damage in Multiple Sclerosis. Mt Sinai J Med. 78(2): 231–243.
- Hains B.C., Saab C.Y., Lo A.C., Waxman S.G. (2004) Sodium channel blockade with phenytoin protects spinal cord axons, enhances axonal conduction, and improves functional motor recovery after contusion SCI. Exp Neurol. 188:365-377.
- Halliwell R.F., Peters J.A., Lambert J.J. (1989) The mechanism of action and pharmacological specificity of the anticonvulsant NMDA antagonist MK-801: a voltage clamp study on neuronal cells in culture. Br J Pharmacol. 96(2):480-94.
- Halpain S., Hipolito A., Saffer L. (1998) Regulation of F-actin stability in dendritic spines by glutamate receptors and calcineurin. J Neurosci. 18(23):9835-44.
- Hare A.W., Dong C.J., Wheeler L. (2011) Excitotoxic Injury to Retinal Ganglion Cells, Glaucoma - Basic and Clinical Concepts, Dr Shimon Rumelt (Ed.), InTech, DOI: 10.5772/20040. Available from: http://www.intechopen.com/books/glaucoma-basic-and-clinical-concepts/excitotoxic-injury-to-retinal-ganglion-cells.
- Hares K., Kemp K., Rice C., Gray E., Scolding N., Wilkins A. (2014) Reduced axonal motor protein expression in non-lesional grey matter in multiple sclerosis. Mult Scler. 20(7):812-21.

- Hares K., Redondo .J, Kemp K., Rice C., Scolding N., Wilkins A. (2016) Axonal motor protein KIF5A and associated cargo deficits in multiple sclerosis lesional and normal-appearing white matter. Neuropathol Appl Neurobiol.
- Harms C., Bösel J., Lautenschlager M., Harms U., Braun J.S., Hörtnagl H., Dirnagl U., Kwiatkowski D.J., Fink K., Endres M. (2004) Neuronal gelsolin prevents apoptosis by enhancing actin depolymerization. Mol Cell Neurosci. 25(1):69-82.
- Hartwick A.T., Hamilton C.M., Baldridge W.H. (2008) Glutamatergic calcium dynamics and deregulation of rat retinal ganglion cells. J Physiol. 586(14):3425-46.
- Hauser S.L., Oksenberg J.R. (2006) The neurobiology of multiple sclerosis: genes, inflammation, and neurodegeneration. Neuron 52(1):61-76.
- Hedström A.K., Bäärnhielm M., Olsson T. and Alfredsson L. (2009) Tobacco smoking, but not Swedish snuff use, increases the risk of multiple sclerosis. Neurology 73(9):696-701.
- Heiduschka P., Schnichels S., Fuhrmann N., Hofmeister S., Schraermeyer U., Wissinger B., Alavi M.V. (2010) Electrophysiological and histologic assessment of retinal ganglion cell fate in a mouse model for OPA1-associated autosomal dominant optic atrophy. Invest Ophthalmol Vis Sci. 51(3):1424-31.
- Hein K., Gadjanski I., Kretzschmar B., Lange K., Diem R., Sättler M.B. and Bähr M. (2012) An optical coherence tomography study on degeneration of retinal nerve fiber layer in rats with autoimmune optic neuritis. Invest Ophthalmol Vis Sci. 53(1):157-63.
- Hellström M., Pollett M.A., Harvey A.R. (2011) Post-injury delivery of rAAV2-CNTF combined with short-term pharmacotherapy is neuroprotective and promotes extensive axonal regeneration after optic nerve trauma. J Neurotrauma. 28(12):2475-83.
- Hildebrand M.E., Xu J., Dedek A., Li Y., Sengar A.S., Beggs S., Lombroso P.J., Salter M.W. (2016) Potentiation of Synaptic GluN2B NMDAR Currents by Fyn Kinase Is Gated through BDNF-Mediated Disinhibition in Spinal Pain Processing. Cell Rep. 17(10):2753-2765.
- Hiruma H., Katakura T., Takahashi S., Ichikawa T., Kawakami T. (2003) Glutamate and amyloid beta-protein rapidly inhibit fast axonal transport in cultured rat hippocampal neurons by different mechanisms. J Neurosci. 23:8967–77.
- Hobom M., Storch M.K., Weissert R., Maier K., Radhakrishnan A., Kramer B., Bähr M. and Diem R. (2004) Mechanisms and time course of neuronal degeneration in experimental autoimmune encephalomyelitis. Brain Pathol. 14(2):148-57.
- Hoffmann D.B., Williams S.K., Bojcevski J., Müller A., Stadelmann C., Naidoo V., Bahr B.A., Diem R. and Fairless R. (2013) Calcium influx and calpain activation mediate preclinical retinal neurodegeneration in autoimmune optic neuritis. J Neuropathol Exp Neurol. 72(8):745-57.

- Hofstetter H.H., Shive C.L. and Forsthuber T.G. (2002) Pertussis toxin modulates the immune response to neuroantigens injected in incomplete Freund's adjuvant: induction of Th1 cells and experimental autoimmune encephalomyelitis in the presence of high frequencies of Th2 cells. J Immunol. 169(1):117-25.
- Hohlfeld R. (1997) Biotechnological agents for the immunotherapy of multiple sclerosis. Principles, problems and perspectives. Brain 120 (Pt 5):865-916.
- Honce J.M. (2013) Gray Matter Pathology in MS: Neuroimaging and Clinical Correlations. Mult Scler Int. 2013:627870.
- Hoyt K.R., Arden S.R., Aizenman E., Reynolds I.J. (1998) Reverse Na^{+}/Ca^{2+} exchange contributes to glutamate-induced intracellular Ca2+ concentration increases in cultured rat forebrain neurons. Mol Pharmacol. 53(4):742-9.
- Huang D., Swanson E.A., Lin C.P., Schuman J.S., Stinson W.G., Chang W., Hee M.R., Flotte T., Gregory K., Puliafito C.A. (1991) Optical coherence tomography. Science 254(5035):1178-81.
- Huang X., Kong W., Zhou Y., Gregori G. (2011) Distortion of axonal cytoskeleton: an early sign of glaucomatous damage. Invest Ophthalmol Vis Sci. 52(6):2879-88.
- Huettner J.E., Bean B.P. (1988) Block of N-methyl-D-aspartate-activated current by the anticonvulsant MK-801: selective binding to open channels. Proc Natl Acad Sci USA 85(4):1307-11.
- Huettner J.E., Bean B.P. (1988) Block of N-methyl-D-aspartate-activated current by the anticonvulsant MK-801: selective binding to open channels. Proc Natl Acad Sci U S A 85(4):1307-11.
- Hunt M.J., Olszewski M., Piasecka J., Whittington M.A., Kasicki S. (2015) Effects of NMDA receptor antagonists and antipsychotics on high frequency oscillations recorded in the nucleus accumbens of freely moving mice. Psychopharmacology (Berl). 232(24):4525-35.
- Inokuchi Y., Shimazawa M., Nakajima Y., Komuro I., Matsuda T., Baba A., Araie M., Kita S., Iwamoto T., Hara H. (2009) A Na^{+}/Ca^{2+} exchanger isoform, NCX1, is involved in retinal cell death after N-methyl-D-aspartate injection and ischemia-reperfusion. J Neurosci Res. 87(4):906-17.
- Isenmann S., Bähr M. (1997) Expression of c-Jun protein in degenerating retinal ganglion cells after optic nerve lesion in the rat. Exp Neurol. 147(1):28-36.
- Johnson GV., Litersky J.M., Jope R.S. (1991) Degradation of microtubule-associated protein 2 and brain spectrin by calpain: a comparative study. J Neurochem. 56(5):1630-8.
- Jung C., Lee S., Ortiz D., Zhu Q., Julien J.P., Shea T.B. (2005) The high and middle molecular weight neurofilament subunits regulate the association of neurofilaments with kinesin:

inhibition by phosphorylation of the high molecular weight subunit. Brain Res Mol Brain Res. 141:151–55.

- Jürgens T., Jafari M., Kreutzfeldt M., Bahn E., Brück W., Kerschensteiner M., Merkler D. (2016) Reconstruction of single cortical projection neurons reveals primary spine loss in multiple sclerosis. Brain 139(Pt 1):39-46.
- Jürgens T., Jafari M., Kreutzfeldt M., Bahn E., Brück W., Kerschensteiner M., Merkler D. (2016) Reconstruction of single cortical projection neurons reveals primary spine loss in multiple sclerosis. Brain 139:39-46.
- Kapoor R., Davies M., Blaker P.A., Hall S.M., Smith K.J. (2003) Blockers of sodium and calcium entry protect axons from nitric oxide-mediated degeneration. Ann Neurol. 53:174-180.
- Kappos L., Radue E.W., O'Connor P., Polman C., Hohlfeld R., Calabresi P., Selmaj K., Agoropoulou C., Leyk M., Zhang-Auberson L., Burtin P.; FREEDOMS Study Group. (2010) A placebo-controlled trial of oral fingolimod in relapsing multiple sclerosis. N Engl J Med. 362(5):387-401.
- Karbowski M., Youle R.J. (2003) Dynamics of mitochondrial morphology in healthy cells and during apoptosis. Cell Death Differ. 10(8):870-80.
- Karschin A., Lipton S.A. (1989) Calcium channels in solitary retinal ganglion cells from post-natal rat. J Physiol. 418:379-96.
- Kaufhold F., Zimmermann H., Schneider E., Ruprecht K., Paul F., Oberwahrenbrock T., Brandt A.U. (2013) Optic neuritis is associated with inner nuclear layer thickening and microcystic macular edema independently of multiple sclerosis. PLoS One 8(8):e71145.
- Kaushik M., Wang C.Y., Barnett M.H., Garrick R., Parratt J., Graham S.L., Sriram P., Yiannikas C., Klistorner A. (2013) Inner nuclear layer thickening is inversley proportional to retinal ganglion cell loss in optic neuritis. PLoS One 8(10):e78341.
- Kawachi I. and Lassmann H. (2017) Neurodegeneration in multiple sclerosis and neuromyelitis optica. J Neurol Neurosurg Psychiatry 88(2):137-145.
- Kawachi I., Lassmann H. (2016) Neurodegeneration in multiple sclerosis and neuromyelitis optica. J Neurol Neurosurg Psychiatry 2016 pii: jnnp-2016-313300.
- Kermer P., Klöcker N., Labes M., Thomsen S., Srinivasan A., Bähr M. (1999) Activation of caspase-3 in axotomized rat retinal ganglion cells in vivo FEBS Lett. 453(3):361-4.
- Kerschensteiner M., Schwab M.E., Lichtman J.W., Misgeld T. (2005) In vivo imaging of axonal degeneration and regeneration in the injured spinal cord. Nat Med. 11(5):572-7.
- Kipp M., van der Valk P. and Amor S. (2012) Pathology of multiple sclerosis. CNS Neurol Disord Drug Targets 11(5):506-17.

- Kitaoka Y., Kitaoka Y., Kumai T., Lam T.T., Kuribayashi K., Isenoumi K., Munemasa Y., Motoki M., Kobayashi S., Ueno S. (2004) Involvement of RhoA and possible neuroprotective effect of fasudil, a Rho kinase inhibitor, in NMDA-induced neurotoxicity in the rat retina. Brain Res. 1018(1):111-8.
- Kitaoka Y1, Kitaoka Y, Kumai T, Lam TT, Kuribayashi K, Isenoumi K, Munemasa Y, Motoki M, Kobayashi S, Ueno S. (2004) Involvement of RhoA and possible neuroprotective effect of fasudil, a Rho kinase inhibitor, in NMDA-induced neurotoxicity in the rat retina. Brain Res. 1018(1):111-8.
- Klistorner A., Arvind H., Garrick R., Yiannikas C., Paine M., Graham S.L. (2010) Remyelination of optic nerve lesions: spatial and temporal factors. Mult Scler. Jul;16(7):786-95.
- Klistorner A., Graham S., Fraser C., Garrick R., Nguyen T., Paine M., O'Day J., Grigg J., Arvind H. and Billson F.A. (2007) Electrophysiological evidence for heterogeneity of lesions in optic neuritis. Invest Ophthalmol Vis Sci. 48(10):4549-56.
- Klugmann M., Schwab M.H., Pühlhofer A., Schneider A., Zimmermann F., Griffiths I.R., Nave K.A. (1997) Assembly of CNS myelin in the absence of proteolipid protein. Neuron 18:59–70.
- Knöferle J., Koch J.C., Ostendorf T., Michel U., Planchamp V., Vutova P., Tönges L., Stadelmann C., Brück W., Bähr M., Lingor P. (2010) Mechanisms of acute axonal degeneration in the optic nerve in vivo. Proc Natl Acad Sci U S A 107(13):6064-9.
- Koeberle P.D., Ball A.K. (1998) Effects of GDNF on retinal ganglion cell survival following axotomy. Vision Res. 38(10):1505-15.
- Koenig K.A., Sakaie K.E., Lowe M.J., Lin J., Stone L., Bermel R.A., Beall E.B., Rao S.M., Trapp B.D., Phillips M.D. (2014) Hippocampal volume is related to cognitive decline and fornicial diffusion measures in multiple sclerosis. Magn Reson Imaging. 32(4):354-8.
- Komatsu M., Wang Q.J., Holstein G.R., Friedrich V.L. Jr., Iwata J., Kominami E., Chait B.T, Tanaka K., Yue Z. (2007) Essential role for autophagy protein Atg7 in the maintenance of axonal homeostasis and the prevention of axonal degeneration. Proc Nat Acad Sci U S A 104(36):14489-94.
- Koo E.H., Sisodia S.S., Archer D.R., Martin L.J., Weidemann A., Beyreuther K., Fischer P., Masters C.L., Price D.L. (1990) Precursor of amyloid protein in Alzheimer disease undergoes fast anterograde axonal transport. Proc Natl Acad Sci USA 87:1561–65.
- Kornek B., Lassmann H. (1999) Axonal pathology in multiple sclerosis. A historical note. Brain Pathol. 9(4):651-6.
- Kornek B., Storch M.K., Bauer J., Djamshidian A., Weissert R., Wallstroem E., Stefferl A., Zimprich F., Olsson T., Linington C., Schmidbauer M. and Lassmann H. (2001) Distribution of a

calcium channel subunit in dystrophic axons in multiple sclerosis and experimental autoimmune encephalomyelitis. Brain 124(Pt 6):1114-24.

- Kornek B., Storch M.K., Weissert R., Wallstroem E., Stefferl A., Olsson T., Linington C., Schmidbauer M. and Lassmann H. (2000) Multiple sclerosis and chronic autoimmune encephalomyelitis: a comparative quantitative study of axonal injury in active, inactive, and remyelinated lesions. Am J Pathol. 157(1):267-76.
- Kothakota S., Azuma T., Reinhard C., Klippel A., Tang J., Chu K., McGarry T.J., Kirschner M.W., Koths K., Kwiatkowski D.J., Williams L.T. (1997) Caspase-3-generated fragment of gelsolin: effector of morphological change in apoptosis. Science 278(5336):294-8.
- Krishnamoorthy G. and Wekerle H. (2009) EAE: an immunologist's magic eye. Eur J Immunol. 39(8):2031-5.
- Krishnamoorthy G., Lassmann H., Wekerle H. and Holz A. (2006) Spontaneous opticospinal encephalomyelitis in a double-transgenic mouse model of autoimmune T cell/B cell cooperation. J Clin Invest. 116(9):2385-92.
- Krizaj D., Demarco S.J., Johnson J., Strehler E.E., Copenhagen D.R. (2002) Cell-Specific Expression of Plasma Membrane Calcium ATPase Isoforms in Retinal Neurons. J Comp Neurol. 451(1): 1–21.
- Krizbai I.A., Deli M.A., Pestenacz A., Siklos L., Szabo C.A., Andras I., Joo F. (1998) Expression of glutamate receptors on cultured cerebral endothelial cells. J Neurosci Res 54:814–819.
- Krnjevic K., Xu .YZ. (1989) Dantrolene suppresses the hyerpolarization or outward current observed during anoxia in hippocampal neurons. Can J Physiol Pharmacol. 67:1602-1604.
- Kuhle J., Disanto G., Dobson R., Adiutori R., Bianchi L., Topping J., Bestwick J.P., Meier U.C., Marta M., Costa G.D., Runia T., Evdoshenko E., Lazareva N., Thouvenot E., Iaffaldano P., Direnzo V., Khademi M., Piehl F., Comabella M., Sombekke M., Killestein J., Hegen H., Rauch S., D'Alfonso S., Alvarez-Cermeño J.C., Kleinová P., Horáková D., Roesler R., Lauda F., Llufriu S., Avsar T., Uygunoglu U., Altintas A., Saip S., Menge T., Rajda C., Bergamaschi R., Moll N., Khalil M., Marignier R., Dujmovic I., Larsson H., Malmestrom C., Scarpini E., Fenoglio C., Wergeland S., Laroni A., Annibali V., Romano S., Martínez A.D., Carra A., Salvetti M., Uccelli A., Torkildsen Ø., Myhr K.M., Galimberti D., Rejdak K., Lycke J., Frederiksen J.L., Drulovic J., Confavreux C., Brassat D., Enzinger C., Fuchs S., Bosca I., Pelletier J., Picard C., Colombo E., Franciotta D., Derfuss T., Lindberg R., Yaldizli Ö., Vécsei L., Kieseier B.C., Hartung H.P., Villoslada P., Siva A., Saiz A., Tumani H., Havrdová E., Villar L.M., Leone M., Barizzone N., Deisenhammer F., Teunissen C., Montalban X., Tintoré M., Olsson T., Trojano M., Lehmann S., Castelnovo G., Lapin S., Hintzen R., Kappos L., Furlan R., Martinelli V., Comi G., Ramagopalan

S.V. and Giovannoni G. (2015) Conversion from clinically isolated syndrome to multiple sclerosis: A large multicentre study. Mult Scler. 21(8):1013-24.

- Kułakowska A., Ciccarelli N.J., Wen Q., Mroczko B., Drozdowski W., Szmitkowski M., Janmey P.A., Bucki R. (2010) Hypogelsolinemia, a disorder of the extracellular actin scavenger system, in patients with multiple sclerosis. BMC Neurol. 10:107.
- Kullmann D.M. (2010) Neurological channelopathies. Annu. Rev. Neurosci. 33:151–172.
- Kupersmith M.J., Garvin M.K., Wang J.K., Durbin M., Kardon R. (2016) Retinal ganglion cell layer thinning within one month of presentation for optic neuritis. Mult Scler. 22(5):641-8.
- Kuribayashi J., Kitaoka Y., Munemasa Y., Ueno S. (2010) Kinesin-1 and degenerative changes in optic nerve axons in NMDA-induced neurotoxicity. Brain Res. 1362:133-40.
- Kusaka S., Kapousta-Bruneau N.V., Puro D.G. (1999) Plasma-induced changes in the physiology of mammalian retinal glial cells: role of glutamate. Glia 25(3):205-15.
- Kusaka S., Kapousta-Bruneau N.V., Puro D.G. (1999) Plasma-induced changes in the physiology of mammalian retinal glial cells: role of glutamate. Glia 25(3):205-15.
- Kutzelnigg A. and Lassmann H. (2005) Cortical lesions and brain atrophy in MS. J Neurol Sci. 233(1-2):55-9.
- Kutzelnigg A., Lucchinetti C.F., Stadelmann C., Brück W., Rauschka H., Bergmann M., Schmidbauer M., Parisi J.E., Lassmann H. (2005) Cortical demyelination and diffuse white matter injury in multiple sclerosis. Brain 128(Pt 11):2705-12.
- Langer-Gould A, Brara S.M., Beaber B.E., Zhang J.L. (2013) Incidence of multiple sclerosis in multiple racial and ethnic groups. Neurobiology. 80(19):1734-9.
- Langer-Gould A., Brara S.M., Beaber B.E., Zhang J.L. (2013) Incidence of multiple sclerosis in multiple racial and ethnic groups. Neurology 80(19):1734-9.
- Lanz T.V., Williams S.K., Stojic A., Iwantscheff S., Sonner J.K., Grabitz C., Becker S., Böhler L.I., Mohapatra S.R., Sahm F., Küblbeck G., Nakamura T., Funakoshi H., Opitz C.A., Wick W., Diem R., Platten M. (2017) Tryptophan-2,3-Dioxygenase (TDO) deficiency is associated with subclinical neuroprotection in a mouse model of multiple sclerosis. Sci Rep. 7:41271.
- Lappe-Siefke C., Goebbels S., Gravel M., Nicksch E., Lee J., Braun P.E., Griffiths I.R., Nave K.A. (2003) Disruption of Cnp1 uncouples oligodendroglial functions in axonal support and myelination. Nat Genet. 33:366–74.
- Lassmann H. (2013) Relapsing-remitting and primary progressive MS have the same cause(s)--the neuropathologist's view: 1. Mult Scler. 19(3):266-7.
- Lebrun C., Bensa C., Debouverie M., et al. (2009) Association between clinical conversion to multiple sclerosis in radiologically isolated syndrome and magnetic resonance imaging,

cerebrospinal fluid, and visual evoked potential: follow-up of 70 patients. Arch Neurol. 66:841–846.

- Lei S.Z., Zhang D., Abele A.E., Lipton S.A. (1992) Blockade of NMDA receptor-mediated mobilization of intracellular Ca2+ prevents neurotoxicity. Brain Res. 598(1-2):196-202.
- Leung C.K., Lindsey J.D., Crowston J.G., Ju W.K., Liu Q., Bartsch D.U., Weinreb R.N. (2008) In vivo imaging of murine retinal ganglion cells. J Neurosci Methods 168(2):475-8.
- Li C., Tropak M.B., Gerlai R., Clapoff S., Abramow-Newerly W., Trapp B., Peterson A., Roder J. (1994) Myelination in the absence of myelin-associated glycoprotein. Nature 369(6483):747-50.
- Lin T.H., Kim J.H., Perez-Torres C., Chiang C.W., Trinkaus K., Cross A.H., Song S.K. (2014) Axonal transport rate decreased at the onset of optic neuritis in EAE mice. Neuroimage 100:244-53.
- Lingor P., Koch J.C., Tönges L., Bähr M. (2012) Axonal degeneration as a therapeutic target in the CNS. Cell Tissue Res. 349(1):289-311.
- Linthicum D.S., Munoz J.J. and Blaskett A. (1982) Acute experimental autoimmune encephalomyelitis in mice. I. Adjuvant action of Bordetella pertussis is due to vasoactive amine sensitization and increased vascular permeability of the central nervous system. Cell Immunol. 73(2):299-310.
- Lipton S.A., Rosenberg P.A. (1994) Excitatory Amino Acids as a Final Common Pathway for Neurologic Disorders. N Engl J Med. 330:613-622.
- Liu J.S., Zhao M.L., Brosnan C.F., Lee S.C. (2001) Expression of inducible nitric oxide synthase and nitrotyrosine in multiple sclerosis lesions. Am J Pathol. 158(6):2057-66.
- Llinas R., Sugimori M., Silver R.B. (1992) Microdomains of high calcium concentration in a presynaptic terminal. Science 256:677-679.
- Lo A.C., Saab C.Y., Black J.A. and Waxman SG. (2003) Phenytoin protects spinal cord axons and preserves axonal conduction and neurological function in a model of neuroinflammation in vivo. J Neurophysiol. 90:3566-71.
- Lo A.C., Saab C.Y., Black J.A., Waxman S.G. (2003) Phenytoin protects spinal cord axons and preserves axonal conduction and neurological function in a model of neuroinflammation in vivo. J Neurophysiol. 90:3566-3571.
- Lovas G., Szilágyi N., Majtényi K., Palkovits M., Komoly S. (2000) Axonal changes in chronic demyelinated cervical spinal cord plaques. Brain 123 (Pt 2):308-17.
- Lu C., Mattson M.P. (2001) Dimethyl sulfoxide suppresses NMDA- and AMPA-induced ion currents and calcium influx and protects against excitotoxic death in hippocampal neurons. Exp Neurol. 170(1):180-5.

- Lublin F.D., Reingold C., Cohen A.J., Cutter R.G., Sørensen S.P, Thompson, J.A., Wolinsky S.J., Balcer J.L., Banwell B., Frederik Barkhof F., Bebo Jr. B., Calabresi P.A., Clanet M., Comi G., Fox J.R., Freedman S.M., Goodman D.A., Inglese,M., Kappos L., Kieseier C.B., Lincoln A.J., Lubetzki Ch., Miller E.A., Montalban X., O'Connor W.P., Petkau J., Pozzilli,C., Rudick A.R., Sormani P.M., Stüve O., Waubant E., Polman H.Ch. (2014) Defining the clinical course of multiple sclerosis: The 2013 revisions. Neurobiology 83: 278-286.
- Lucas D.R., Newhouse J.P. (1957) The toxic effect of Sodium L-Glutamine on the inner layers of the Retina. AMA Arch Ophthalmol. 58(2):193-201.
- Lucas R.M., Hughes A.M., Lay M.L., Ponsonby A.L., Dwyer D.E., Taylor B.V. and Pender MP. (2011) Epstein-Barr virus and multiple sclerosis. J Neurol Neurosurg Psychiatry 82(10):1142-8.
- Lucchinetti C., Brück W., Parisi J., Scheithauer B., Rodriguez M., Lassmann H. (2000) Heterogeneity of multiple sclerosis lesions: implications for the pathogenesis of demyelination. Ann Neurol. 47(6):707-17.
- Lucchinetti C.F., Popescu B.F., Bunyan R.F., Moll N.M., Roemer S.F., Lassmann H., Brück W., Parisi J.E., Scheithauer B.W., Giannini C., Weigand S.D., Mandrekar J., Ransohoff R.M. (2011) Inflammatory cortical demyelination in early multiple sclerosis. N Engl J Med. 365(23):2188-97.
- Luchtman D., Gollan R., Ellwardt E., Birkenstock J., Robohm K., Siffrin V., Zipp F. (2016) In vivo and in vitro effects of multiple sclerosis immunomodulatory therapeutics on glutamatergic excitotoxicity. J Neurochem. 136(5):971-80.
- Lukinavičius G., Reymond L., D'Este E., Masharina A., Göttfert F., Ta H., Güther A., Fournier M., Rizzo S., Waldmann H., Blaukopf C., Sommer C., Gerlich D.W., Arndt H.D., Hell S.W., Johnsson K. (2014) Fluorogenic probes for live-cell imaging of the cytoskeleton. Nat Methods 11:731–733.
- Luo X., Heidinger V., Picaud S., Lambrou G., Dreyfus H., Sahel J., Hicks D. (2001) Selective excitotoxic degeneration of adult pig retinal ganglion cells in vitro. Invest Ophthalmol Vis Sci. 42(5):1096-106.
- Ma M. (2013) Role of calpains in the injury-induced dysfunction and degeneration of the mammalian axon. Neurobiol Dis. 60:61-79.
- Ma M., Ferguson T.A., Schoch K.M., Li J., Qian Y., Shofer F.S., Saatman K.E., Neumar R.W. (2013) Calpains mediate axonal cytoskeleton disintegration during Wallerian degeneration. Neurobiol Dis. 56:34-46.
- Macrez R., Stys P.K., Denis V., Lipton S.A., Fabian D. (2016) Mechanisms of glutamate toxicity in multiple sclerosis: biomarker and therapeutic opportunities. Lancet Neurol. 15: 1089–102.

- Madsen L.S., Andersson E.C., Jansson L., krogsgaard M., Andersen C.B., Engberg J., Strominger J.L., Svejgaard A., Hjorth J.P., Holmdahl R., Wucherpfennig K.W. and Fugger L. (1999) A humanized model for multiple sclerosis using HLA-DR2 and a human T-cell receptor. Nat Genet. 23(3):343-7.
- Mahad D.H., Trapp B.D., Lassmann H. (2015) Pathological mechanisms in progressive multiple sclerosis. Lancet Neurol. 14:183–93.
- Maier K., Merkler D., Gerber J., Taheri N., Kuhnert A.V., Williams S.K., Neusch C., Bähr M., Diem R. (2007) Multiple neuroprotective mechanisms of minocycline in autoimmune CNS inflammation. Neurobiol Dis. 25(3):514-25.
- Manabe S., Lipton S.A. (2003) Divergent NMDA signals leading to proapoptotic and antiapoptotic pathways in the rat retina. Invest Ophthalmol Vis Sci. 44(1):385-92.
- Massey S.C., Miller R.F. (1990) N-methyl-D-aspartate receptors of ganglion cells in rabbit retina. J Neurophysiol. 63(1):16-30.
- Matsuda T., Arakawa N., Takuma K., Kishida Y., Kawasaki Y., Sakaue M., Takahashi K., Takahashi T., Suzuki T., Ota T., Hamano-Takahashi A., Onishi M., Tanaka Y., Kameo K., Baba A. (2001) SEA0400, a novel and selective inhibitor of the Na^{+}-Ca^{2+} exchanger, attenuates reperfusion injury in the in vitro and in vivo cerebral ischemic models. J Pharmacol Exp Ther. 298(1):249-56.
- Matthews P.M., Pioro E., Narayanan S., De Stefano N., Fu L., Francis G., Antel J., Wolfson C., Arnold D.L. (1996) Assessment of lesion pathology in multiple sclerosis using quantitative MRI morphometry and magnetic resonance spectroscopy. Brain 119:715–722.
- McCormack J.G., Halestrap A.P., Denton R.M. (1990) Role of calcium ions in regulation of mammalian intramitochondrial metabolism. Physiol Rev. 70(2):391-425.
- McDonald L.J., Moss J. (1993) Stimulation by nitric oxide of an NAD linkage to glyceraldehyde-3-phosphate dehydrogenase. Proc Natl Acad Sci U S A 90(13):6238-41.
- McKay S., Bengtson C.P., Bading H., Wyllie D.J., Hardingham G.E. (2013) Recovery of NMDA receptor currents from MK-801 blockade is accelerated by Mg^{2+} and memantine under conditions of agonist exposure. Neuropharmacology 74:119-25.
- Mead B., Thompson A., Scheven A.B., Logan A., Berry M., Leadbeater W. (2014) Comparative Evaluation of Methods for Estimating Retinal Ganglion Cell Loss in Retinal Sections and Wholemounts. PLoS ONE 9(12): e116116.
- Mead B., Tomarev S. (2016) Evaluating retinal ganglion cell loss and dysfunction. Exp Eye Res. 151:96-106.
- Melena J., Osborne N.N. (2001) Voltage-dependent calcium channels in the rat retina: involvement in NMDA-stimulated influx of calcium. Exp Eye Res. 72(4):393-401.

- Melo C.V., Okumoto S., Gomes J.R., Baptista M.S., Bahr B.A., Frommer W.B., Duarte C.B. (2013) Spatiotemporal resolution of BDNF neuroprotection against glutamate excitotoxicity in cultured hippocampal neurons. Neuroscience 237:66-86.
- Menè P., Pugliese F., Cinotti G.A. (1993) Cyclic nucleotides inhibit Na+/Ca2+ exchange in cultured human mesangial cells. Exp Nephrol. 1(4):245-52.
- Meyer R., Weissert R., Diem R., Storch M.K., de Graaf K.L., Kramer B. and Bahr M. (2001) Acute neuronal apoptosis in a rat model of multiple sclerosis. J Neurosci. 21(16):6214-20.
- Meyer-Franke A., Wilkinson G.A., Kruttgen A., Hu M., Munro E., Hanson M.G. Jr., Reichardt L.F., Barres B.A. (1998) Depolarization and cAMP elevation rapidly recruit TrkB to the plasma membrane of CNS neurons. Neuron 21(4):681-93.
- Micu I., Plemel J.R., Lachance C. (2016) The molecular physiology of the axo-myelinic synapse. Exp Neurol. 276: 41–50.
- Miller D.H., Leary S.M. (2007) Primary-progressive multiple sclerosis. Lancet Neurol. 6(10):903-12.
- Muhlert N., Atzori M., De Vita E. (2014) Memory in multiple sclerosis is linked to glutamate concentration in grey matter regions. J Neurol Neurosurg Psychiatr. 85: 833–39.
- Munemasa Y., Ohtani-Kaneko R., Kitaoka Y., Kumai T., Kitaoka Y., Hayashi Y., Watanabe M., Takeda H., Hirata K., Ueno S. (2006) Pro-apoptotic role of c-Jun in NMDA-induced neurotoxicity in the rat retina. J Neurosci Res. 83(5):907-18.
- Munemasa Y., Ohtani-Kaneko R., Kitaoka Y., Kuribayashi K., Isenoumi K., Kogo J., Yamashita K., Kumai T., Kobayashi S., Hirata K., Ueno S. (2005) Contribution of mitogen-activated protein kinases to NMDA induced neurotoxicity in the rat retina. Brain Res. 1044:227–240.
- Munger K.L., Levin L.I., Hollis B.W., Howard N.S. and Ascherio A. (2006) Serum 25-hydroxyvitamin D levels and risk of multiple sclerosis. JAMA 296(23):2832-8.
- Muriel P., Castañeda G., Ortega M., Noël F. (2003) Insights into the mechanism of erythrocyte Na+/K+-ATPase inhibition by nitric oxide and peroxynitrite anion. J Appl Toxicol. 23(4):275-8.
- Nadal-Nicolás F.M., Jiménez-López M., Salinas-Navarro M., Sobrado-Calvo P., Alburquerque-Béjar J.J. (2012) Whole Number, Distribution and Co-Expression of Brn3 Transcription Factors in Retinal Ganglion Cells of Adult Albino and Pigmented Rats. PLoS ONE 7(11): e49830.
- Nadal-Nicolás F.M., Sobrado-Calvo P., Jiménez-López M., Vidal-Sanz M., Agudo-Barriuso M. (2015) Long-Term Effect of Optic Nerve Axotomy on the Retinal Ganglion Cell Layer. Invest Ophthalmol Vis Sci. 56(10):6095-112.

- Nakagawa T., Zhu H., Morishima N., Li E., Xu J., Yankner B.A., Yuan J. (2000) Caspase-12 mediates endoplasmic-reticulum-specific apoptosis and cytotoxicity by amyloid-beta. Nature 403(6765):98-103.
- Nawaz S., Sánchez P., Schmitt S., Snaidero N., Mitkovski M., Velte C., Brückner B.R., Alexopoulos I., Czopka T., Jung S.Y., Rhee J.S., Janshoff A., Witke W., Schaap I.A., Lyons D.A., Simons M. (2015) Actin filament turnover drives leading edge growth during myelin sheath formation in the central nervous system. Dev Cell. 34(2):139-51.
- Neely M.D., Gesemann M. (1994) Disruption of microfilaments in growth cones following depolarization and calcium influx. J Neurosci. 14(12):7511-20.
- Nicot A., Ratnakar P.V., Ron Y., Chen C.C., Elkabes S. (2003) Regulation of gene expression in experimental autoimmune encephalomyelitis indicates early neuronal dysfunction. Brain 126(Pt 2):398-412.
- Nikic I., Merkler D., Sorbara C., Brinkoetter M., Kreutzfeldt M., Bareyre F.M., Brück W., Bishop D., Misgeld T., Kerschensteiner M. (2011) A reversible form of axon damage in experimental autoimmune encephalomyelitis and multiple sclerosis. Nat Med. 17(4):495-9.
- Nikić I., Merkler D., Sorbara C., Brinkoetter M., Kreutzfeldt M., Bareyre F.M., Brück W., Bishop D., Misgeld T., Kerschensteiner M. (2011) A reversible form of axon damage in experimental autoimmune encephalomyelitis and multiple sclerosis. Nat Med. 17(4):495-9.
- Noseworthy J.H., Lucchinetti C., Rodriguez M., Weinshenker B.G. (2000) Multiple sclerosis. N Engl J Med. 343(13):938-52.
- Nuschke A.C., Farrell S.R., Levesque J.M., Chauhan B.C. (2015) Assessment of retinal ganglion cell damage in glaucomatous optic neuropathy: Axon transport, injury and soma loss. Exp Eye Res. 141:111-24.
- Obrenovitch T.P., Urenjak J., Zilkha E., Jay T.M. (2000) Excitotoxicity in neurological disorders--the glutamate paradox. Int J Dev Neurosci. 18(2-3):281-7.
- Ohno N., Chiang H., Mahad D.J., Kidd G.J., Liu L., Ransohoff R.M., Sheng Z.H., Komuro H., Trapp B.D. (2014) Mitochondrial immobilization mediated by syntaphilin facilitates survival of demyelinated axons. Proc Natl Acad Sci U S A 111(27):9953-8.
- Oksenberg J.R., Barcellos L.F., Cree B.A., Baranzini S.E., Bugawan T.L., Khan O., Lincoln R.R., Swerdlin A., Mignot E., Lin L., Goodin D., Erlich H.A., Schmidt S., Thomson G., Reich D.E., Pericak-Vance M.A., Haines J.L., Hauser S.L. (2004) Mapping multiple sclerosis susceptibility to the HLA-DR locus in African Americans. Am J Hum Genet. 74:160–7.
- Olney J.W. (1969) Brain lesions, obesity, and other disturbances in mice treated with monosodium glutamate. Science 164(3880):719-21.

- Orrenius S., Zhivotovsky B., Nicotera P. (2003) Regulation of cell death: the calcium-apoptosis link. Nat Rev Mol Cell Biol. 4(7):552-65.
- Pacheco R., Oliva H., Martinez-Navío J.M. (2006) Glutamate released by dendritic cells as a novel modulator of T cell activation. J Immunol. 177: 6695–704.
- Pampliega O., Domercq M., Soria F.N., Villoslada P., Rodríguez-Antigüedad A., Matute C. (2011) Increased expression of cystine/glutamate antiporter in multiple sclerosis. J Neuroinfl ammation 8: 63.
- Pang I.H., Wexler E.M., Nawy S., DeSantis L., Kapin M.A. (1999) Protection by eliprodil against excitotoxicity in cultured rat retinal ganglion cells. Invest Ophthalmol Vis Sci. 40(6):1170-6.
- Pant HC, Veeranna (1995) Neurofilament phosphorylation. Biochem Cell Biol. 73, 575-592.
- Parrilla-Reverter G., Agudo M., Sobrado-Calvo P., Salinas-Navarro M., Villegas-Pérez M.P., Vidal-Sanz M. (2009) Effects of different neurotrophic factors on the survival of retinal ganglion cells after a complete intraorbital nerve crush injury: a quantitative in vivo study. Exp Eye Res. 89(1):32-41.
- Paul C., Manero F., Gonin S., Kretz-Remy C., Virot S., Arrigo A.P. (2002) Hsp27 as a negative regulator of cytochrome C release. Mol Cell Biol. 22: 816–834.
- Pedre X., Mastronardi F., Bruck W., López-Rodas G., Kuhlmann T., Casaccia P. (2011) Changed histone acetylation patterns in normal-appearing white matter and early multiple sclerosis lesions. J Neurosci. 31(9):3435-45.
- Pellegrini J.W., Lipton S.A. (1993) Delayed administration of memantine prevents N-methyl-D-aspartate receptor-mediated neurotoxicity. Ann Neurol. 33(4):403-7.
- Perfettini J.L., Roumier T., Kroemer G. (2005) Mitochondrial fusion and fission in the control of apoptosis. Trends Cell Biol. 15(4):179-83.
- Perry V.H. (1981) Evidence for an amacrine cell system in the ganglion cell layer of the rat retina. Neuroscience 6(5):931-44.
- Peterson J.W., Bö L., Mörk S., Chang A., Trapp BD. (2001) Transected neurites, apoptotic neurons, and reduced inflammation in cortical multiple sclerosis lesions. Ann Neurol. 50(3):389-400.
- Pinton P., Brini M., Bastianutto C., Tuft R.A., Pozzan T., Rizzuto R. (1998) New light on mitochondrial calcium. Biofactors 8(3-4):243-53.
- Pinton P., Giorgi C., Siviero R., Zecchini E., Rizzuto R. (2008) Calcium and apoptosis: ER-mitochondria Ca2+ transfer in the control of apoptosis. Oncogene 27(50):6407-18.
- Piri N., Kwong J.M., Song M., Caprioli J. (2006) Expression of hermes gene is restricted to the ganglion cells in the retina. Neurosci. Lett. 405:40–45.

- Pitt D., Werner P., Raine C.S. (2000) Glutamate excitotoxicity in a model of multiple sclerosis. Nat Med. 6(1):67-70.
- Polman C.H., Reingold S.C., Banwell B., Clanet M., Cohen J.A., Filippi M., Fujihara K., Havrdova E., Hutchinson M., Kappos L., Lublin F.D., Montalban X., O'Connor P., Sandberg-Wollheim M., Thompson A.J., Waubant E., Weinshenker B., Wolinsky J.S. (2011) Diagnostic criteria for multiple sclerosis: 2010 revisions to the McDonald criteria. Ann Neurol. 69(2):292-302.
- Raftopoulos R., Hickman S.J., Toosy A., Sharrack B., Mallik S., Paling D., Altmann D.R., Yiannakas M.C., Malladi P., Sheridan R., Sarrigiannis P.G., Hoggard N., Koltzenburg M., Gandini Wheeler-Kingshott C.A., Schmierer K., Giovannoni G., Miller D.H., Kapoor R. (2016) Phenytoin for neuroprotection in patients with acute optic neuritis: a randomised, placebo-controlled, phase 2 trial. Lancet Neurol. 15(3):259-69.
- Renganathan M., Cummins T.R., Waxman S.G. (2002) Nitric oxide blocks fast, slow, and persistent Na+ channels in C-type DRG neurons by S-nitrosylation. J Neurophysiol. 87(2):761-75.
- Riedhammer C., Weissert R. (2015) Antigen presentation, autoantigens, and immune regulation in multiple sclerosis and other autoimmune diseases. Front Immunol. 2015; 6: 322.
- Rintoul G.L., Filiano A.J., Brocard J.B., Kress G.J., Reynolds I.J. (2003) Glutamate decreases mitochondrial size and movement in primary forebrain neurons. J. Neurosci. 23(21):7881-8.
- Robitaille R., Garcia M.L., Kaczorowski G.J., Charlton M.P. (1993) Functional colocalization of calcium and calcium-gated potassium channels in control of transmitter release. Neuron 11:645-655.
- Rocca M.A., Mesaros S., Preziosa P., Pagani E., Stosic-Opincal T., Dujmovic-Basuroski I., Drulovic J., Filippi M. (2013) Wallerian and trans-synaptic degeneration contribute to optic radiation damage in multiple sclerosis: a diffusion tensor MRI study. Mult Scler. 19(12):1610-7.
- Rodriguez A.R., de Sevilla Müller L.P., Brecha N.C. (2014) The RNA binding protein RBPMS is a selective marker of ganglion cells in the mammalian retina. J Comp Neurol. 522(6):1411-43.
- Roed H., Frederiksen J., Langkilde A., Sørensen T.L., Lauritzen M., Sellebjerg F. (2005) Systemic T-cell activation in acute clinically isolated optic neuritis. J Neuroimmunol. 162(1-2):165-72.
- Rosati G. (2001) The prevalence of multiple sclerosis in the world: an update. Neurol Sci. 22:117-139.
- Rosenmund C., Westbrook G.L. (1993) Calcium-induced actin depolymerization reduces NMDA channel activity. Neuron 10(5):805-14.

- Rudrabhatla P. (2014) Regulation of Neuronal Cytoskeletal Protein Phosphorylation in Neurodegenerative Diseases. J Alzheimers Dis. 41(3):671-84.
- Rui Y., Tiwari P., Xie Z., Zheng J.Q. (2006) Acute impairment of mitochondrial trafficking by beta amyloid peptides in hippocampal neurons. J Neurosci. 26:10480–87.
- Saab A.S., Tzvetanova I.D., Nave K.A. (2013) The role of myelin and oligodendrocytes in axonal energy metabolism. Curr Opin Neurobiol. 23(6):1065-72.
- Saab A.S., Tzvetavona I.D., Trevisiol A., Baltan S., Dibaj P., Kusch K., Möbius W., Goetze B., Jahn H.M., Huang W., Steffens H., Schomburg E.D., Pérez-Samartín A., Pérez-Cerdá F., Bakhtiari D., Matute C., Löwel S., Griesinger C., Hirrlinger J., Kirchhoff F., Nave K.A. (2016) Oligodendroglial NMDA Receptors Regulate Glucose Import and Axonal Energy Metabolism. Neuron 91(1):119-32.
- Saab A.S., Tzvetavona I.D., Trevisiol A., Baltan S., Dibaj P., Kusch K., Möbius W., Goetze B., Jahn H.M., Huang W., Steffens H., Schomburg E.D., Pérez-Samartín A., Pérez-Cerdá F., Bakhtiari D., Matute C., Löwel S., Griesinger C., Hirrlinger J., Kirchhoff F., Nave K.A. (2016) Oligodendroglial NMDA Receptors Regulate Glucose Import and Axonal Energy Metabolism. Neuron 91(1):119-32.
- Sadovnick A.D., Ebers G.C., Dyment D.A., Risch N.J. (1996) Evidence for genetic basis of multiple sclerosis. The Canadian Collaborative Study Group Lancet. 347(9017):1728-30.
- Saggu S.K., Chotaliya H.P., Blumbergs P.C., Casson R.J. (2010) Wallerian-like axonal degeneration in the optic nerve after excitotoxic retinal insult: an ultrastructural study. BMC Neurosci. 11:97.
- Saidha S., Syc S.B., Ibrahim M.A., Eckstein C., Warner C.V., Farrell S.K., Oakley J.D., Durbin M.K., Meyer S.A., Balcer L.J., Frohman E.M., Rosenzweig J.M., Newsome S.D., Ratchford J.N., Nguyen Q.D. and Calabresi P.A. (2011) Primary retinal pathology in multiple sclerosis as detected by optical coherence tomography. Brain 134(Pt 2):518-33.
- Sakamoto K., Hiraiwa M., Saito M., Nakahara T., Sato Y., Nagao T., Ishii K. (2010) Protective effect of all-trans retinoic acid on NMDA-induced neuronal cell death in rat retina. Eur J Pharmacol. 635(1-3):56-61.
- Sánchez-Migallón M.C., Nadal-Nicolás F.M., Jiménez-López M., Sobrado-Calvo P., Vidal-Sanz M., Agudo-Barriuso M. (2011) Brain derived neurotrophic factor maintains Brn3a expression in axotomized rat retinal ganglion cells. Exp Eye Res. 92(4):260-7.
- Sanes J.R., Masland R.H. (2015) The types of retinal ganglion cells: current status and implications for neuronal classification. Annu Rev Neurosci. 38:221-46.
- Sawcer S., Franklin R.J., Ban M. (2014) Multiple sclerosis genetics. Lancet Neurol. 13(7):700-9.

- Schattling B., Eggert B., Friese M.A. (2014) Acquired channelopathies as contributors to development and progression of multiple sclerosis. Exp Neurol. 262 Pt A:28-36.
- Schlaepfer W.W., Zimmerman U.J. (1985) Mechanisms underlying the neuronal response to ischemic injury: Calcium-activated proteolysis of neurofilaments. Prog Brain Res. 63:185-196.
- Schulz R., Vogel T., Mashima T., Tsuruo T., Krieglstein K. (2009) Involvement of Fractin in TGF-beta-induced apoptosis in oligodendroglial progenitor cells. Glia 57(15):1619-29.
- Schwab B.L., Guerini D., Didszun C., Bano D., Ferrando-May E., Fava E., Tam J., Xu D., Xanthoudakis S., Nicholson D.W., Carafoli E., Nicotera P. (2002) Cleavage of plasma membrane calcium pumps by caspases: a link between apoptosis and necrosis. Cell Death Differ. 9(8):818-31.
- Schwartzkroin P.A., Stafstrom C.E. (1980) Effects of EGTA on the calcium-activated after-hyperpolarization in hippocampal CA3 pyramidal cells. Science 210:1125-1126.
- Secondo A., Esposito A., Sirabella R., Boscia F., Pannaccione A., Molinaro P., Cantile M., Ciccone R., Sisalli M.J., Scorziello A., Di Renzo G., Annunziato L. (2015) Involvement of the Na+/Ca2+ exchanger isoform 1 (NCX1) in neuronal growth factor (NGF)-induced neuronal differentiation through Ca2+-dependent Akt phosphorylation. J Biol Chem. 290(3):1319-31.
- Seitz A., Kojima H., Oiwa K., Mandelkow E.M., Song Y.H., Mandelkow E. (2002) Single-molecule investigation of the interference between kinesin, tau and MAP2c. EMBO J. 21:4896–905.
- Seki M., Soussou W., Manabe S., Lipton S.A. (2010) Protection of retinal ganglion cells by caspase substrate-binding peptide IQACRG from N-methyl-D-aspartate receptor-mediated excitotoxicity. Invest Ophthalmol Vis Sci. 51(2):1198-207.
- Semra Y.K., Seidi O.A., Sharief M.K. (2002) Heightened intrathecal release of axonal cytoskeletal proteins in multiple sclerosis is associated with progressive disease and clinical disability. J Neuroimmunol. 122(1-2):132-9.
- Sharp C.D., Hines I., Houghton J., Warren A., Jackson IV T.H., Jawahar A., Nanda A., Elrod J.W., Long A., Chi A., Minagar A., Alexander J.S. (2003) Glutamate causes a loss in human cerebral endothelial barrier integrity through activation of NMDA receptor. Am J Physiol Hear Circ Physiol. 285:H2592–H2598.
- Shen S., Wiemelt A.P., McMorris F.A., Barres B.A. (1999) Retinal ganglion cells lose trophic responsiveness after axotomy. Neuron 23(2):285-95.
- Shriver L.P., Dittel B.N. (2006) T-cell-mediated disruption of the neuronal microtubule network: correlation with early reversible axonal dysfunction in acute experimental autoimmune encephalomyelitis. Am J Pathol. 169(3):999-1011.

- Siffrin V., Birkenstock J., Luchtman D.W., Gollan R., Baumgart J., Niesner R.A., Griesbeck O., Zipp F. (2015) FRET based ratiometric Ca^{2+} imaging to investigate immune-mediated neuronal and axonal damage processes in experimental autoimmune encephalomyelitis. J Neurosci Methods. 249:8-15.
- Siliprandi R., Canella R., Carmignoto G., Schiavo N., Zanellato A., Zanoni R., Vantini G. (1992) N-methyl-D-aspartate-induced neurotoxicity in the adult rat retina. Vis Neurosci. 8(6):567-73.
- Smith K.J., Lassmann H. (2002) The role of nitric oxide in multiple sclerosis. Lancet Neurol. 1(4):232-41.
- Smith S.J., Augustine G.J. (1988) Calcium ions, active zones, and synaptic transmitter release. Trends Neurosci. 11:458-464.
- Smith T., Groom A., Zhu B., Turski L. (2000) Autoimmune encephalomyelitis ameliorated by AMPA antagonists. Nat Med. 6(1):62-6.
- Söderström M., Link H., Xu Z., Fredriksson S. (1993) Optic neuritis and multiple sclerosis: anti-MBP and anti-MBP peptide antibody-secreting cells are accumulated in CSF. Neurology 43(6):1215-22.
- Soilu-Hänninen M., Airas L., Mononen I., Heikkilä A., Viljanen M. and Hänninen A. (2005) 25-Hydroxyvitamin D levels in serum at the onset of multiple sclerosis. Mult Scler. 11(3):266-71.
- Sokolowski J.D., Gamage K.K., Heffron D.S., Leblanc A.C., Deppmann C.D., Mandell J.W. (2014) Caspase-mediated cleavage of actin and tubulin is a common feature and sensitive marker of axonal degeneration in neural development and injury. Acta Neuropathol Commun. 2:16.
- Sorbara C.D., Wagner N.E., Ladwig A., Nikić I., Merkler D., Kleele T., Marinković P., Naumann R., Godinho L., Bareyre F.M., Bishop D., Misgeld T., Kerschensteiner M. (2014) Pervasive axonal transport deficits in multiple sclerosis models. Neuron 84(6):1183-90.
- Srinivasan R., Sailasuta N., Hurd R., Nelson S., Pelletier D. (2005) Evidence of elevated glutamate in multiple sclerosis using magnetic resonance spectroscopy at 3 T. Brain 128(Pt 5):1016-25.
- Sriram P., Graham S.L., Wang C., Yiannikas C., Garrick R., Klistorner A. (2012) Transsynaptic retinal degeneration in optic neuropathies: optical coherence tomography study. Invest Ophthalmol Vis Sci. 53(3):1271-5.
- Staal J.A., Dickson T.C., Gasperini R., Liu Y., Foa L., Vickers J.C. (2010) Initial calcium release from intracellular stores followed by calcium dysregulation is linked to secondary axotomy following transient axonal stretch injury. J Neurochem. 112(5):1147-55.

- Staal J.A., Dickson T.C., Gasperini R., Liu Y., Foa L., Vickers J.C. (2010) Initial calcium release from intracellular stores followed by calcium dysregulation is linked to secondary axotomy following transient axonal stretch injury. J Neurochem. 112(5):1147-55.
- Stefferl A., Brehm U., Storch M., Lambracht-Washington D., Bourquin C., Wonigeit K., Lassmann H. and Linington C. (1999) Myelin oligodendrocyte glycoprotein induces experimental autoimmune encephalomyelitis in the "resistant" Brown Norway rat: disease susceptibility is determined by MHC and MHC-linked effects on the B cell response. J Immunol. 163(1):40-9.
- Stokin G.B., Lillo C., Falzone T.L., Brusch R.G., Rockenstein E., Mount S.L., Raman R., Davies P., Masliah E., Williams D.S., Goldstein L.S. (2005) Axonopathy and transport deficits early in the pathogenesis of Alzheimer's disease. Science 307(5713):1282-8.
- Stone J.R., Okonkwo D.O., Dialo A.O., Rubin D.G., Mutlu L.K., Povlishock J.T., Helm G.A. (2004) Impaired axonal transport and altered axolemmal permeability occur in distinct populations of damaged axons following traumatic brain injury. Exp Neurol. 190(1):59-69.
- Storch M.K., Stefferl A., Brehm U., Weissert R., Wallström E., Kerschensteiner M., Olsson T., Linington C., Lassmann H. (1998) Autoimmunity to myelin oligodendrocyte glycoprotein in rats mimics the spectrum of multiple sclerosis pathology. Brain Pathol. 8(4):681-94.
- Stüve O., Marra C.M., Jerome K.R., Cook L., Cravens P.D., Cepok S., Frohman E.M., Phillips J.T., Arendt G., Hemmer B., Monson N.L. and Racke M.K. (2006) Immune surveillance in multiple sclerosis patients treated with natalizumab. Ann Neurol. 59(5):743-7.
- Stys P.K. (2013) Pathoetiology of multiple sclerosis: are we barking up the wrong tree? F1000 Prime Rep. 5: 20.
- Stys P.K., Lehning E., Saubermann A.J. and LoPachin RM Jr. (1997) Intracellular concentrations of major ions in rat myelinated axons and glia: calculations based on electron probe X-ray microanalyses. J Neurochem. 68(5):1920-8.
- Stys P.K., Sontheimer H., Ransom B.R., Waxman S.G. (1993) Noninactivating, tetrodotoxin-sensitive Na^+ conductance in rat optic nerve axons. Proc Natl Acad Sci U S A 90, 6976-6980.
- Stys P.K., Waxman S.G., Ransom B.R. (1992a) Effects of temperature on evoked electrical activity and anoxic injury in CNS white matter. J Cereb Blood Flow Metab. 12:977-986.
- Stys P.K., Waxman S.G., Ransom B.R., (1992b) Ionic mechanisms of anoxic injury in mammalian CNS white matter: role of Na+ channels and NCX. J Neurosci. 12:430-439.
- Stys P.K., Zamponi G.W., van Minnen J., Geurts J.J. (2012) Will the real multiple sclerosis please stand up? Nat Rev Neurosci. 13(7):507-14.

- Sühs K.W., Fairless R., Williams S.K., Heine K., Cavalié A., Diem R. (2014) N-methyl-D-aspartate receptor blockade is neuroprotective in experimental autoimmune optic neuritis. J Neuropathol Exp Neurol. 73(6):507-18.
- Sühs K.W., Hein K., Sättler M.B., Görlitz A., Ciupka C., Scholz K., Käsmann-Kellner B., Papanagiotou P., Schäffler N., Restemeyer C., Bittersohl D., Hassenstein A., Seitz B., Reith W., Fassbender K., Hilgers R., Heesen C., Bähr M., Diem R. (2012) A randomized, double-blind, phase 2 study of erythropoietin in optic neuritis. Ann Neurol. 72(2):199-210.
- Suhy J., Rooney W.D., Goodkin D.E., Capizzano A.A., Soher B.J., Maudsley A.A., Waubant E., Andersson P.B., Weiner M.W. (2000) 1H MRSI comparison of white matter and lesions in primary progressive and relapsing-remitting MS. Mult Scler. 6(3):148-55.
- Syc S.B., Saidha S., Newsome S.D., Ratchford J.N., Levy M., Ford E., Crainiceanu C.M., Durbin M.K., Oakley J.D., Meyer S.A., Frohman E.M., Calabresi P.A.(2012) Optical coherence tomography segmentation reveals ganglion cell layer pathology after optic neuritis. Brain 135(Pt 2):521-33.
- Szalai G., Krishnamurthy R., Hajnóczky G. (1999) Apoptosis driven by IP(3)-linked mitochondrial calcium signals. EMBO J. 18(22):6349-61.
- Taschenberger H., Grantyn R. (1995) Several types of Ca^{2+} channels mediate glutamatergic synaptic responses to activation of single Thy-1-immunolabeled rat retinal ganglion neurons. J Neurosci. 15(3 Pt 2):2240-54.
- Thor H., Hartzell P., Orrenius S. (1984) Potentiation of oxidative cell injury in hepatocytes which have accumulated Ca2+. J Biol Chem. 259:6612–6615.
- Tisell A., Leinhard O.D., Warntjes J.B.M. (2013) Increased concentrations of glutamate and glutamine in normal-appearing white matter of patients with multiple sclerosis and normal MR imaging brain scans. PLoS One 8: e61817.
- Trapp B.D., Nave K.A. (2008) Multiple sclerosis: an immune or neurodegenerative disorder? Annu Rev Neurosci. 31:247-69.
- Trapp B.D., Peterson J., Ransohoff R.M., Rudick R., Mörk S., Bö L. (1998) Axonal transection in the lesions of multiple sclerosis. N Engl J Med. 338(5):278-85.
- Traynelis S.F., Wollmuth L.P., McBain C.J., Menniti F.S., Vance K.M., Ogden K.K., Hansen K.B., Yuan H., Myers S.J., Dingledine R. (2010) Glutamate receptor ion channels: structure, regulation, and function. Pharmacol Rev. 62(3):405-96.
- Trifaro J.M., Vitale M.L. (1993) Cytoskeleton dynamics during neurotransmitter release. Trends Neurosci. 16:466-472.

- Tur C., Goodkin O., Altmann D.R., Jenkins T.M., Miszkiel K., Mirigliani A., Fini C., Gandini Wheeler-Kingshott C.A., Thompson A.J., Ciccarelli O., Toosy A.T.(2016) Longitudinal evidence for anterograde trans-synaptic degeneration after optic neuritis. Brain 139(Pt 3):816-28.
- Tymianski M. (1996) Cytosolic calcium concentrations and cell death in vitro. In: B.K. Siesjo, T. Wieloch (Eds.), Advances in Neurology: Cellular and Molecular Mechanisms of Ischemic Brain Damage, Lippincott-Raven, Philadelphia, pp. 85–105.
- Tymianski M., Charlton M.P., Carlen P.L., Tator C.H. (1993) Source specificity of early calcium neurotoxicity in cultured embryonic spinal neurons. J Neurosci. 13:2085–2104.
- Tymianski M., Tator, Ch. (1996) Normal and Abnormal Calcium Homeostasis in Neurons: A Basis for the Pathophysiology of Traumatic and Ischemic Central Nervous System Injury. Neurosurgery pp 1176-1195.
- Ullian E.M., Barkis W.B., Chen S., Diamond J.S., Barres B.A. (2004) Invulnerability of retinal ganglion cells to NMDA excitotoxicity. Mol Cell Neurosci. 26(4):544-57.
- Utsumi T., Sakurai N., Nakano K., Ishisaka R. (2003) C-terminal 15 kDa fragment of cytoskeletal actin is posttranslationally N-myristoylated upon caspase-mediated cleavage and targeted to mitochondria. FEBS Lett. 539(1-3):37-44.
- van Horssen J., Brink B.P., de Vries H.E., van der Valk P., Bø L. (2007) The blood-brain barrier in cortical multiple sclerosis lesions. J Neuropathol Exp Neurol. 66(4):321-8.
- Vanagas L., de La Fuente M.C., Dalghi M., Ferreira-Gomes M., Rossi R.C., Strehler E.E., Mangialavori I.C., Rossi J.P. (2013) Differential effects of G- and F-actin on the plasma membrane calcium pump activity. Cell Biochem Biophys. 66(1):187-98.
- Vazana U., Veksler R., Pell G.S., Prager O., Fassler M., Chassidim Y., Roth Y., Shahar H., Zangen A., Raccah R., Onesti E., Ceccanti M., Colonnese C., Santoro A., Salvati M., D'Elia A., Nucciarelli V., Inghilleri M., Friedman A. (2016) Glutamate-Mediated Blood-Brain Barrier Opening: Implications for Neuroprotection and Drug Delivery. J Neurosci. 36(29):7727-39.
- Vercellino M., Masera S., Lorenzatti M., Condello C., Merola A., Mattioda A., Tribolo A., Capello E., Mancardi G.L., Mutani R., Giordana M.T. and Cavalla P. (2009) Demyelination, inflammation, and neurodegeneration in multiple sclerosis deep grey matter. J Neuropathol Exp Neurol. 68(5):489-502.
- Vercellino M., Plano F., Votta B., Mutani R., Giordana M.T., Cavalla P. (2005) Grey matter pathology in multiple sclerosis. J Neuropathol Exp Neurol. 64(12):1101-7.
- Vercellino, M.M., Merola, A.A., Piacentino, C.C., Votta, B.B., Capello, E.E., Mancardi, G.L.G., Mutani, R.R., Giordana, M.T.M., Cavalla, P.P., (2007) Altered glutamate reuptake in relapsing–remitting and secondary progressive multiple sclerosis cortex: correlation with

microglia infiltration, demyelination, and neuronal and synaptic damage. J Neuropathol Exp Neurol. 66: 732–739.

- Wagner O.I., Ascano J., Tokito M., Leterrier J.F., Janmey P.A., Holzbaur E.L. (2004) The interaction of neurofilaments with the microtubule motor cytoplasmic dynein. Mol Biol Cell 15:5092–100.
- Waller A. (1850) Experiments on the section of the glossopharyngeal and hypoglossal nerves of the frog, and observations of the alternations produced thereby in the structure of their primitive fibers. Phil Trnas R Soc Lond. 140:423-29.
- Walter S.D., Ishikawa H., Galetta K.M. (2013) Ganglion cell loss in relation to visual disability in multiple sclerosis. Ophthalmology 119:1250–1257.
- Wang J.T., Medress Z.A., Barres B.A. (2012) Axon degeneration: molecular mechanisms of a self-destruction pathway. J Cell Biol. 196(1):7-18.
- Wang X., Ng Y.K., Tay S.S. (2005) Factors contributing to neuronal degeneration in retinas of experimental glaucomatous rats. J Neurosci Res. 82:674-89.
- Waxman S.G., Black J.A., Ransom B.R., Stys P.K. (1994) Anoxic injury of rat optic nerve: ultrastructural evidence for coupling between Na+ influx and Ca2+-mediated injury in myelinated CNS axons. Brain Res. 644(2):197-204.
- Webb R.H., Hughes G.W., Pomerantzeff O. (1980) Flying spot TV ophthalmoscope. Appl Opt. 19(17):2991-7.
- Wegner C., Esiri M.M., Chance S.A., Palace J., Matthews P.M. (2006) Neocortical neuronal, synaptic, and glial loss in multiple sclerosis. Neurology 67(6):960-7.
- Werner P., Pitt D., Raine C.S. (2001) Multiple sclerosis: altered glutamate homeostasis in lesions correlates with oligodendrocyte and axonal damage. Ann Neurol. 50: 169–80.
- Werner P., Pitt D., Raine C.S. (2001) Multiple sclerosis: altered glutamate homeostasis in lesions correlates with oligodendrocyte and axonal damage. Ann Neurol. 50: 169–80.
- Wessendorf M.W. (1991) Fluoro-Gold: composition, and mechanism of uptake. Brain Res. 553(1):135-48.
- Wong E.H., Kemp J.A., Priestley T., Knight A.R., Woodruff G.N., Iversen L.L. (1986) The anticonvulsant MK-801 is a potent N-methyl-D-aspartate antagonist. Proc Natl Acad Sci U S A 83(18):7104-8.
- Xu K., Zhong G., Zhuang X. (2013) Actin, spectrin and associated proteins form a periodic cytoskeletal structure in axons. Science 339:452–456.
- Yang J., Weimer R.M., Kallop D., Olsen O., Wu Z., Renier N., Uryu K., Tessier-Lavigne M. (2013) Regulation of axon degeneration after injury and in development by the endogenous calpain inhibitor calpastatin. Neuron 80(5):1175-89.

- Yednock T.A., Cannon C., Fritz L.C., Sanchez-Madrid F., Steinman L. and Karin N. (1992) Prevention of experimental autoimmune encephalomyelitis by antibodies against alpha 4 beta 1 integrin. Nature 356(6364):63-6.
- Yi M., Weaver D., Hajnóczky G. (2004) Control of mitochondrial motility and distribution
- Yin X., Crawford T.O., Griffin J.W., Tu Ph., Lee V.M., Li C., Roder J., Trapp B.D. (1998) Myelin-associated glycoprotein is a myelin signal that modulates the caliber of myelinated axons. J Neurosci. 18:1953–62.
- Yoles E., Muller S., Schwartz M. (1997) NMDA-receptor antagonist protects neurons from secondary degeneration after partial optic nerve crush. J Neurotrauma 14(9):665-75.
- Yuan A., Rao M.V., Sasaki T., Chen Y., Kumar A., Veeranna Liem R.K., Eyer J., Peterson A.C., Julien J.P., Nixon R.A. (2006) Alpha-internexin is structurally and functionally associated with the neurofilament triplet proteins in the mature CNS. J Neurosci. 26(39):10006-19.
- Yuan, A.,Rao M.V.,Veeranna, Nixon R.A. (2012) Neurofilamentsata glance. J Cell Sci. 125, 3257–3263.
- Zeis T., Probst A., Steck A.J., Stadelmann C., Brück W., Schaeren-Wiemers N. (2009) Molecular changes in white matter adjacent to an active demyelinating lesion in early multiple sclerosis. Brain Pathol. 19(3):459-66.
- Zuchero J.B., Fu M.M., Sloan S.A., Ibrahim A., Olson A., Zaremba A., Dugas J.C., Wienbar S., Caprariello A.V., Kantor C., Leonoudakis D., Lariosa-Willingham K., Kronenberg G., Gertz K., Soderling S.H., Miller R.H., Barres B.A. (2015) CNS myelin wrapping is driven by actin disassembly. Dev Cell. 2015 34(2):152-67.

Abbreviations

AD	Alzheimer's disease
ALS	Amyloid lateral sclerosis
AMPA	α-amino-3-hydroxyl-5-methyl-isoxazol-4-propionic acid
AON	Autoimmune optic neuritis
APP	Amyloid precursor protein
ATP	Adenosine triphosphate
Aβ	β-amyloid protein
BBB	Blood-brain barrier
BN	Brown Norway
BRB	Blood-retinal barrier
cAON	Clinical phase of autoimmune optic neuritis
CDMS	Clinically diagnosed MS
CIS	Clinically Isolated Syndrome
CNS	Central nervous system
CSF	Cerebrospinal fluid
EAE	Experimental autoimmune encephalomyelitis
ER	Endoplasmic reticulum
F-actin	Filamentous actin
FC	Fast component axonal transport
G-actin	Globular actin (monomer)
GM	Grey matter
HLA – DRB1	DR beta 1 gene
iAON	Induction phase of autoimmune optic neuritis
IL2R	Interleukin‑2 receptor
IL7R	Interleukin-7 receptor
INL	Inner nuclear layer
iNOS	Inducible nitric oxide synthases
IVI	Intravitreal injection
Kif21B	Kinesin family member 21B
LGN	Lateral geniculate nucleus
MAG	Myelin-associated glycoprotein
MBP	Myelin basic protein
MHC	Major histocompatibility complex

MOG	Myelin oligodendrocyte glycoprotein
MS	Multiple sclerosis
NaV	Voltage-gated Na^+ channels
NAWM	Normal-appearing white matter
NCX	Na^+-Ca^{2+} exchangers
NFH	Neurofilament medium
NFL	Neurofilament light
NFM	Neurofilament medium
NFs	Neurofilaments
NMDA	N-methyl-D-aspartate
NMDAR	N-methyl-D-aspartate receptor
NO	Nitric oxide
ON	Optic neuritis
ONH	Optic nerve head
PD	Parkinson's disease
PI3K	Phosphoinositide 3-kinase
PLP	Proteolipid protein
PMCA	Plasma membrane Ca^{2+} ATPases
PPMS	Primary Progressive MS
RGC	Retinal ganglion cell
RIS	Radiologically Isolated Syndrome
RNFL	Retinal nerve fibre layer
RNS	Reactive nitrogen species
ROS	Reactive oxygen species
RRMS	Relapsing remitting MS
SC	Slow component axonal transport
SPMS	Secondary Progressive MS
TUNEL	Terminal deoxynucleotidyl transferase dUTP nick end labelling
VGCC	Voltage-gated Ca^{2+} channels
WM	White matter
βAPP	β-amyloid precursor protein